SULPHUR BEHAVIOUR AND CAPTURING DURING A FIXED-BED GASIFICATION PROCESS OF COAL

A thesis submitted to the NORTH-WEST UNIVERSITY, Potchefstroom. In fulfilment of the requirements for the degree PhD (Chemistry)

By

Madoda Pet Skhonde

BSc Chemistry and Maths (WITS, 2000)

BSc, Honours Chemistry (WITS, 2001)

GDE Coal Technology (WITS, 2004)

MSc Chemical Engineering (WITS, 2006)

Promoter: Prof CA Strydom

Co-Promoters: Prof HH Schobert and Dr JR Bunt

School of Physical and Chemical Sciences

North-West University

Potchefstroom

South Africa

March 2009

SULPHUR BEHAVIOUR AND CAPTURING DURING A FIXED-BED GASIFICATION PROCESS OF COAL

M P SKHONDE

March 2009

Declaration

I, the undersigned, declare that the work contained in this thesis is my own original study and has not previously been submitted at any university for a degree

M P Skhonde **Date**

ACKNOWLEDGEMENTS

The author would like to extend his thanks and appreciation to the following people and organizations for their assistance throughout the study:

Firstly, Prof Christien Strydom (study promoter), Prof Harold Schobert and Dr John Bunt (study co-promoters) for their outstanding assistance and guidance throughout the course of the study. Secondly, Dr Henry Matjie for his extremely valuable insight, assistance, motivation and advice at crucial times.

Dr Johannes van Heerden and the Sasol Technology (Syngas and Coal Technology R&D) team for their financial as well as technical and moral support.

Colleagues Arno Ooms, Rudi Coetzer, Elias Nana, Sarel DuPlessis, Ishmael Nkadimeng, Thomas Mokgotsi, Joseph Mpinga and Adam Baran for their practical assistance in various aspects of the work conducted. Special thanks to Adam who conducted XRD analysis.

CMT laboratories for conducting ultimate analysis, proximate analysis, sulphur forms analysis and ash analysis.

My wife Conny and son Njabulo for their encouragement, interest and support during the write-up phase of this project.

Finally, to God, the almighty, for blessing me with the intellect and perseverance to successfully complete this project.

SYNOPSIS

During coal gasification, sulphur is liberated from the coal structure and released as H_2S and COS. However, widespread concern about environmental emissions from coal utilization has started to limit the growth in use of coal as an energy source. The primary objective of the study reported in this thesis was to investigate the possibility of sulphur capturing through injection of SO_2 into a packed coal bed, under controlled conditions that simulates the zones of a fixed-bed gasifier. The secondary objective of the study was to investigate the sulphur behaviour in a commercial fixed-bed gasifier.

In the study conducted, the behaviour of sulphur occurring within a fixed-bed gasification process was studied using a commercial Sasol-Lurgi fixed-bed gasifier, using the gasifier turnout sampling method. The investigation of sulphur capturing in a packed coal bed under controlled conditions was conducted in two different experimental set-ups, namely: a laboratory-scale furnace that simulates the combustion zone as well as a pilot-scale pipe reactor that simulates all the various zones of the gasifier.

Sulphur behaviour across a commercial fixed bed gasifier was found to be influenced mainly by minerals-based sulphur such as sulphur in pyrite. Pyrite decomposition to pyrrhotite was found to be the predominant process in the top half of the gasifier, leading to the formation of H_2S and COS. Pyrrhotite was found to be undergoing further transformation towards the formation of iron oxides, leading to formation of more H_2S, or SO_2 and SO_3, depending on whether reducing or oxidising conditions prevail. Sulphur was found to be retained in the ash in different forms, with one being

sulphur oxides that reacted with the high temperature transformation product (CaO) of calcite or dolomite to form anhydrite.

Findings from the investigation of sulphur capturing in a packed coal bed suggests that SO_2 injection into a packed coal bed under controlled conditions leads to sulphur capturing in the coal minerals, particularly CaO from the decomposition of limestone and dolomite. Notable amounts of CaS were found to be the sulphur-capture product; this was associated with high carbon content that favours formation of CaS over $CaSO_4$. A linear relationship between carbon content and the amount of CaS formed was obtained.

OORSIG

Swael word as H_2S en COS uit die steenkoolstruktuur vrygestel tydens die steenkoolgasifiseringsproses. Wydverspreide bekommernis oor die omgewingsvrystellings tydens die gebruik van steenkool het egter begin om die gebruik daarvan as 'n energiebron te beperk. Die primêre doel van die studie soos in hierdie tesis bespreek, is om die opname van swael deur inlating van SO_2 in 'n gepakte bed te ondersoek onder gekontroleerde omstandighede wat die sones binne 'n vaste-bed vergasser simuleer. Die sekondêre doel van hierdie studie was om die gedrag van swael in 'n kommersiële vaste-bed gasifiseerder te ondersoek.

Vir hierdie studie is die gedrag van swael tydens die vaste-bed vergassingsproses bestudeer binne 'n kommersiële Sasol-Lurgi vaste-bed vergasser deur gebruik te maak van die vergassingsuitkeermetode. Die ondersoek na die opname van swael in 'n vaste steenkoolbed onder gekontroleerde omstandighede is in twee verskillende eksperimentele opstellings gemaak, naamlik: 'n laboratorium-grootte oond wat die verbrandingsone simuleer, asook 'n loodsaanleg-skaal pypreaktor wat die verskillende sones binne 'n vergasser simuleer.

Daar is bevind dat swael gedrag binne 'n kommersiële vaste-bed vergasser hoofsaaklik beinvloed word deur die mineraal-gebonde swaelverbindings, soos die swael in pirriet. Die dominante proses in die boonste gedeelte van die vergasser blyk die ontbinding van pirriet na pirhotiet te wees, wat lei tot die vorming van H_2S en COS. Pirhotiet ondergaan verdere transformasie na die vorming van ysteroksiede, wat lei tot die vorming van meer H_2S of SO_2 en SO_3, afhanklik daarvan of die atmosfeer reduserend of oksiderend is. Dit is bevind dat swael in verskillende vorme in die as

behoue bly, waarvan een vorm die is van swaeloksiede wat met die hoë temperatuur transformasieproduk van kalksteen (CaO) of dolomiet reageer om kalsiumanhidriet te vorm.

Bevindings tydens die ondersoek na die swaelopname in 'n vaste steenkoolbed dui daarop dat SO_2 inlaat in die gepakte steenkoolbed onder gekontroleerde omstandighede lei tot die vasvang daarvan in steenkoolminerale, veral CaO, wat uit kalksteen en dolomiet vorm. Merkbare hoeveelhede van CaS is aangedui as die swaelproduk. Hierdie produk word geassossieer met die hoë koolstof inhoud wat die vorming van CaS bo die van $CaSO_4$ bevoordeel. 'n Liniêre verwantskap tussen die koolstofinhoud en die hoeveelheid CaS wat gevorm is, is gevind

INDEX

LIST OF ABBREVIATIONS

AGR	**Acid gas removal**
ASTM	**American Society for Testing and Materials**
C	**Carbon**
CCSEM	**Computer-controlled scanning electron microscopy**
CCT	**Clean Coal Technology**
CGCU	**Conventional cold gas clean-up**
CFB	**Circulating fluidised bed boiler**
CMT	**Coal and Materials Technologies**
DOE	**US department of energy**
DSRP	**Direct sulphur recovery process**
EPRI	**Electric Power Research Institute**
FT	**Fischer-Tropsch**
HGCU	**Hot gas clean-up**
ID	**Inner Diameter**
IGCC	**Integrated Gasification Combined Cycle**
ISO	**International Organisation for Standardization**
MDEA	**Methyldiethanolamine**
METC	**Morgantown Energy Technology Centre**
MK IV	**Mark Four (ID 3.848 diameter) gasifier**
NETL	**National Energy Technology Laboratory**
PCD	**Particulates Control Device**
PSD	**Particle size distribution**
PSDF	**Power Systems Development Facility**

R&D	**Research and Development**
RSF	**Reactive semi-fusinite**
RTI	**Research Triangle Institute**
S	**Sulphur**
SABS	**South African Bureau of Standards**
SCT	**Syngas and Coal Technology R&D group**
SEM	**Scanning Electron Microscopy**
SHOS	**Super high organic sulphur**
SRU	**Sulphur Recovery Unit**
SWPC	**Siemens Westinghouse Power Corporate**
T	**Temperature**
WHO	**World Health Organisation**
XRD	**X-ray diffraction**
XRF	**X-ray fluorescence**

LIST OF FIGURES

Chapter 1: Background and literature review

Chapter 2: Experimental procedures

Chapter 3: Results and discussions

LIST OF TABLES

Chapter 1: Background and literature review

Chapter 2: Experimental Procedures

Chapter 3: Results and discussions

LIST OF APPENDICES

LIST OF ABBREVIATIONS

AGR	Acid gas removal
ASTM	American Society for Testing and Materials
C	Carbon
CCSEM	Computer-controlled scanning electron microscopy
CCT	Clean Coal Technology
CGCU	Conventional cold gas clean-up
CFB	Circulating fluidised bed boiler
CMT	Coal and Materials Technologies
DOE	US department of energy
DSRP	Direct sulphur recovery process
EPRI	Electric Power Research Institute
FT	Fischer-Tropsch
HGCU	Hot gas clean-up
ID	Inner Diameter
IGCC	Integrated Gasification Combined Cycle
ISO	International Organisation for Standardization
MDEA	Methyldiethanolamine
METC	Morgantown Energy Technology Centre
MK IV	Mark Four (ID 3.848 diameter) gasifier
NETL	National Energy Technology Laboratory
PCD	Particulates Control Device
PSD	Particle size distribution
PSDF	Power Systems Development Facility

R&D	**Research and Development**
RSF	**Reactive semi-fusinite**
RTI	**Research Triangle Institute**
S	**Sulphur**
SABS	**South African Bureau of Standards**
SCT	**Syngas and Coal Technology R&D group**
SEM	**Scanning Electron Microscopy**
SHOS	**Super high organic sulphur**
SRU	**Sulphur Recovery Unit**
SWPC	**Siemens Westinghouse Power Corporate**
T	**Temperature**
WHO	**World Health Organisation**
XRD	**X-ray diffraction**
XRF	**X-ray fluorescence**

LIST OF FIGURES

Chapter 1: Background and literature review

Chapter 2: Experimental procedures

Chapter 3: Results and discussions

LIST OF TABLES

Chapter 1: Background and literature review

Chapter 2: Experimental Procedures

Chapter 3: Results and discussions

LIST OF APPENDICES

Chapter 1

Background and literature review

Coal is the largest and most widespread fossil fuel resource, providing 23% of the world's energy. With coal gasification processes, acid gas removal from raw gases produced, has become one of the areas with a very high research and development focus. Utilisation of the H_2S once removed from the gas stream is necessary for the reduction of the amount of H_2S emitted to the atmosphere. H_2S emission reduction from gasification has received more attention recently due to increased pressure put on the coal processing industry from an environmental point of view [Korens et al, 2002].

Sulphur is introduced to the coal processing plant with the coal, where it is bound in the coal structure, or present in various minerals such as pyrite. With coal combustion processes, sulphur is liberated from the coal structure and released mainly as SO_2 and SO_3, whereas, with coal gasification processes, sulphur is liberated from the coal structure and released as H_2S and COS [Ozum et al., 1993; Mastral et al., 1999; Day, 2004; Ocampo et al., 2003]. Sulphur emissions from various coal processing plants have become one of the environmental footprints that need to be addressed.

1.1. Objectives of this study

Understanding of sulphur behaviour during the fixed bed gasification process is an important step towards devising means for the reduction of sulphur emissions from the gasification processes. In the study presented in this thesis, sulphur behaviour in a commercial fixed bed gasifier and the possibility of sulphur capturing via injection of SO_2 in a packed coal bed was investigated. The hypothesis of the study carried out was that injection of SO_2 in a packed coal bed, under controlled conditions such as in the fixed bed gasification process, can lead to sulphur capturing by high temperature transformation products of coal mineral matrix through a series of reactions involving Ca-bearing minerals such as limestone and dolomite.

The main objective of the study was to test the hypothesis that the injection of SO_2 into a packed coal bed, at controlled conditions, can lead to sulphur capturing through the series of the reactions indicated below (equations 1, 2, 3 and 4). Part of the primary objective was to understand the sulphur capturing mechanism. In order to achieve in-situ sulphur capturing, it is necessary to understand the behaviour of sulphur in coal as the coal is exposed to thermal treatment under controlled conditions. The second objective of the study was to understand the behaviour of sulphur in the coal as the coal is exposed to various conditions in a fixed bed gasifier. This was done by following the sulphur profile from the top of the gasifier to the base of the reactor.

During a fixed-bed coal gasification process, coal is introduced to the gasifier from the top with the agent (i.e. steam and oxygen) introduced from the bottom of the

reactor. The interaction of the coal and the agent (steam and oxygen) in counter-current mode gives rise to the gasification reaction in the coal structure. This leads to liberation of various gases from the coal structure. These gases are the constituents of the syngas such as CO, CH_4 and H_2, as well as impurities including CO_2, and H_2S and various hydrocarbons.

During the coal gasification process, sulphur is liberated from the coal structure and released as H_2S. The H_2S forms part of the raw synthesis gas composition and is released with the raw gas out of the gasifier. The coal as fed to the gasifiers also contains calcium in the form of dolomite ($CaMg(CO_3)_2$) and limestone ($CaCO_3$). $CaCO_3$ and $CaMg(CO_3)_2$ are reported to undergo decomposition to form lime (CaO) and periclase (MgO) respectively, together with CO_2, at temperatures above 400 °C, as shown in equations 1 and 2 [Raask, 1984; Hem and Debaprasad, 1986; Hu et al., 2006; Macias-Perez et al., 2007].

$$CaCO_3 \rightarrow CaO + CO_2 \quad \text{.....1}$$

$$CaMg(CO_3)_2 \rightarrow CaO + MgO + CO_2 \text{.....2}$$

Most of the H_2S is released higher up in a fixed-bed gasifier under strongly reducing conditions that prevail, before the coal reaches the combustion zone where decomposition of limestone and dolomite leads to the formation of CaO and MgO as shown in equation 1 and 2 [Raask, 1984; Hem and Debaprasad, 1986; Hu et al., 2006; Macias-Perez et al., 2007]. The sulphur released in these regions of the gasifier as H_2S cannot react with the calcium in the limestone and dolomite, as the decomposition of limestone and dolomite only takes place lower down in the gasifier. However with the

injection into a packed coal bed of sulphur (in a form of H_2S or SO_2), the H_2S is expected to be converted to SO_2/SO_3 due to the oxidising conditions that prevail, i.e. high temperature and presence of oxygen, and the sulphur can then possibly react with the calcium oxide at elevated temperatures to produce $CaSO_4$, as shown in reactions 3 and 4.

$$CaO + SO_2 + {}^1/_2O_2 \rightarrow CaSO_4 \quad \text{.....3}$$

$$CaO + SO_3 \rightarrow CaSO_4 \quad \text{.....4}$$

1.2 Introduction to coal

This section covers background and reviews relevant literature on coal and coal classification. Mineral matter formation in coal is also briefly discussed in this section.

1.2.1 Definition of coal

Coal is a heterogeneous mixture of organic compounds consisting predominantly of altered plant material [Osborne, 1988], together with a certain amount of inorganic material in the form of moisture and mineral components. The organic part of the coal originally grew up to 300 million years ago [Horsfall, 1993]. Coal is also defined as a readily combustible rock containing more than 50 % by weight, and more than 70 % by volume of carbonaceous material [Horsfall, 1993]. Coal is formed through an apparently continuous series of alterations:

living material→ peat→lignite→subbituminous coal→anthracite

This succession of changes in the properties and structure of coal is called metamorphism. The degree of metamorphism is called "rank".

The nature of the organic constituents depends on the relative proportions of the various kinds of plant debris (woods, leaves, spores, etc.) in the initial accumulation of peat, and on the diagenetic or metamorphic changes that have occurred since the peat was originally laid down. Together with the nature and relative amount of any mineral matter that may be present, this assemblage of organic compounds is reflected in the physical appearance of the coal, and determines its behaviour when used.

It is generally accepted that there were at least two stages of coal formation from plant material:

- The biochemical period of accumulation and preservation of plant material as peat, and
- The geochemical period of conversion of peat to coal. [Vlakovic, 1983]

Although most coal researchers accept this theory, agreement on the details of the actual chemical and physical changes that occur in the process is not widespread.

The Northern Hemisphere (Laurasian) coals were formed by sedimentation of plant material in swamps in warm, moist climate conditions. The accumulated plant material decayed under anaerobic conditions (due to accumulation beneath the surface of swamps) and after a gel-like phase, eventually metamorphised into coal. Elevation

changes and accumulation of water-borne mud and silt interrupted the growth and decay cycle. Growth re-asserted itself and the cycle recommenced forming a number of coal seams [England et al., 2002; Speight, 1994].

In the Southern Hemisphere (Gondwana), the coal formation vegetation differed from the Northern Hemisphere vegetation. Coal-forming vegetation grew in shallow lakes that were fed by rivers flowing from elevated lakes. Glaciers fed the rivers during the formation phase, which resulted in a greater degree of aerobic decay. Due to the rivers being glacier-fed, a lot of mineral matter was introduced. When the water drained from the gel-like phase, the peat was buried. The increase in temperature and pressure initiated the coalification process [Teichmuller and Teichmuller, 1967; Speight, 1994].

1.2.2 Classification of coal

During the coal formation process, the most important characteristics that are used for coal classification were established namely: coal grade, coal type and coal rank. Coalification is known as the transformation process of peat via the steps of lignite, sub-bituminous, bituminous, anthracite and graphite. Various authors have presented data indicating the main chemical changes that occur during coalification processes [Falcon, 1977; Teichmuller and Teichmuller, 1967; Hawke et al., 1999].

1.2.3 Grade of Coal

The grade of coal is determined by the amount of mineral matter that is left as residue after combustion (ash content). The higher the amount of inorganic residue, the lower the grade of the coal.

1.2.4 Coal Type

The type of plant material that was part of the vegetation of the coal formation process determines the type of coal. During the process of decay the cellulose is biochemically converted to peat in the presence of adequate air and restricted decomposition with a gradual increase in carbon-rich compounds. During this stage of coalification process, microscopic constituents called macerals are formed [Smith, 1984; Coetzee, 1976]. Four main groups of macerals can be distinguished in South African coals:

- Vitrinite
- Exinite
- Reactive semi-fusinite (RSF) and
- Inertinite.

Reactive semi-fusinite can only be found in the Gondwana coal area [Smith, 1984]. The macerals are also subdivided as shown in the following table.

Table 1.1: Sub-division of main maceral groups [Tsai, 1982 and Smith, 1984]

Vitrinite	Colinite Telinite
Exinite	Sporinite Cutinite Algenite Resinite
Inertinite	Scleronite Semifusinite Fusinite
Reactive semi-fusinite	Micrinite Macrinite

Vitrinite is derived from the cell wall material or woody tissue of plants, and it is the most abundant group that makes up to 50 to 90 % of most American coals. Vitrinite is the main maceral found in Northern Hemisphere coal with a content of 70 to 80 % of the seam. Exinite contains the highest hydrogen content and the lowest oxygen content of all the macerals. Inertinite contains the lowest amount of hydrogen and the highest oxygen content of all the macerals [Meyers, 1982]. The vitrinite content for South African coals varies between 14 and 90 %.

From an isometamorphic maceral group evaluation on a 84 % (m/V) carbon content coal, it was clear that larger aromatic clusters are present in vitrinite, and that the aromaticity of a certain coal rank is the highest for inertinite [Tsai, 1982].

1.2.5 Rank of Coal

The rank of coal is determined by the degree of maturity of the coal. The change is the result of metamorphosis that the coal layers undergo over a period of millions of years. Pressure within the sediment layer, heat from the mantle of the earth, and secondary heat as a result of weathering of the earth's crust caused the volatiles and

moisture content to decrease. This resulted in higher carbon contents. High-rank coal has lower oxygen contents, and lower rank coal can have oxygen contents up to 30 % [Fuerstenau, 1976].

With an increase in rank, the structure of the coal tends to become less porous and the carbon becomes more aromatic in chemical structure. An increase of aromaticity is found with an increase in rank, therefore anthracite will be more aromatic than brown coal [Meyers, 1982; Ibarra et al., 1996]. The structure of the coal becomes more ordered for higher rank coals: the aromatic lamellae grow in proportion and size and their alignment becomes more perfect [Horsfall, 1993].

1.2.6 Mineral matter in coal

The inorganic composition of coal consists mainly of minerals and to a lesser extent organically associated components and exchangeable cations [Galuskina, 2004]. When burned at high temperatures in the presence of O_2, the inorganic components are left behind as a residue, called ash. In the reducing and oxidising environment of a combustion chamber, mineral matter undergoes a variety of transformations. Clays are transformed to aluminosilicates and mullite ($Al_6Si_2O_{13}$), calcite forms CaO, and quartz may remain unchanged [Reyes et al., 2004].

The presence of minerals in coal is due to finely divided mineral precursors that are captured during the sedimentation phase and are bound to the organic structure of the coal, or occur in the cleats of the coal structure as excluded minerals. There are two ways in which the minerals are captured, namely:

(1) Syngenitic (minerals formed or incorporated during the coalification process), and

(2) Epigenetic (minerals were rinsed into the structure via holes and cracks after coalification was completed)

The removal of minerals from the coal matrix depends on the type of mineral [Horsfall, 1993]. Syngenetic minerals are more difficult to remove than epigenetic minerals. The minerals forms is represented in figure 1.1 [Horsfall, 1993].

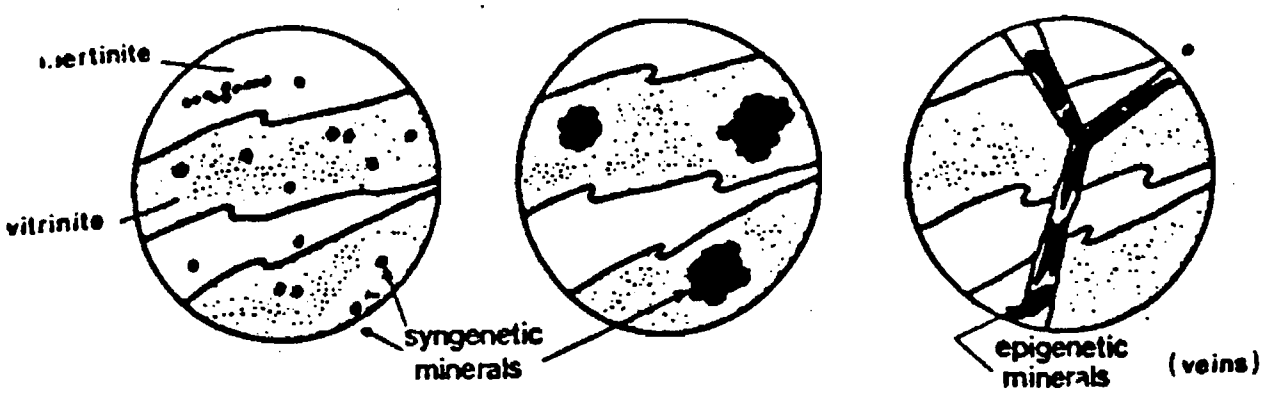

Figure 1.1 Syngenetic and epigenetic mineral matter in a coal structure [Horsfall, 1993].

South African coals differ from Northern Hemisphere coals in mineral content. The South African coals have higher percentages of finely included minerals in the coal, which requires extensive milling to very small particle sizes for liberation of the minerals [Botha, 1980].

1.3 Introduction to coal gasification

Coal gasification is a process used to produce syngas (a mixture of H_2 and CO) from coal using various process configurations. The gasification process employed depends on the type of coal as well as the conditions necessary to produce syngas through a high-efficiency process.

The Sasol-Lurgi fixed-bed dry bottom gasifier is an example of a commercial fixed bed gasification process. The Sasol-Lurgi gasifier operates on lump-sized coal. Therefore once the coal is mined, it is crushed down to less than 100 mm and screened at a bottom size of 5 to 8 mm. The coal enters at the top of the gasifier through a coal lock hopper system, while reactants (steam and oxygen) are introduced at the bottom of the gasifier (figure 1.2). As a result, there is a counter-current flow of the coal and reactants, which leads to a temperature drop across the length of the gasifier. This gives rise to the various reaction zones as indicated in figure 1.2.

On top of the gasifier, as the coal enters, it is exposed to the drying zone where the moisture is driven off. Below the drying zone, the devolatilization zone commences, where the volatile matter is driven from the coal structure. It is in this region where char formation takes place. The gasification zone or reduction zone follows below the devolatilization zone, where the coal gasification reactions take place, leading to the consumption of the char formed in the devolatilization zone. In the combustion zone the char is burnt off to ash with more gases being formed [Slaghuis, 1993].

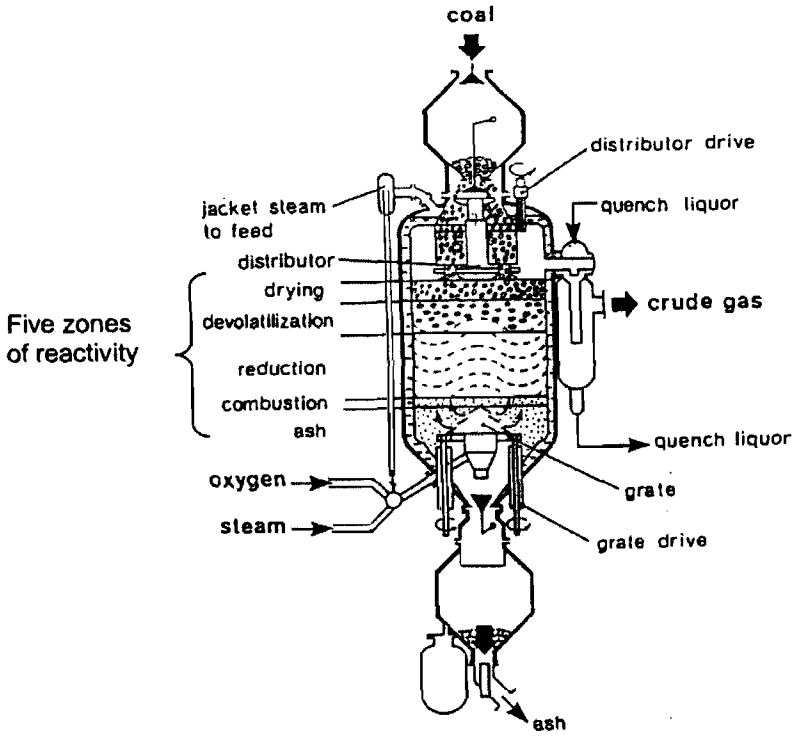

Figure 1.2. Representation of the gasifier showing the zones of reactivity [Slaghuis, 1993].

1.4 Sulphur in coal

In this section the different forms of sulphur in coal are described. Transformation of coal minerals, including the sulphur-bearing ones, during the coalification process is discussed. The different forms of sulphur-containing gases that are released from different coal processing options are also mentioned.

1.4.1 Sulphur during coal formation

Sulphur in coal can originate from sea water, fresh water, vegetation and extraneous mineral matter. Abundance of sulphur in coals is controlled by depositional environments and the diagenetic history of the coal seams and overlying strata. The seawater interaction with the peat results in elevated levels of sulphur in coals [Ryan

and Ledda, 1997]. Low-sulphur coal seams, such as the Tertiary coals in the Powder River Basin in the USA, were deposited in an alluvial environment and the peat was not influenced by seawater. The sulphur in these low-sulphur coals is derived mostly from their parent plant materials. In contrast, high-sulphur coal seams are generally associated with marine strata. For example, the Herrin Coal in the Illinois Basin in the USA is predominantly a high-sulphur containing coal, and the seam is mostly overlain by the marine Anna Shale and Brereton Limestone [Benson, 1987]. The rare, yet characteristically superhigh-organic-sulphur (SHOS) coal of Guidin, Guizhou, China, was deposited during the Late Permian on a carbonate platform where there was plenty of seawater sulphate but a lack of iron [Shao et al., 1998].

During the formation of high-sulphur coal, seawater sulphate diffuses into peat and is reduced by microorganisms to hydrogen sulphide, elemental sulphur and polysulphides. During early diagenesis in a reducing environment, ferric iron is reduced to ferrous iron, which reacts with hydrogen sulphide to form iron monosulphide. Iron monosulphide is later transformed by reaction with elemental sulphur into pyrite. Organic sulphur is formed by reaction of reduced sulphur species with the premaceral humic substances formed by bacterial decomposition of the accumulated organic matter. Organic sulphur species in coals are mainly thiols, sulphides, disulphides, and thiophene and its derivatives. The thiophenic fraction of organic sulphur increases with the carbon content of coals. Organic sulphur compounds formed in peat are mostly thiols and sulphides, which gradually convert to thiophenes with increasing coal maturation [Ryan and Ledda, 1997; Casagrande, 1979].

1.4.2 Types of sulphur in coals

Sulphur may occur in coal in a number of forms, including sulphides, organic sulphur, and sulphates [Spears et al., 1999]. The most important forms are sulphides (mainly pyrite) and organic sulphur.

- Sulphide minerals, such as pyrite, are associated with the inorganic fractions. Pyrite in coal typically forms from H_2S and Fe in solution. The process involves bacterial reduction of SO_4^{-2} to H_2S, followed by the combination of H_2S, elemental sulphur and ferrous iron oxide (FeO) to form pyrite and water [Ryan and Ledda, 1997].
- Organic sulphur is incorporated into the hydrocarbon structure of the coal substance. Organic sulphur forms also vary depending on the manner in which the sulphur is bound to the organic structure. These forms include: aliphatic or aromatic thiols; aliphatic, aromatic or mixed sulphides; aliphatic-aromatic or mixed disulphides; and heterocyclic compounds of thiophene type [Ryan and Ledda, 1997].
- Sulphate minerals (mostly hydrous iron or calcium sulphates) are usually produced by atmospheric oxidation of the sulphides. Pearson and Kwong [1979] suggested that in coals with high proportion of organic sulphur, organic sulphur can oxidise to form gypsum [Pearson and Kwong, 1979; Ryan and Ledda, 1997].

During ultimate analysis of coal, the total sulphur content is determined; this represents sulphur occurring in all the possible forms mentioned above. Although the total sulphur content provides sufficient data for most commercial applications,

knowledge of the amounts present in each of the three principal forms (viz. sulphides, organic sulphur and sulphates) is useful for the following purposes:

- To assess the level to which the total sulphur content might be reduced by coal preparation processes. It is possible that a preparation plant may remove much of the pyritic sulphur and sulphate sulphur, but such a plant is unlikely to reduce the organic sulphur component.
- To assess, by normative calculation, the amount of mineral matter in the coal.

1.4.3 Transformation of coal minerals that impact on sulphur behaviour during coal processing

During coal processing such as combustion or gasification, coal minerals play a major role as they are transformed into various forms that contribute to the overall behaviour of that particular coal in the process. During coal combustion processes, Bryers [1986], and Srinivasachar et al. [1990] found that the excluded minerals experience more oxidising combustion conditions than included minerals. Therefore the excluded minerals may increase the rate of fusion, enlarge the clinker size, and also reduce the devolatilisation of inorganic elements during coal combustion [Bryers, 1986; Srinivasachar et al., 1990]. During coal combustion, the included minerals generally reach temperatures in excess of the surrounding gas temperature and react quickly by coalescence due to the close proximity to one another, and may have lower melting points. Some inorganic species in the heated particles of the included minerals may undergo reduction and start to volatilise in the form of submicron particles or gases under the conditions of the burning char [Bryers, 1986; Srinivasachar et al., 1990].

Major minerals, such as kaolinite ($Al_4Si_4O_{10}(OH)_8$), illite ($K_{1.5}Al_4(Si_{6.5}\ Al_{1.5})O(OH)_4$), and quartz ($SiO_2$), undergo transformation as they are exposed to elevated temperatures (of more than 600 °C) to form various new minerals. Kaolinite transforms and forms metakaolinite, which transforms to mullite ($3Al_2O_3.2SiO_2$), alumina (Al_2O_3) and cristoballite (SiO_2) with an increase in temperature [Grim and Bradley, 1940; Benson, 1987]. Illite transforms to form spinnel and mullite, which are in the glass phase [Grim and Bradley, 1940; Benson, 1987]. Ward and French [2004] reported that illite and other clays, excluding kaolinite, fuse at around 1200°C to 1350 °C to form glassy components, resulting in relatively low ash fusion temperatures and possible slag development. Results from studies of Srinivasachar et al. [1990] show that illite particles start to decompose at temperatures above 1167 °C, lose their crystalline structure, and completely transform to a glass. During the investigation, no vaporisation of the potassium species from the molten solution of both the excluded and included illite particles occurred, but the formation of cenospheres (ash component that contains unburnt carbon particles of different types) from coal combustion, unaltered quartz, other mineral grains and hollow silicate spheres that float on water were observed.

Combustion of synthetic chars containing illite inclusions indicated coalescence of these inclusions to form larger ash agglomerates [Srinivasachar et al., 1990]. Comparison of these results with ash-particle compositional data, obtained from the combustion of a bituminous coal containing illite, showed intermediate composition, indicating interaction between the molten illite and quartz, kaolinite, and pyrite [Srinivasachar et al., 1990]. From the results by these researchers it was concluded

that the molten solution of illite is responsible for the dissolution of ash particles at 1167 °C during the pulverised coal combustion process.

Quartz is often regarded as essentially non-reactive during the combustion process but upon heating it undergoes a series of phase transitions, in lignites [Bryers, 1986]. At room temperature quartz is known as low quartz. At 573 °C it changes into other polymorphs, α-quartz, β-quartz (573-870 °C), β_2-tridymite (870-1470 °C), and β_2–cristobalite (>1470 °C), to form liquid. Watt [1969] mentioned that in the last two transformations of quartz, the structure of its polymorphs can open and react with sodium ions at temperatures ranging from 760 to 1250 °C to form nepheline ($NaAlSiO_4$).

It is well documented that the trace amounts of excluded carbonate minerals, including calcite ($CaCO_3$), dolomite ($CaMg(CO_3)_2$), siderite ($FeCO_3$), and ankerite ((Fe, Ca, Mg) CO_3)), are found in most bituminous coals. Bryers [1986], Ward and French [2004], and Raask [1984] indicated that calcite decomposes at elevated temperatures from 500 to 1000 °C to form quicklime (CaO). This lime may react with water and sulphur oxides to form portlandite ($Ca(OH)_2$) and anhydrite ($CaSO_4$) respectively. At high temperatures, CaO interacts with more reactive aluminium silicate, such as meta-kaolinite, to form gehlenite ($Ca_2Al_2SiO_7$) and anorthite ($CaAl_2Si_2O_8$), which fuse at approximately 1400 to 1500 °C.

1.4.4 Sulphur emissions from coal processing

Sulphur in the coal structure is converted at elevated temperatures during coal processing and liberated in various forms, which include SO_x (SO_2 and SO_3) and H_2S (and COS) from combustion plants and gasification plants respectively. These sulphur-containing gases are formed during the various transformations that the coal structure and minerals undergo in a particular process.

Sulphur emissions contribute to air pollution since sulphur is emitted in gaseous form and is exposed to the environment. The gases enter the body by inhalation, ingestion with food or liquids where the sulphur is absorbed, as well as by skin absorption. The World Health Organisation (WHO) estimates that 3 million people die each year because of air pollution [Fischlowitz-Roberts, 2002]. Millions more suffer health problems. Around 30 to 40 % of asthma cases and 20 to 30 % of all respiratory diseases are linked to air pollution. Exposure to concentrations of more than or equal to 700 mg/m^3 H_2S can lead to human death [Fischlowitz-Roberts, 2002].

Of the sulphur gases emitted from the gasification plants, H_2S is the most notable due to its characteristic smell, which leads to public outcry and media criticism. This, as well as tougher legislation and enforcement of environmental policies from the countries' authorities has forced companies to review their operations and emission strategy with regard to H_2S emissions.

1.5 Sulphur removal from coal processing gases.

This section summarises various options for sulphur removal from coal processing gases. A review of sulphur removal from coal processing gases is presented with emphasis on both the conventional cold gas cleanup as well as the warm/hot gas cleanup options.

1.5.1. Conventional cold gas clean-up

In this section conventional cold gas cleanup processes for sulphur removal is discussed.

1.5.1.1 Acid gas removal processes

Gas cleanup, which involves removal of primary fuel gas contaminants such as particulates, CO_2 and sulphur (mostly present as hydrogen sulphide (H_2S)), and a number of secondary contaminants such as ammonia, chloride, alkali vapour, and heavy metals (As, Se, Hg, etc.), can be carried out using conventional cold-gas cleanup or advanced hot-gas cleanup methods [Gangwal et al., 1995]. There are a variety of commercial acid gas removal (AGR) processes available to treat various gas streams. The principal challenge of the AGR processes is to decrease the concentrations of the contaminants (sulphur, CO_2, trace elements etc.) from the synthesis gas to as low a level as possible, consistent with prevailing emission regulations, and as economically as possible.

In cold-gas cleanup, H_2S is removed from syngas by first concentrating it with amine-based chemical solvents (e.g. MDEA, methyldiethanolamine), or physical solvents such as Selexol (a refrigerated glycol) or Rectisol (refrigerated methanol). These systems are very effective in removing nearly all of the undesirable contaminants. The major drawback of cold-gas cleanup is that the entire syngas stream must be cooled prior to H_2S removal, to 37 °C for amine-based absorption processes, and to -40 to -62 °C for the refrigerated physical solvent processes [Korens et al., 2002]. Cooling the syngas to these temperatures condenses most of the water vapour present and thereby significantly reduces the energy efficiency of the overall production process. These low temperatures also significantly increase the capital cost of the IGCC (integrated gasification combined cycle) plant or chemical synthesis plant. The most suitable gas purification process is selected with respect to the specification of the final product syngas, fuel gas, pipeline gas and by-products required such as pure CO_2. Rectisol is a preferred process for chemical synthesis and is also often used as a beneficial process for other applications. Rectisol treatment of raw gas leads to purified gases with very low impurities compared to other processes as shown in table 1.2, as taken from Koss and Schlichting [2005].

Table 1.2: Pure gas specification from various gas cleaning processes [Koss and Schlichting, 2005]

Product gas Quality		
Process	**Purified Gas quality**	**Impurities**
Rectisol ®	0.1 to1 ppm 10 to 50 ppm 5ppm	Total sulphur (H_2S + COS) CO_2 H_2S in CO_2 by-product
Purisol®	5 to 50 ppm	H_2S, no COS removal
MDEA	3 to 50 ppm	H_2S, no COS removal
aMDEA®	1 to 50 ppm 5 to 50 ppm	H_2S CO_2

The processes employed for IGCC facilities and chemical synthesis are MDEA-based acid-gas removal processes, physical solvents-based processes, as well as processes based on employing mixed chemical and physical solvents.

1.5.1.2 Sulphur recovery

Sulphur recovery employing the Claus-based process remains the mainstay of sulphur recovery. For a sulphur recovery unit (SRU) usually based on the Claus process to operate properly, it requires a H_2S-rich acid gas feed, meaning the H_2S has to be removed preferentially to CO_2 in the AGR. In IGCC, AGR units are normally preceded by COS hydrolysis units to convert COS to H_2S [Undengaard and Berzins, 1984; Korens et al., 2002]. It is therefore desirable to choose a process that will selectively remove H_2S. The various selected acid gas removal processes achieve sulphur removal to different extents as shown in table 1.2. However, Rectisol appears to be the best process for sulphur removal. One of the key advantages of the Rectisol process is that it offers the possibility of recovering sulphur-containing compounds independently from CO_2.

1.5.2 Hot- and warm-gas clean-up

Hot gas cleanup was initially developed for air-blown gasification systems which produce over twice the volume of syngas (due to N_2 dilution) than the O_2-blown gasifiers produce, and therefore secures better thermal process efficiency and lower capital cost penalties related to syngas cooling to comparable temperature levels. Conventional cold gas cleanup (CGCU) with an air-blown system is uneconomical for

air-blown gasifiers [Korens et. al, 2002]. Therefore the success of air-blown gasification combined cycle power plants depends on the success of the HGCU developments.

Hot-gas cleanup is carried out at temperatures approaching those of the gasifier (about 800 °C). Hot-gas cleanup works well for H_2S removal but does little to remove Hg and other volatile components. Research in advanced hot-gas cleanup methods is conducted primarily in the US, Europe, and Japan, with the US Department of Energy (DOE), National Energy Technology Laboratory (NETL), formerly Morgantown Energy Technology Centre (METC), in the leadership role. The DOE/NETL programme has focused on hot-gas particulate removal and hot-gas desulphurisation (HGD) technologies that match or nearly match the temperature and pressure of the gasifier, gas cleanup system, and the combustion turbine. Warm-gas cleanup is conducted at moderate temperatures (about 200 °C) and has the advantage of being able not to only remove H_2S, but can also remove other troublesome contaminants such as Hg, Se, As, and Cd that cannot be removed by hot-gas sorbents [Korens et al., 2002].

While some cooling of the gas is required for warm-gas cleanup (which means there is some energy efficiency penalty), unlike cold-gas cleanup, warm-gas cleanup operates above the steam dew point of the syngas. Therefore, the warm-gas energy penalty is much lower than that of the cold-gas cleanup. Warm-gas cleanup permits removing multiple contaminants with lower cost equipment (lower cost alloys can be used) while minimising the energy efficiency penalty.

The goals of the high-temperature gas treatment are to eliminate the need for expensive heat-recovery equipment, reduce efficiency losses due to quenching, and minimise wastewater treatment costs associated with conventional cold-gas cleanup [Gangwal et al., 1995].

1.5.2.1 Hot- or Warm-Gas Desulphurisation (HGD)

Economic studies have indicated that hot gas desulphurisation results in lower capital and operating costs than for the conventional cold-gas desulphurisation process [Gangwal, 1995]. The only two large-scale "hot-gas" desulphurisation systems installed in the US, both in DOE CCT (clean coal technology) IGCC demonstration projects have never been demonstrated. Consequently, their ultimate commercial feasibility may never be known. Both systems were similarly based on the reaction of H_2S with zinc oxide or nickel oxide solid sorbents in an absorption column, followed by regeneration of the sorbent by contact with air in a separate column. The regenerator off-gas contains SO_2, which must be converted to elemental sulphur or sulphuric acid in a final recovery operation [Korens et al., 2002].

The main requirement for a metal oxide sorbent is that it should selectively react with H_2S in a reducing fuel-gas environment at desired conditions (2 to 3 MPa, 400 to 750°C) without undergoing reduction itself. Metal oxide reduction could result in loss of valuable fuel-gas, volatile metal loss due to evaporation, and weakening of the mechanical structure of the sorbent due to loss of oxygen [Gangwal et al., 1995; Hepol, 2000].

Metal oxide sorbents can be classified as disposable or regenerable. Disposable sorbents, typically calcium-based (e.g. limestone, dolomite, or lime), are employed in the bed near the combustion zone of the gasifier to remove H_2S in-situ via the reaction indicated in equation 5 [Maes et al., 1997; Hu et al., 2006]:

$$CaO + H_2S \rightarrow CaS + H_2O \quad \ldots\ldots 5$$

The CaS formed is then converted into the stable $CaSO_4$ form for disposal along with the gasifier bottom ash. A lower-than-required or desirable level of sulphur removal (about 80 to 90 % removal instead of 95 to 99 %) necessitates the use of an additional polishing sorbent, which is typically air-regenarable.

Regenerable sorbents can be employed in a polishing mode or in a bulk mode, where no in-bed disposable sorbent is employed for the total removal of H_2S from fuel gas. Various metal oxide sorbents and processes have been researched and reported. These include sorbents and processes based on oxides of copper, cerium, manganese, cobalt, tin, iron, and zinc, both individually and in combination, with up to >97 % sulphur removal achieved with temperatures less than 600 °C [Kay and Wilson, 1978; Xie et al., 2007; Gangwal et al., 1995; Slimane et al., 2007; Siriwardane et al., 2007].

All HGD reactor systems (e.g. fixed, moving or fluidized-bed), operate with air-regenerable sorbents, which results in a dilute SO_2 tail gas that must be treated further. The primary options for tail gas treatment include conversion of the SO_2 to sulphur products, including elemental sulphur and sulphuric acid. A promising process called "Direct Sulphur Recovery Process" (DSRP) has been under development since 1998

at Research Triangle Institute (RTI) [Schlather and Turk, 2007] for recovery of elemental sulphur from SO_2 at high-temperature, high-pressure conditions.

Another option for high-temperature H_2S removal from gas streams is reported by TDA Research Inc., where H_2S is oxidised with small amounts of air (O_2) to produce elemental sulphur without any H_2 consumption [Vidaurri et al., 2007].

1.5.2.2 Ongoing Warm-Gas Clean-up Programmes

Three long-running DOE-supported R&D programmes on warm-gas cleanup continues at Siemens Westinghouse Power Corporate (SWPC), Research Triangle Institute (RTI), and the Power Systems Development Facility (PSDF) operated by Southern Company Services at Wilsonville, Alabama. EPRI are also providing support for the PSDF programme, along with the Southern Company.

RTI and Eastman Chemical Company (Eastman) have successfully demonstrated a transport reactor-based desulphurisation technology suitable for warm (250 to 600 °C) syngas [Merkel et al., 2007, Schlather and Turk, 2007]. RTI is investigating a conceptual multi-step process that includes $HCl/H_2S/CO_2/H_2O$ removal by a solubility-selective polymer membrane, removal of HCl upfront through reaction with an alkali carbonate supported on a high surface area support, recovery of elemental sulphur by RTI's Direct Sulphur Recovery Process (DSRP), and removal of ammonia by zeolite molecular sieves, as shown in figure 1.3.

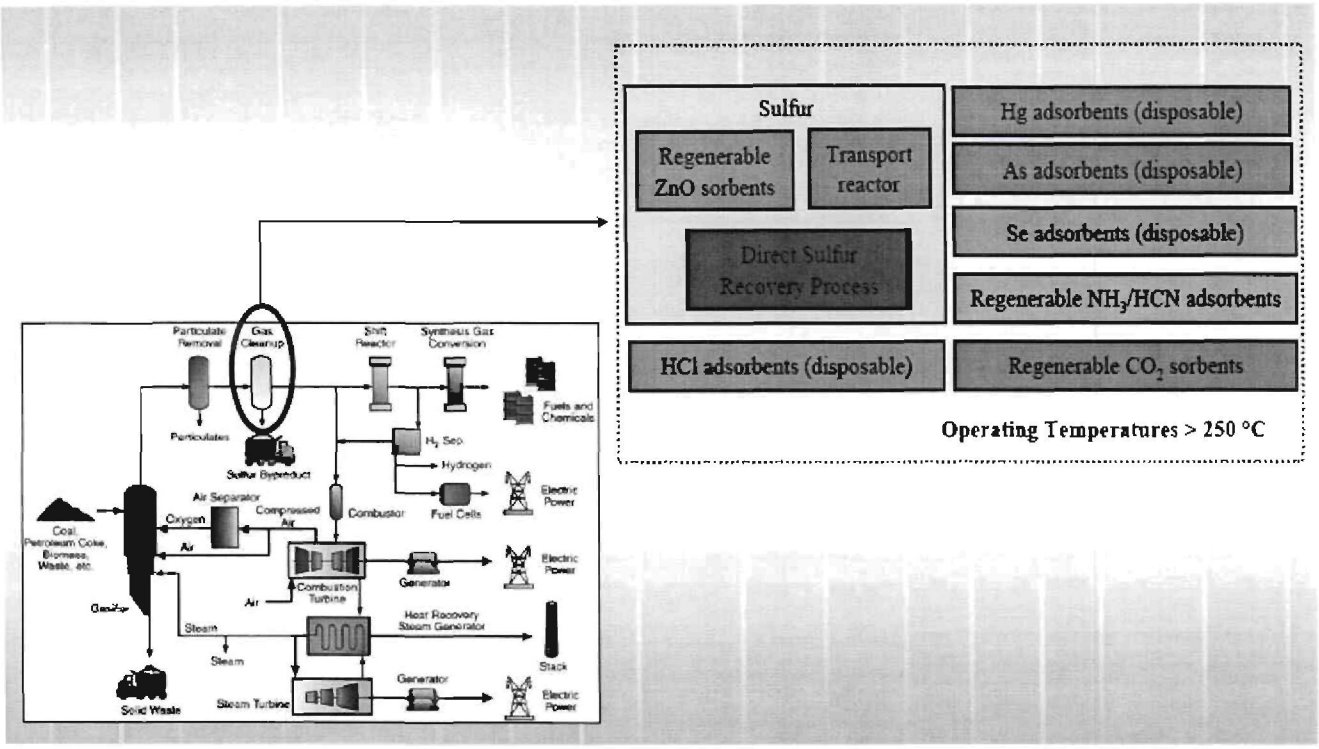

Figure 1.3: Schematic process flow of RTI's warm gas cleanup process [Schlather and Turk, 2007].

While the work at RTI is targeting very low levels, rapidly decreasing membrane selectivity as temperature increases above 25 °C is a challenge. The target temperature for the sulphur, HCl, and NH_3 removal process is in the 150 to 260 °C range. This range is ideal for producing of chemicals (such as methanol, FT products, and H_2) and also for phosphoric acid and solid oxide fuel cells [Merkel et al., 2007, Schlather and Turk, 2007].

SWPC's activities include the assessment of barrier filter materials and filter performance, the development of a candle filter safeguard device (SGD), and R&D on a conceptual 4-stage process that the investigators are calling the "Ultra-Clean Process". While this process is targeting removal of H_2S, HCl, and particulates to sub-ppm levels, it does not remove NH_3, HCN, or mercury [Slimane et al., 2007].

The Power Systems Development Facility (PSDF) is an engineering-scale demonstration of advanced coal-fired power systems and high-temperature, high-pressure gas filtration systems. As shown in figure 1.4, coal gasification at the PSDF is achieved with a KBR Transport gasifier, and a Siemens Westinghouse particulate control device (PCD) is used for filtration of gasification ash from syngas. As a critical process in the gasification system, hot-gas filtration in the PCD removes the particulates so that the syngas can be utilised in a downstream gas turbine or a fuel cell. Results obtained from the testing and demonstration of the PCD system has significantly increased readiness towards commercialisation of the hot-gas filtration technology [Davidson et al., 1999; Dahlin and Landhman, 2005; Guan et al., 2007].

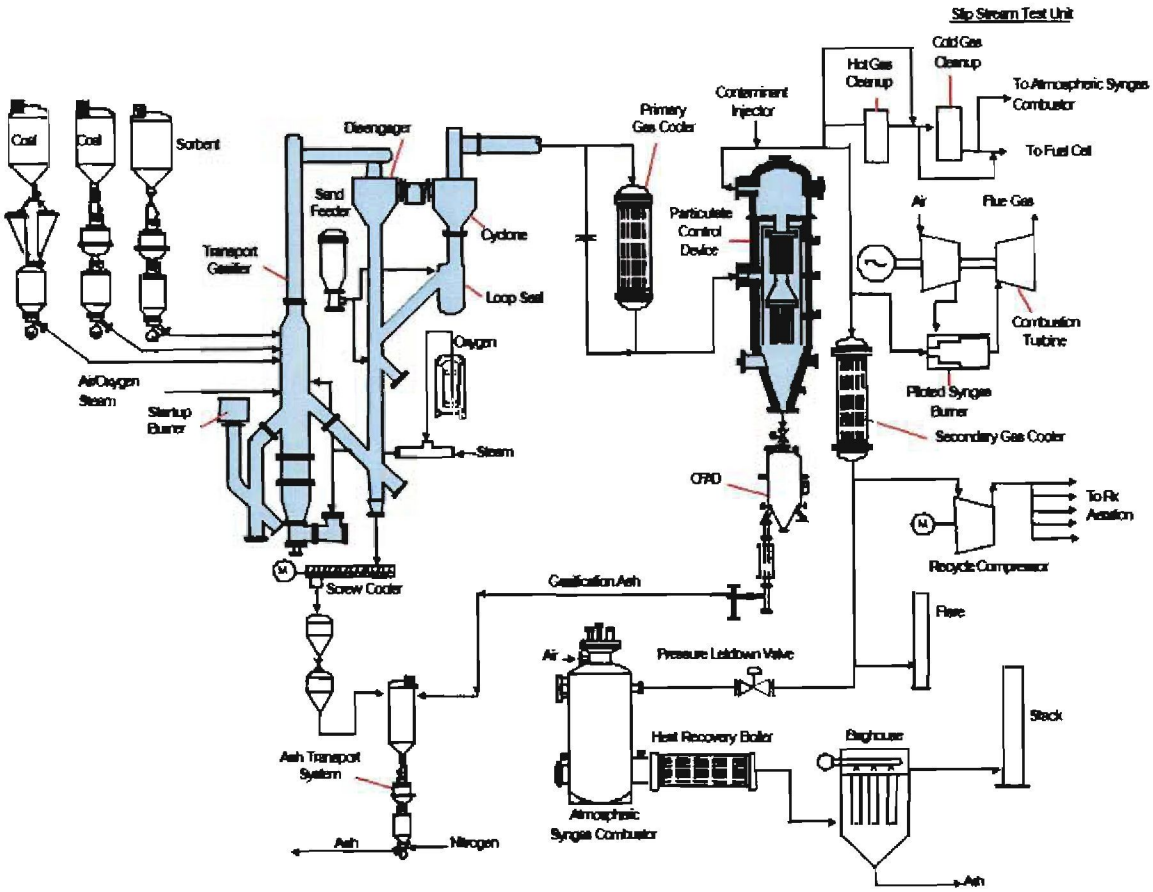

Figure 1.4: PSDF gasification process diagram [Guan et al., 2007].

TDA Research Inc. is developing a warm-gas cleanup process where H_2S is oxidised with small amounts of air (or O_2) to elemental sulphur in-situ without hydrogen consumption. Simultaneously, Hg is removed by reacting it with liquid elemental sulphur to form stable HgS. In the work conducted at TDA, a catalyst (activated carbon) has been developed that can convert H_2S to sulphur at temperatures ranging from 110 to 220 °C with essentially no H_2 oxidation [Vidaurri et al., 2007; Gardner et al., 2002; Dalai and Tollefson 1998]. While the focus of the work done by the TDA Research Inc. is the development of the H_2S oxidation catalyst, their overall process consists of several additional units, as shown in the process flow diagram in figure 1.5.

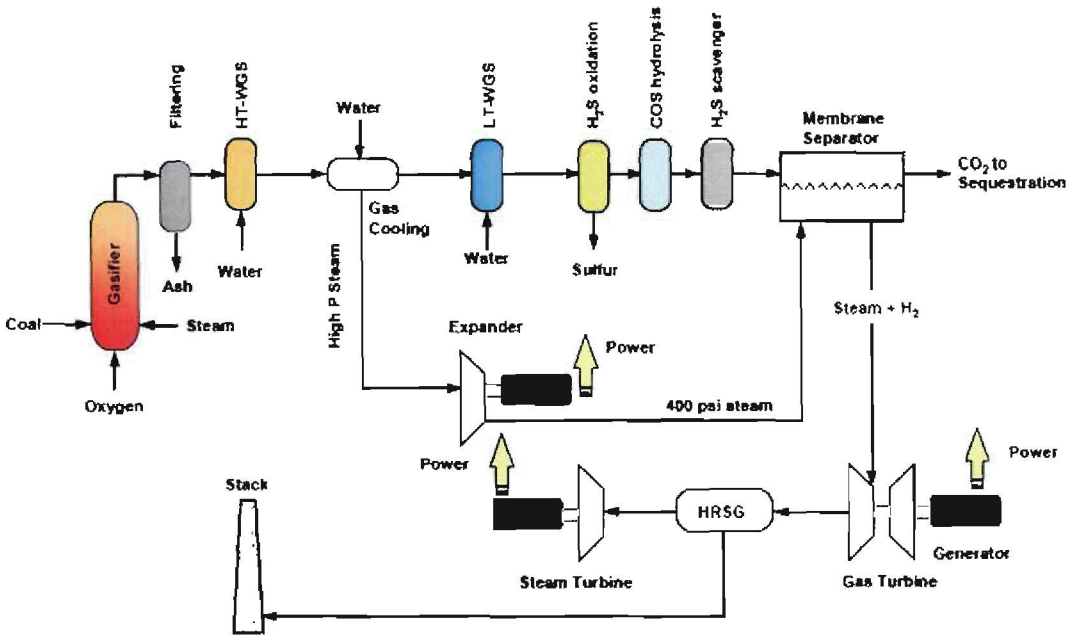

Figure 1.5: Schematic of TDA multi-contaminant warm gas cleanup process for IGCC [Vidaurri et al., 2007]

In the process flow diagram shown in figure 1.5, the main steps are 1) coal gasification, 2) hot particulate filtering, and 3) intermediate gas cooling from 815 to 315 °C (used to generate high pressure steam for power), 4) high-temperature water gas shift (inlet at 315°C), 5) further gas cooling to 250 °C for low-temperature water-gas-shift (additional steam is generated), 6) direct oxidation of H_2S into sulphur and water with minimal COS formation, 7) COS hydrolysis to convert the small amounts of COS that are inevitably formed back into H_2S for scavenging by 8) an H_2S scavenger that is used as a tail gas polisher, and finally 9) a membrane to separate H_2 from CO_2. The H_2 stream with steam is sent to the turbines with the CO_2 sent for sequestration.

TDA's catalysts oxidises H_2S into sulphur and water without any significant reduction in the H_2 content of gas and without any SO_2 formation. Also, because elemental

sulphur is formed, it reacts with Hg vapour to form stable HgS. The HgS is concentrated in the recovered sulphur and can be landfilled. In addition to Hg sequestration, equilibrium calculations suggest that As, Se, and Cd can also be removed with >90 % efficiency by reaction with sulphur to form stable sulphides [Vidaurri et al., 2007].

1.6 Options for H_2S emission reduction from gasification plants

The reduction of H_2S emissions from gasification plants is becoming crucial as environmental pressures on coal gasification plants increase. Several alternatives to reduce H_2S emissions exist, and are discussed further in this section.

1.6.1 Sulpholin process for sulphur production

In the Sulpholin process the H_2S is recovered and converted to elemental sulphur by means of chemical absorption, flotation, decanting and melting processes, as shown in figure 1.6 [Deberry, 1998]. The molten sulphur is then taken to the granulation plant, to convert it into granules in which form it can be transported to the clients. Some of the sulphur is sold in the liquid form. During the sulphur recovery using the Sulpholin process, sodium sulphate is formed as a by-product. The salt is recovered via a bleed stream from the main process, concentrated, purified and sold.

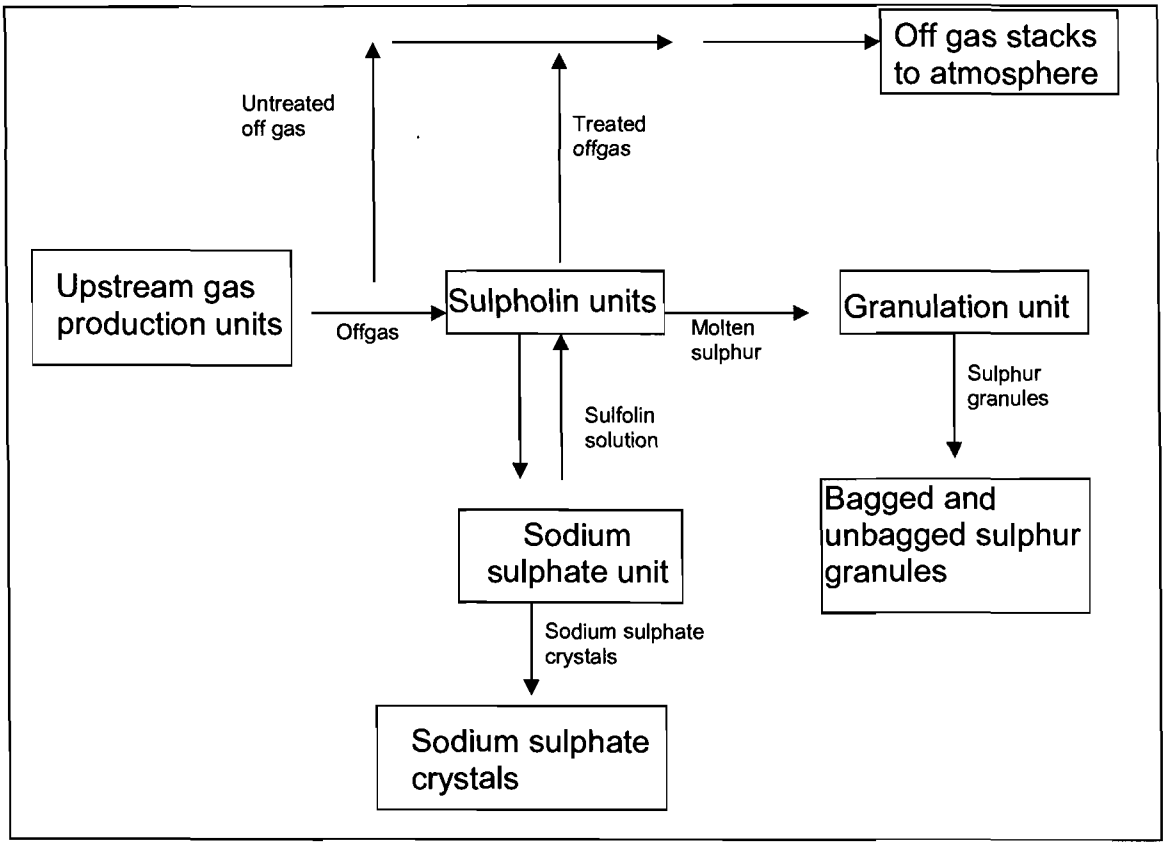

Figure 1.6: Schematic representation of a Sulpholin plant for sulphur recovery and sodium sulphate production [Vermaire et al., 1988; Deberry, 1998].

1.6.2 Coal destoning for sulphur removal

Coal destoning involves the physical removal of sulphur-bearing minerals associated with rock fragments, from coal before gasification. Most of the sulphur in South African coals is present in the form of pyrite, and is more predominant in particles with a higher ash (stone) content. These particles are usually higher in density than "clean" coal particles. The difference in density makes it possible to separate the high-ash (sulphur-rich) coal from cleaner coal by some physical separation methods [Keyser et al., 2001].

The layout of the process is shown in figure 1.7, where the coal is first subjected to coal screening, after which physical separation is done. Various processes are used for density separation, with the most common ones being jigging and dense medium separation. Jigging involves the stratification of a coal, based on density, by pulsating the bed with water. The coal particles that accumulate on the top layers are separated from the lower (refuse) layers. Dense medium separation processes most commonly use cyclones or baths to separate heavier particles from lighter ones, using magnetite or ferrosilicon as a medium [England et al., 2002].

It has been proven that the process of coal destining of coarse coal can achieve more than 30% sulphur removal; however, some of the carbon is lost through the process [Keyser et al., 2001]. Disposal of the discard product also poses other environmental concerns related to toxic substances in the discards that can be exposed to the atmosphere. This makes coal destoning unattractive since it cannot remove included pyrite particles or cleats as well as organic sulphur.

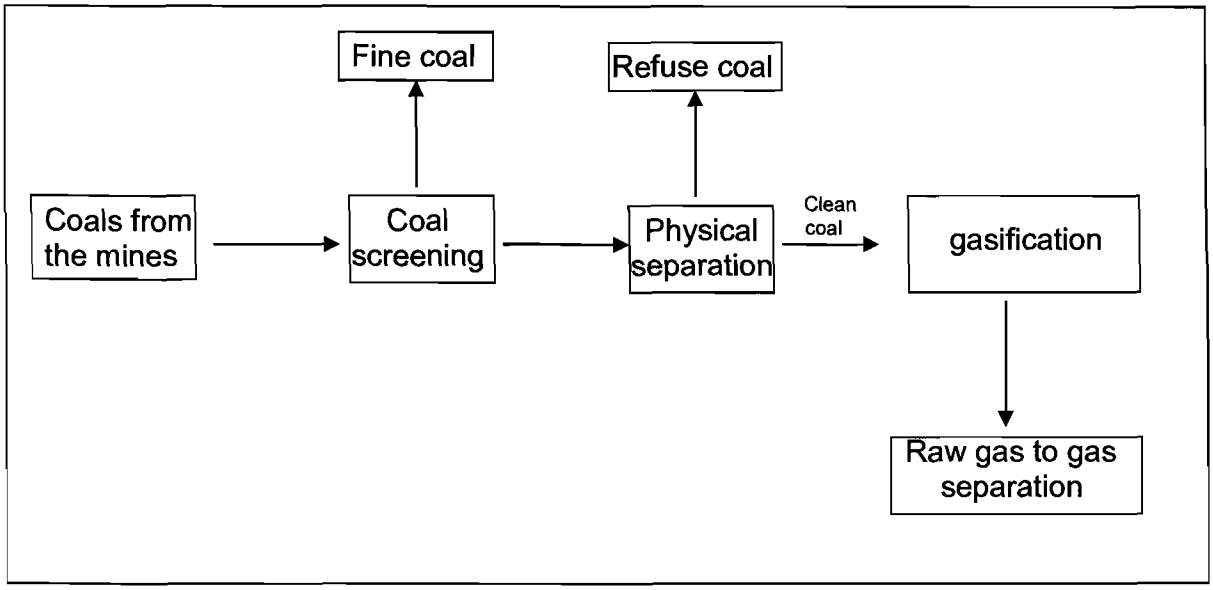

Figure 1.7: Coal destoning for sulphur removal before the gasification process.

1.6.3 Sulphur production by chemical absorption

Chemical absorption, as illustrated in figure 1.8, involves the reaction of offgas constituents with chemical solvents. Amines are the most common solvents used for acid gas removal and selective amines such as methyl diethanolamine (MDEA) can be used to selectively remove H_2S from the offgas stream.

The H_2S-rich solvent stream is regenerated, by breaking of the chemical bonds and steam stripping of newly formed compounds, producing a concentrated H_2S stream with about 15 % H_2S. This stream can be further concentrated to about 60 % H_2S in a gas enrichment unit, through removal of CO_2. This stream can then be used as a feed to the sulphur production unit of a Claus-type process. In this process H_2S is combusted with air to form SO_2. The SO_2 and the remaining H_2S are combined in catalytic reactors to form elemental sulphur. The sulphur product can then be granulated and sold.

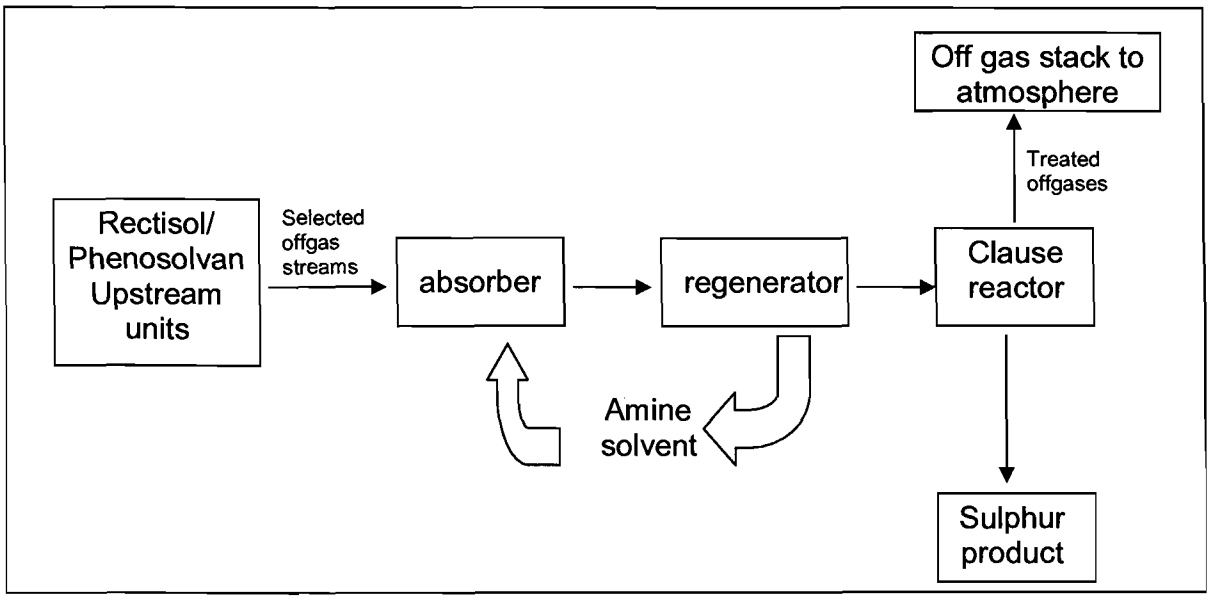

Figure 1.8: Sulphur production by chemical absorption.

1.6.4 Sulphuric acid production

The conversion of H_2S to sulphuric acid is a proven and commercially available technology. The process involves incineration of H_2S to form SO_2, as shown in figure 1.9. This gas is then processed in a physical absorption unit, producing a concentrated SO_2-bearing gas, which is then sent to the acid plant section. The acid plant utilises steam to produce sulphuric acid.

The SO_2 feedgas is converted to SO_3 inside the SO_2 converter. The SO_3 reacts instantly with the moisture to produce sulphuric acid in the vapour phase. The process is to an extent determined by temperature. Liquid acid is subsequently formed by condensation of the H_2SO_4 vapour and not by absorption of the sulphur trioxide in concentrated sulphuric acid, as is the case with contact processes based on dry gases. The process is known as a wet sulphuric acid process.

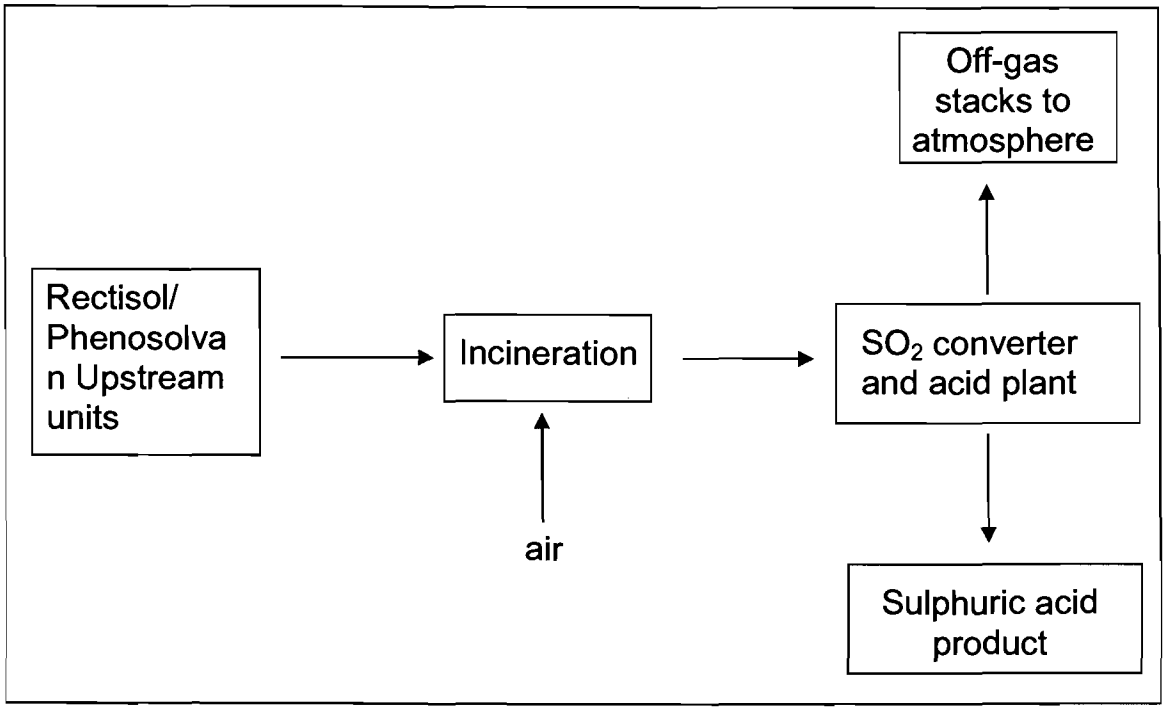

Figure 1.9: Sulphuric acid production from H_2S.

H_2S can also be used for the manufacture of inorganic sulphides, thiophenes, thiols, thioaldehydes, and thioketones. These processes are characterized by high capital costs with market constraints for the products.

1.7 Previous work done on sulphur capturing during coal processing

The use of calcium-based sorbents for flue gases and fuel gas desulphurisation has been widely researched and reported by various authors [Ulerich, 1980; Widemann and Boller, 1990; Zhang et al.2002; Crnkovic, 2006]. The process is mainly employed for combustion applications as well as for fluidised gasification processes. In a paper by Zhang et al., [2002], the use of a limestone co-feed with coal for reduction of SO_2 emission was reported. In the study, a SO_2 removal efficiency of up to 80% was reported using a drop tube-furnace [Zhang et al., 2002]. The practice of adding limestone and/or dolomite with the feed for sulphur emission reduction is being researched and used worldwide. In papers by Crnkovic [2006], Ulerich et al. [1980], and Wiedemann and Boller, [1990], dolomite and limestone were used to study SO_2 sorption onto Ca in limestone and dolomite. The processes utilise the calcium oxide which reacts with SO_2 leading to the formation of $CaSO_4$ as well as gypsum ($CaSO_4.2H_2O$) from 700 °C [Zevenhoven and Kilpinen, 2005].

In papers by Sotichos, [1998], Saxena et al., [1981], and Haji-Sulaiman et al., [1990], the use of limestone and dolomite as a sorbent with feed coal for high-pressure fluidised combustion was illustrated. The process involves the reaction of calcium oxide with SO_2 in the presence of O_2 to form $CaSO_4$ [Sotichos, 1998; Saxena et al., 1981]. Mathematical models for dolomite and limestone absorption of SO_2 through

calcium reactions have been developed by various authors [Bethell et al., 1973; Chen and Saxena, 1977].

The use of calcium-based sorbents for H_2S emission reduction in the fluidised-bed gasification process has been widely research and reported. In papers by Hu et al.[2006] and Maes et al.[1997], both limestone and dolomite were employed for sulphur emission reduction from a pressurised fluidised-bed gasification system. In the system, the CaO produced from limestone and dolomite reacts with the produced H_2S to form CaS, which needs to be oxidised to form $CaSO_4$ for disposal purposes [Hu et al., 2006; Maes et al., 1997]. In a paper by Abbasian et al. [1990], the kinetics of the reaction between the sulphur in coal and calcium in dolomite and limestone was reported.

The amount of work done and reported in literature on sulphur capturing is limited to the use of Ca-based sorbent for flue gases and fuel gases desulphurisation for fine coal combustion applications, as well as for fluidised bed applications. There is limited in-situ sulphur capturing work reported in literature where lump coal is used during fixed bed gasification process. In the study undertaken and reported in this thesis, the possibility of capturing sulphur in-situ through injection of the SO_2 into a packed coarse coal bed under controlled conditions, simulating various zones of a fixed-bed gasification process, was investigated. The objective of this study was to utilise the high-temperature transformation products of limestone and dolomite in the coal for in-situ capturing of the injected sulphur in the form of SO_2.

Chapter 2

Experimental Procedures

This chapter covers the procedures that were used to carry out the experimental work. Sample analysis as well all sample characterisation techniques employed are discussed in this chapter.

The hypothesis of the study is that sulphur emissions from a fixed-bed gasification process can be reduced by in-situ sulphur capturing by the high temperature transformation products of coal minerals. This will give rise to sulphur reporting to the ash as disposable sulphates, instead of it being emitted to the raw gas stream. To test this hypothesis, three separate approaches were adopted for the study; these are:

- Investigation of sulphur behaviour in a commercial-scale fixed-bed gasifier
- Laboratory-scale tests of sulphur capturing in a laboratory-scale furnace; and
- Pilot-scale test of sulphur capturing in an air blown pipe reactor.

2.1 Sulphur behaviour in a Sasol-Lurgi gasifier.

In this section experimental procedures used for studying the sulphur behaviour occurring axially within the Sasol-Lurgi fixed-bed dry-bottom gasifier, are described. The Sasol-Lurgi fixed-bed gasification system was selected to study the sulphur behaviour, as it is one of the commercial fixed-bed gasifier in operation. Methods

employed for sample acquisition, sample preparation and characterisation are described in this section.

2.1.1 Sample acquisition and preparation for analysis

Coal, char and ash samples of gasifier turnout test material were taken from a Sasol-Lurgi gasifier, using a modified sampling procedure that was employed for the work reported by Bunt [2006]. The gasifier turnout method was initially developed and used earlier for gathering of turnout samples from a Sasol-Lurgi Mark IV gasifier in Sasolburg [Glover, 1988 Part 1 and 2]. It was also used on an Indian pilot-scale gasifier, the procedure being published by Krishnudu et al., [1989 a and b].

A total of 32 samples were taken from the top to the bottom of a gasifier using a 3 m^3 sampler (front end loader shovel) by turning the samples out through the gasifier grate, as described in Bunt [2006]. However, only five samples were chosen for monitoring of the sulphur behaviour through the gasifier. The samples were taken from the different reaction zones of the gasifier as indicated in figure 2.1. The selected representative samples (A, B, C, D and E) were crushed to obtain 100% <1 mm particles.

Sample Number	zone
E	drying
D	pyrolysis
C	gasification
B	combustion
A	Ash bed

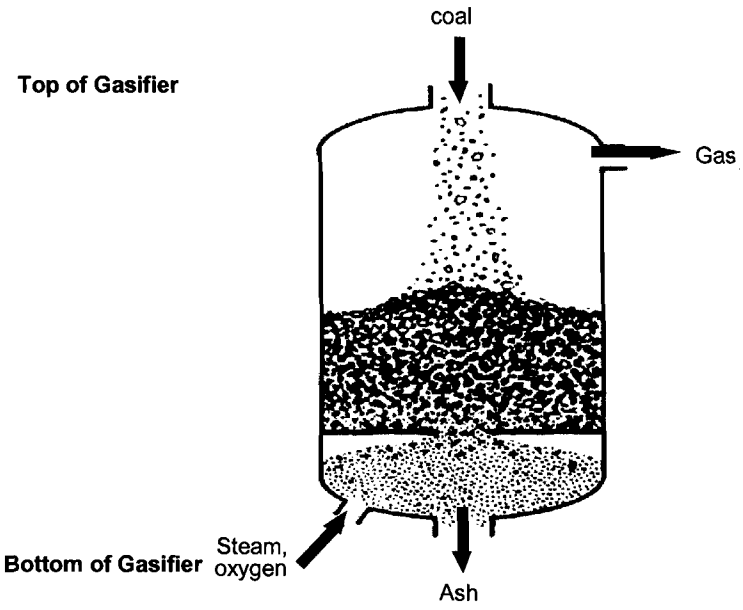

Figure 2.1: Schematic representation showing sampling zones.

2.1.2 Sample characterisation

The turnout samples were prepared by crushing to -1 mm size and split to get representative samples for different characterisation techniques that are discussed in this section. These include elemental analysis and mineralogical analysis.

2.1.2.1 Chemical analysis

Elemental analysis (C, H, N, S and O) was carried out to determine the elements in the various samples; especially the amount of total sulphur, used to determine the extent of sulphur capturing. X-ray fluorescence analysis was conducted to determine the elemental composition of the ash samples.

2.1.2.1.1 Sulphur analysis (Ultimate analysis)

The total sulphur content was determined from the ultimate analysis, which also indicates the content of carbon, hydrogen, nitrogen, and oxygen by difference. The South African Bureau of Standards, Coal and Mineral Technologies (CMT) laboratories determined the elements carbon, hydrogen and nitrogen using the ASTM D5373 method [ASTM D5373, 2002]. Total sulphur was determined using the ASTM D4239 method, and oxygen was calculated by difference.

2.1.2.1.2 X-ray fluorescence (XRF)

XRF is used to determine the elemental composition of the ash with the elements reported as oxides. This technique is widely used together with XRD results for confirmation of the results obtained from XRD analysis [Pearce et al., 1990]. The prepared samples were submitted to Setpoint laboratories for X-ray fluorescence (XRF) analysis. An XRF spectrometer (ARL9800XP (SIM-SEQ)) at Set Point laboratories was used to investigate the characteristic spectra of elements present in the solid sample. For quantification analysis, the intensity of characteristic line of the element analysed was measured.

2.1.2.2 Mineralogical analysis

Mineralogical analysis was carried out to investigate the mineralogy changes in coal as it is exposed to the conditions in the gasifier. The techniques used include sulphur forms determination, XRD, and CCSEM analysis.

2.1.2.2.1 Sulphur forms

The samples were submitted to CMT laboratories for sulphur forms analysis. Sulphur forms analysis includes determination of the following: total sulphur determined using ASTM D4239 [ASTM D4239, 2002], organic sulphur, mineral sulphur and sulphate sulphur analysis, all determined using ISO 157 [ISO 157, 1996].

2.1.2.2.2 X-ray diffraction (XRD)

X-ray analysis is a well established method for process and quality control in the coal industry. X-ray diffraction (XRD) is used to distinguish between structural and phase properties of compounds, where X-ray fluorescence (XRF) is used to determine the elements in the compounds. The crushed representative samples were submitted to the Sasol Technology R&D division (Materials Characterisation Group) for qualitative and quantitative X-ray diffraction (XRD) analyses. The XRD system used to analyse the samples is the X'Pert PRO PANalytical (Philips) – Unit 2. Phase quantification was performed by Rietveld analysis using Siroquant software. The following experimental parameters were used during the analysis of the samples:

Goniometer:	PW3050/60 (T / T configuration)
X-ray detector:	X'Celerator (Solid State, RTMS)
X-ray tube:	Cobalt target, ceramic, LFF-type; λ Co Kα = 1.7889 Å
Voltage:	40 KV
Amperage:	40 mA

Prog. Divergence Slit: 1.0° (fixed)

Anti-scatter Slit:	2.0°
Scan from:	5° 2T
Scan to:	135° 2T
Soller slits:	0.02 Rad
Scanning:	Continuous
Duration of scan:	6 - 14 hrs

2.1.2.2.3 Computer controlled scanning electron microscope analysis (CCSEM)

Computer controlled scanning electron microscopy (CCSEM) has been widely used as a tool to study mineralogy in coal and coal ash, where minerals in crystalline and glassy phases are identified and quantified [van Alphen and Falcon, 2000; Zhang et al., 2002; Matjie et al., 2006; van Alphen, 2007]. All the prepared samples were submitted to van Alphen Consultancy for CCSEM analysis. Back-scattered electron (BSE) images of pyrite transformation were also recorded using CCSEM.

2.2. Sulphur capture in a fixed coal bed in a laboratory-scale furnace

In this section all the experimental procedures employed for the evaluation of the extent of sulphur capturing in a laboratory-scale furnace, are discussed. Characterisation techniques employed for the coal and resulting ash that were carried out are also discussed.

2.2.1 Sample preparation

The bench-scale experiments were conducted using one of the coals used at the Secunda Gasification plant in South Africa. The coal used is a Medium C rank bituminous coal, from a Highveld mine in South Africa, which will be referred to as Coal A. Coal A was used to test the hypothesis for all the experimental conditions tested and reported in this thesis. The coal was crushed and screened to a particle size of 4 mm to 13 mm for testing. This particle size was found to be the optimum size that could be used for the furnace employed.

2.2.2 Sulphur-capture reactions in the laboratory-scale furnace

The sulphur-capture experiments were conducted in a laboratory-scale furnace as shown in figure 2.2. The furnace consists of a lined steel jacket that has an 8 cm internal diameter and 30 cm height, where 300 g of coal is packed in the furnace with air flow at 5 litres per minute and SO_2 flow at 40 cm^3 per minute. The flow rates were found to be optimum conditions for the reaction setup employed as well as for the conditions tested.

The furnace was operated by firstly loading the coal and allowing the flow of air while heating up the elements to the required temperature. SO_2 flow was started as soon as the internal temperature of the furnace reached 600 °C. It was decided to start the flow of SO_2 at this temperature since the decomposition of $CaCO_3$ and $CaMg(CO_3)_2$ also starts to take place at these temperatures, as described under literature. The SO_2 flow was maintained until the internal temperature reached the

desired temperature. The reaction was then kept at the desired temperature for the desired period of time. Once the reaction time elapsed, the reaction was stopped by stopping both the air flow and the SO_2 flow. The reaction was left to cool down and the sample was collected for analysis.

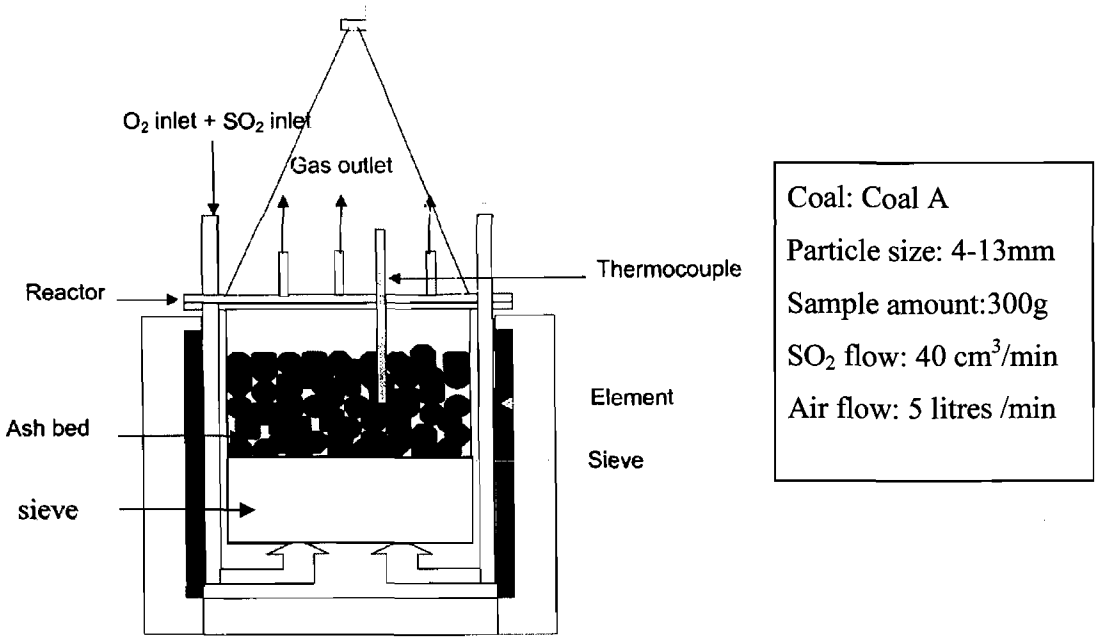

Figure 2.2: Laboratory scale furnace used for SO_2 experiments.

Different parameters, as listed in the following sections, were investigated for their impact on sulphur capturing in the coal bed. The parameters investigated include the effect of temperature, residence time, as well as monitoring of the SO_2 evolution from the reaction.

2.2.2.1 Effect of temperature

The impact of temperature on sulphur capturing in a coal bed under the conditions stated in section 2.2.2, was investigated. This was conducted by treatment of batch samples at various temperatures ranging from 900 to 1250°C, in increments of 50°C. These temperatures were chosen as they are within the range of temperatures experienced by coal at the combustion zone of a fixed-bed gasification process. At each temperature, blank reactions (without SO_2 flow) as well as reactions with SO_2 flow were conducted for comparison. Ash samples resulting from the reaction were taken and prepared for further analysis as described in section 2.2.3.

2.2.2.2 Effect of residence time

The effect of residence time was investigated by treatment of the coal samples at the temperature that was found to be optimal for sulphur capturing, as discussed in section 2.2.2.1. Batch samples were then treated at the fixed optimum temperature, while the time of reaction was set at 20 min, 40 min, 60 min, 80 min, 120 min and 240 min. The reactions were conducted for both the blank reaction (without SO_2 flow) as well as for reaction with SO_2 flow, for comparison purposes.

2.2.2.3 Monitoring of SO_2 emissions during the reaction

The monitoring of sulphur evolution and emission of the off-gas during the reaction was conducted by collecting the off-gas throughout the reaction, and scrubbing it in an aqueous water solution. The off-gas was collected by bubbling it through 20 ml of

distilled water, as illustrated in set-up in figure 2.3. The vacuum pump was used to create a positive pressure flow for collection of the off-gas from the furnace to the scrubbing water solution. The first sample was collected after a temperature of 600°C was reached, with subsequent samples collected in 10-min intervals. Each time a fresh 20 ml sample was used for bubbling the gas through and further analysis. Thereafter, the collected water solutions were then measured for their pH using a calibrated pH meter. Acid concentration determinations were conducted using the standard titration technique using a standardised solution of 0.02 M NaOH.

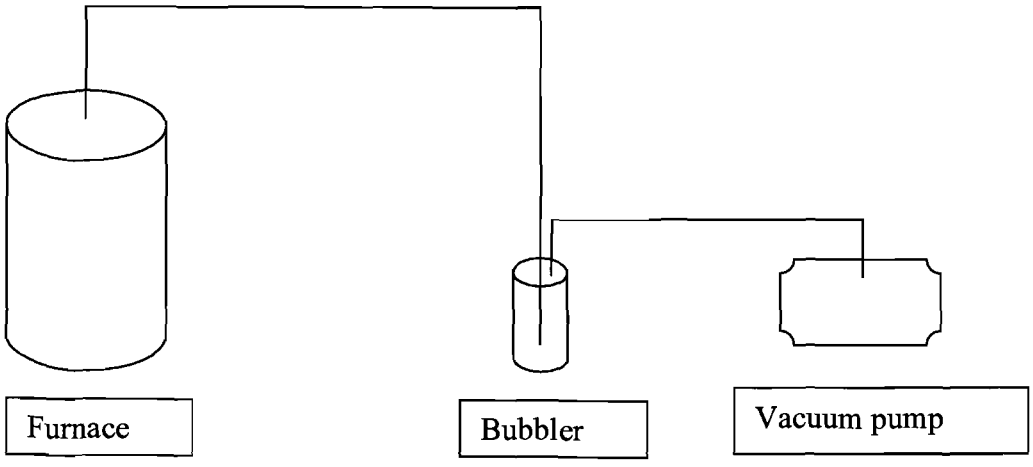

Figure 2.3: Set-up for the off-gas capturing.

2.2.3 Samples characterisation

The ash samples obtained from each of the experiments were subjected to different analyses and characterisation techniques, which included elemental analysis, physical analysis and mineralogical analyses.

2.2.3.1. Chemical analyses

Refer to section 2.1.2.1.1.

2.2.3.2 Effect of thermal exposure on the captured sulphur

The determination of the rate of loss of sulphur at various temperatures was conducted by treating the samples with the highest SO_2 capture, at elevated temperatures ranging from 1150 to 1350 °C, in increments of 50 °C, in a tube furnace. Air flow at 40 cm^3/min was maintained throughout the exercise to maintain an oxidising atmosphere. All of these samples were subjected to total sulphur analysis. The total sulphur data were then used to calculate the percentage sulphur permanently retained in each of the samples. This was done by comparison of the remaining sulphur after thermal treatment to sulphur in the starting sample.

2.2.3.3 Mineralogical analysis

Mineralogical analysis was conducted using XRD. The procedure is described in section 2.1.2.2.2.

2.3. Sulphur capture in a fixed coal bed in a pipe reactor

The description of the pipe reactor equipment and operation as well as the coal characterization techniques applied are discussed in this section.

2.3.1 Sample preparation

The feed coal used in this study was labelled coal A, the same coal used for the experimental work described in section 2.2. The coal that was used was prepared by screening and sizing according to the particle size distribution and masses shown in table 2.1. The fractions shown in table 2.1 were all mixed and homogenised before being loaded to the pipe reactor. The total mass loaded was 240 kg, as discussed in the section to follow.

Table 2.1: Feed coal particle size distribution of pipe reactor feed

Screen size (mm)	Mass (kg)	Fractional % retained
+75	21.12	8.80
+53	21.12	8.80
+ 37.5	36.96	15.40
+26.5	27.60	11.50
+19	28.80	12.00
+13.2	33.60	14.00
+9.5	23.52	9.80
+6.7	24.72	10.30
+4.75	10.56	4.40
+3.35	5.52	2.30
+2.36	1.92	0.80
+1.70	0.96	0.40
-1.70	3.6	1.50
Total	240	100.00

2.3.2 Sulphur capture reaction in a pipe reactor

The pipe reactor consists of a lined steel jacket with outside diameter of 0.8 m and an inner diameter (ID) of 0.4 m and 3 m in length. The refractory lining is approximately 0.2 m thick. A high-strength, abrasive-resistant alumina lining with maximum operating temperature of 1700 °C covered the inside of the pipe reactor. The reactor is designed to burn coal particles in an air atmosphere at atmospheric pressure, and temperature is controlled with nitrogen. The reactor is equipped with thermocouples for temperature measurements, pressure transmitters for pressure measurements and rota meters to control the air, SO_2 and nitrogen flow to the reactor (Photograph 2.1).

Photograph 2.1: The pipe reactor combustor unit.

The required amount of 240 kg of coarse coal was mixed and loaded into the pipe reactor using buckets to minimise segregation of the packed coal bed. The bed was packed to a height of 2 m using the 240 kg coal increment. The bed was heated for an hour with a gas burner to get the coal to a temperature where it will burn in an air atmosphere. After the hour, the gas burner was turned off and the air flow was set to 25 Nm^3/h (normal cubic metres per hour) to allow the coal to ignite. Upon reaching a bottom thermocouple temperature of 600 °C, the air flow was increased to a flow of 35-45 Nm^3/h until the required temperature of 1250 °C was reached.

The air flow was then maintained at approximately 35 to 45 Nm^3/h. The bed temperature was controlled by adjusting the air and nitrogen flow through the bed. The ash bed temperature was controlled at 1250 °C (maximum) for all runs (thermocouples 20 to 16, as shown in photograph 2.1) and the temperature, pressure and flow to the reactor were logged for each run with a Delta V data logging system. For blank reactions without SO_2 flow, the reactor was allowed to burn for approximately 18 hrs before it was cooled down with nitrogen to 25 °C, overnight.

For reactions with a SO_2 flow, the pipe was heated in air for 14 hours to allow the ash bed (thermocouple 16) temperature to reach 1250 °C. Then the SO_2 flow was switched on at 40 ml/min for 2 hrs, after which it was stopped and nitrogen was used for overnight cooling down of the reactor to 25 °C.

After cooling, the combustor was tilted onto its side and opened up like a coffin to allow sample taking and visual inspection of the bed profile (Photograph 2.2). Seven equal-sized fractions were dissected from the entire bed (sample 1 at the top of the

bed, and sample 7 the ash bed sample at the bottom of the reactor). These were analysed further.

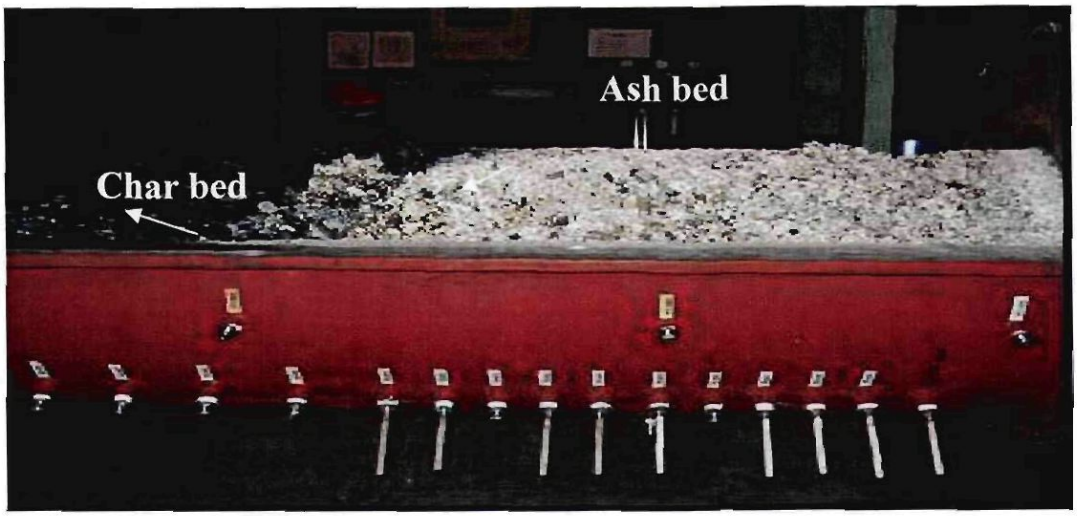

Photograph 2.2: The bed profile of the pipe reactor.

2.3.3 Sample analysis

The seven fractions taken after a single run were subjected to sample preparation for various analyses including: elemental analysis, physical analysis and mineralogical analysis. The fractions were all crushed to -1 mm, followed by splitting to take smaller samples for analysis. All the analysis conducted on the samples as described in section 2.2 were also conducted on the pipe reactor samples.

Chapter 3

Results and Discussion

Results obtained from all of the experimental work reported in this thesis, as well as from all of the characterisation techniques employed in the study, are presented and discussed in this chapter. The chapter is divided into three sections, covering results obtained for sulphur monitoring within a commercial gasifier as well as sulphur capture experiments at laboratory-scale reactor and pilot scale for comparison purposes. The three sections that make up this chapter are:

- Sulphur behaviour in a Sasol-Lurgi fixed-bed gasifier
- Sulphur capture in a fixed coal bed in a laboratory-scale furnace; and
- Sulphur capture in a fixed coal bed in a pipe reactor

Sulphur behaviour in a fixed-bed gasifier was evaluated using the gasifier turnout approach used for the commercial fixed-bed gasifier, in this case a Sasol-Lurgi fixed-bed dry-bottom gasification system. Sulphur capture reactions were conducted on a laboratory-scale furnace as well as pilot scale pipe reactor for comparison and verification of the results.

3.1 Sulphur behaviour in a Sasol-Lurgi gasifier.

This section covers results and discussion of the results obtained for the evaluation of the sulphur behaviour axially within a Sasol-Lurgi fixed-bed gasifier.

3.1.1 Chemical analysis

Total sulphur was obtained from the ultimate analysis and the forms of sulphur were determined to study the sulphur behaviour within the gasifier. XRF results are presented for sulphur, and the results for all of the other elements are given in the appendix.

3.1.1.1 Sulphur analysis

The amount of sulphur in each of the fractions sampled was determined from the total sulphur content and calculated from the mass of the sample. The amount of sulphur in each of the fractions is indicated in table 3.1. From the table it can be deduced that the amount of sulphur tends to decrease from the top sample (E), where there was about 11 kg of sulphur per 516 kg of coal (equivalent to 11 kg of sulphur per 516 kg of ash), all the way to the sample at the bottom of the gasifier, sample A, where there is about 3 kg of sulphur per 860 kg of ash.

Most of the sulphur loss seems to be taking place in the area of the top two samples; which are in the drying and pyrolysis zones, samples E and D. This suggests that most of the sulphur evolution takes place in the top half of the gasifier where reducing conditions prevail, in agreement with findings by Garcia-Labiano et al. [1995].

Table 3.1 Mass of sulphur in the different gasifier turnout fractions

sample	Zone where sample was taken	Mass of coal (kg)	sulphur %	mass of S (kg)
A	Ash bed	859.67	0.39	3.35
B	Combustion	785.67	0.45	3.54
C	Gasification	736.33	0.85	6.26
D	Pyrolysis	570.67	1.11	6.33
E	Drying	515.67	2.12	10.93

The graph in figure 3.1 shows the distribution of the different sulphur forms from the top of the gasifier to the bottom.

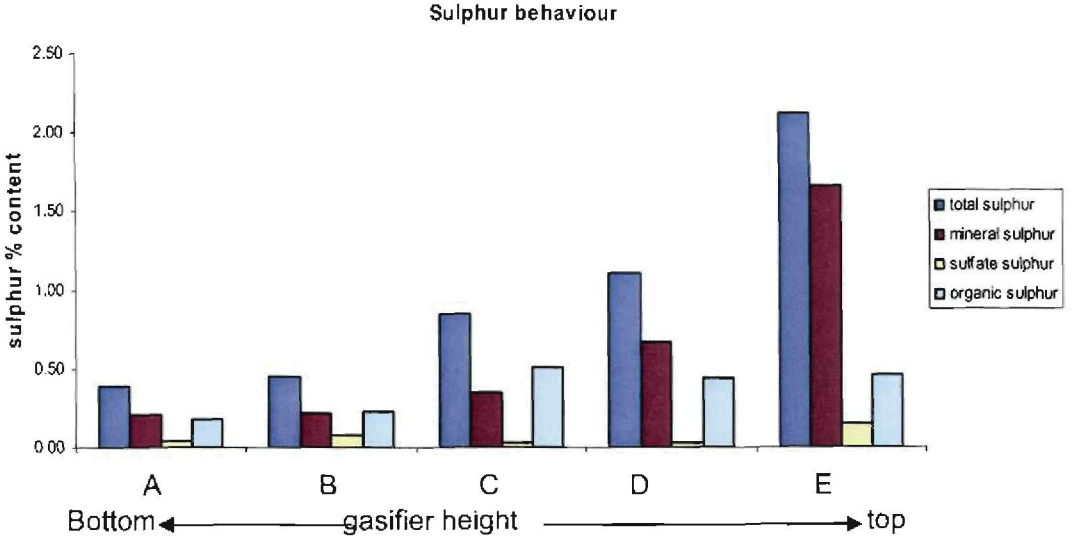

Figure 3.1: Forms of sulphur from the top to the bottom of the gasifier

From the graph in figure 3.1 it can be deduced that the total sulphur content decreases from the top of the gasifier to the bottom of the gasifier, in agreement with the results shown in table 3.1. It can be deduced that the total sulphur content is mainly made up of mineral sulphur for samples E, which is coal sample at the top of the gasifier. The loss of the mineral sulphur within the gasifier was found to correlate to the loss of the total sulphur, as shown in figure 3.2, where a linear correlation with R^2 of 0.97 was

obtained. This also suggests that for the coal used for this gasifier, mineral sulphur is the predominant form of sulphur in the feed coal and its behaviour influences the total sulphur behaviour throughout the gasifier.

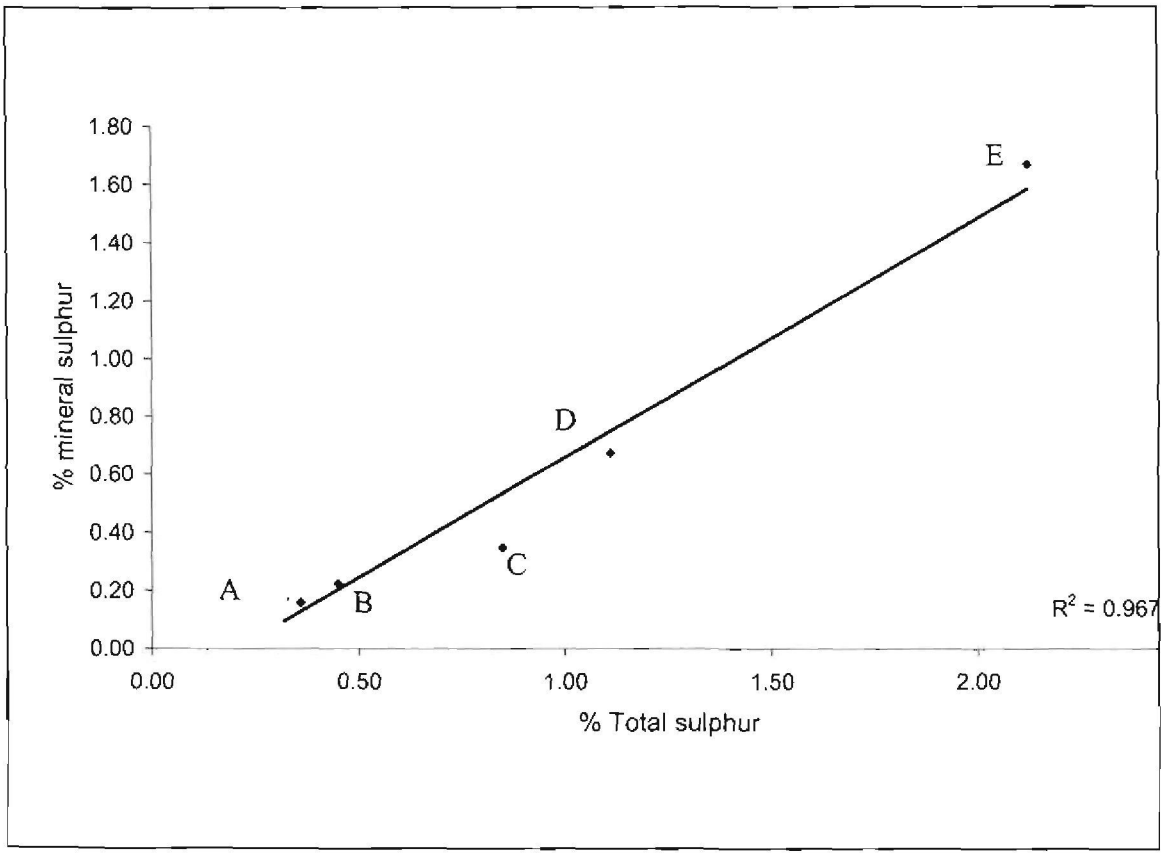

Figure 3.2: Correlation between total sulphur and mineral sulphur

A notable loss of mineral sulphur was observed with the first two samples from the top (E and D), which are the samples in the drying and pyrolysis zones. This loss in total sulphur and mineral sulphur can be attributed to the decomposition of pyrite to form pyrrhotite and H_2S. The reaction, shown in equation 6, has been reported and proven by various authors to be taking place from 500 °C in a reducing atmosphere in the presence of hydrogen [Popiel et al., 1990; Coburn et al., 1991; Ripley et al., 2000; Lambert et al., 1998].

$$FeS_2 + H_2 \rightarrow Fe_{(1-x)}S + H_2S \qquad 6$$

On the other hand, the organic sulphur does not show any major changes in the top half of the gasifier, with a slight relative increase when compared to the total sulphur amount in pyrolysis zone. This increase is an artifact of the decrease in the mineral sulphur that decreases the total sulphur. It thus seems that the amount of organic sulphur remains constant in the pyrolysis zone. This is in agreement with work published earlier by Gryglewicz and Jasieńko [1992] and Gryglewicz [1995], where organic sulphur enrichment was reported to take place during coal pyrolysis at temperatures of up to 700 °C, which corresponds to a temperature representing the start of the gasification zone. In these papers, during coal pyrolysis up to 1700 °C in a fixed bed in an atmosphere of the evolved gases, an enrichment of the organic sulphur was observed between 300 to 600 °C. This was observed to be taking place when conversion of pyrite into ferrous sulphide occurred, which was accompanied by accumulation of organic sulphur in the char [Gryglewicz and Jasieńko, 1992; Gryglewicz, 1995].

A slight decrease in the organic sulphur is noted in the bottom half of the gasifier, with some of the organically associated sulphur still identified in unburned carbon in the carbonaceous shale in the ash sample. A further decrease in the amount of mineral sulphur is noted in the bottom half of the gasifier. This further reduction in mineral sulphur can be due to further decomposition of some of the pyrrhotite leading to the formation of more H_2S and metallic iron that will react with oxygen further down in the gasifier in the presence of oxygen to form various oxides of iron as presented in the proposed equation 7.

$$5Fe_{(1-x)}S + 9O_2 \rightarrow FeO.Fe_2O_3 + Fe_2O_3 + 4SO_2 + SO_3 \quad 7$$

Pyrrhotite transforms to metallic iron (which in turn transforms mainly to hematite and magnetite) and mainly sulphur dioxide and sulphur trioxide at temperatures higher than 700°C under oxidising conditions in the late gasification zone and the combustion zone, which will correspond with the loss of total sulphur from sample C to sample B [Guilin et al., 2006].

3.1.1.2 X-ray fluorescence analysis

The normalised sulphur content for coal and ash samples determined by XRF are given in table 3.2. The table containing the detailed elemental composition is presented in appendix A as table A.2. From table 3.2, it can be deduced that there is a decrease in the amount of sulphur determined through XRF analysis as SO_3 as the coal moves through the gasifier from the top sample (Sample E) all the way to the bottom sample (Sample A). From these results it can also be deduced that most of the sulphur reduction takes place between the top three samples, which are in the drying, pyrolysis and gasification zones. This is indicative of the regions of major loss of sulphur from the coal as it is exposed to the conditions in the gasifier, which follows the same trend as that observed for total sulphur based on ultimate analysis results (table 3.1).

Table 3.2: Elemental analysis by XRF, showing SO_3 results.

Sample number	A	B	C	D	E
Zones where samples were taken	Ash bed	combustion	gasification	pyrolysis	drying
% SO_3 (XRF, normalised in ash,)	0.25	0.73	2.39	4.29	5.61

3.1.2 Mineralogical analysis

In this section results from the XRD and CCSEM analysis are presented and discussed. XRD was used for the identification and quantification of crystalline phases in the mineral matter of the coal and ash. CCSEM analysis was used for identification as well as quantification of all associated minerals as well as their modes of occurrence. The results from the CCSEM analysis include identification of phases within the glass phase.

3.1.2.1 X-ray diffraction

X-ray diffraction was used to monitor the behaviour of sulphur-bearing crystalline phases during coal gasification. The XRD analysis results obtained for the turnout samples are shown in table 3.3. From the results it can be deduced that sample E, which is the feed coal to gasification, consists mainly of kaolinite and quartz, with minor amounts of gorceixite, greigite, rutile, pyrite, calcite, aragonite, dolomite and muscovite.

As the temperature of the gasifier increases, minerals in the coal transform to form high-temperature transformation products. The presence of mullite, cristobalite, anorthite and diopside in some of the ash samples indicates that these minerals were derived from the mineral transformation at elevated temperatures during gasification, since these minerals were not present in the feed coal to generate the ash. Pyrite is observed in the first sample (Sample E) and transformed at elevated temperatures as the coal was exposed to higher temperatures in the gasifier. For the sake of brevity, discussion in this thesis is focused on the sulphur-bearing mineral transformation in all the samples.

Table 3.3: XRD results for the turnout samples (as received)

Minerals identified (%)	**A**	**B**	**C**	**D**	**E**
Zones where samples were taken	Ash bed	combustion	gasification	pyrolysis	Drying
Anorthite $[(Ca,Na)(Si,Al)_2O_6]$	18.1	7.7	1.8	0.4	n/d
α-Quartz $[\alpha\text{-}SiO_2]$	14.4	14.3	11.7	6.2	6.0
Mullite $[Al_6Si_2O_{13}]$	11.8	5.3	2.4	3.9	n/d
Cristobalite $[SiO_2]$	0.5	0.1	<0.1	n/d	n/d
Diopside $[Ca(Mg,Al)(Si,Al)_2O_6]$	<0.1	0.7	1.0	0.2	n/d
***Mayenite** $[Ca_{12}A_{114}O_{33}]$	0.3	n/d	n/d	n/d	n/d
Anhydrite $[CaSO_4]$	0.2	0.1	0.4	n/d	n/d
Muscovite $[KAl_2(Si_3Al)O_{10}(OH,F)_2]$	0.8	0.8	<0.1	1.2	1.1
Hematite $[\alpha\text{-}Fe_2O_3]$	0.3	0.2	<0.1	n/d	n/d
Magnetite $[FeFe_2O_4]$	0.2	0.3	n/d	n/d	n/d
Kaolinite $[Al_2Si_5(OH)_4]$	n/d	n/d	1.4	6.7	6.7
Calcite $[CaCO_3]$	n/d	2.6	3.4	1.5	1.2
Aragonite $[CaCO_3]$	n/d	n/d	n/d	1.0	1.2
Dolomite $[CaMg(CO_3)_2]$	n/d	n/d	n/d	2.4	2.0
Pyrite $[FeS_2]$	n/d	n/d	<0.1	0.2	0.4
Pyrrhotite $[Fe_7S_8]$	n/d	<0.1	0.4	n/d	n/d
***Greigite** $[Fe_3S_4]$	n/d	n/d	n/d	0.2	0.2
Rutile $[TiO_2]$	n/d	0.3	0.1	0.2	0.3
***Anatase** $[TiO_2]$	n/d	n/d	<0.1	n/d	n/d
***Gorceixite** $[BaAl_3(PO_4)PO_3OH)(OH)_6]$	n/d	n/d	n/d	0.2	0.2
Non-crystalline content (mainly, glass and/or carbon)	53.3	67.5	76.9	75.7	80.7

Note: * - possibility only; n/d – not detected

The graph in figure 3.3 shows the proportions of sulphur and iron-bearing minerals in the coal and ash samples analysed. The XRD results were normalised and calculated as the amounts of crystalline phases in mineral matter in the coal and ash samples.

The results as shown in figure 3.3 indicate the presence of pyrite in the feed coal (sample E) at the top of the gasifier. A decrease in the proportion of pyrite in the coal,

with an increase in temperature is noted as the coal is exposed to the conditions further downwards in the gasifier. Formation of anhydrite as well as pyrrhotite is noted in the third sample (C). Samples C, D and E are from the top half of the gasifier where reducing conditions prevail.

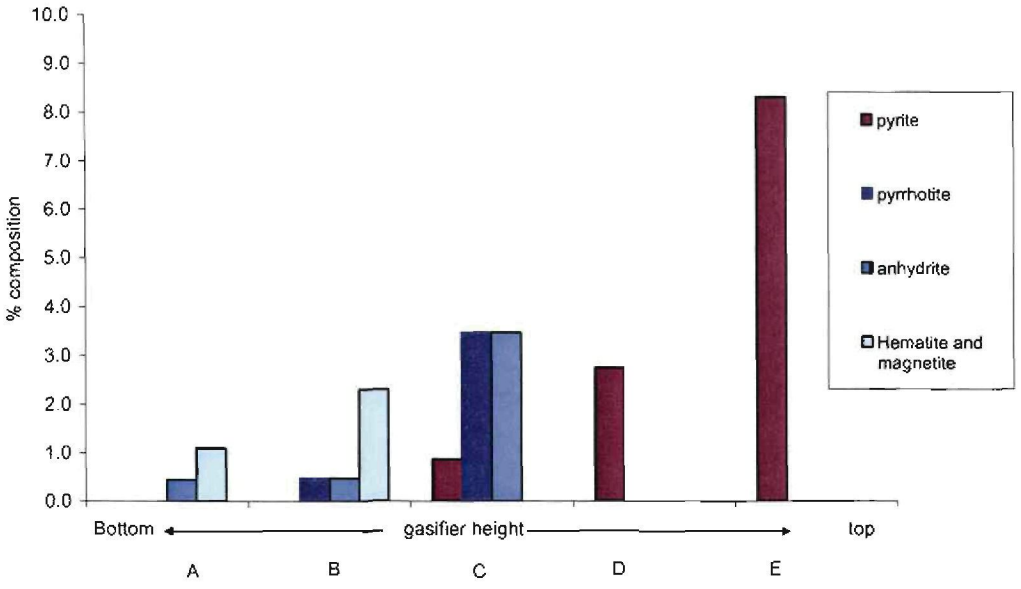

Figure 3.3: Sulphur- and iron-bearing minerals in coal and ash (based on XRD, normalised in crystalline matter in ash)

A decrease in the pyrite content is accompanied by the formation of pyrrhotite in sample C, which is in agreement with the results of the total sulphur content as well as the mineral sulphur analysis, and is also in agreement with equation 6. This suggests that the second and the third samples from the top of the gasifier were exposed to temperatures of more than 500 °C. This is in agreement with the observation by Bunt [2006] (figure 3.4) that the second sample (D) was taken from the pyrolysis zone where the particle surface temperature is about 800 °C. From figure 3.4 it can also be

deduced that the third sample (C) was taken further down at the start of the gasification zone where the particle surface temperature was 1000 °C.

The loss of pyrite is even more notable for the second sample (D) when compared to the third sample (C). In this region, sample D to sample C, from figure 3.1 it is noted that there is no major decrease in the amount of total sulphur, and yet figure 3.3 indicates a notable decrease in the amount of pyrite, leading to the formation of pyrrhotite. This suggests that the transformation of pyrite to pyrrhotite is predominant within this area of the gasifier. This is in agreement with equation 6.

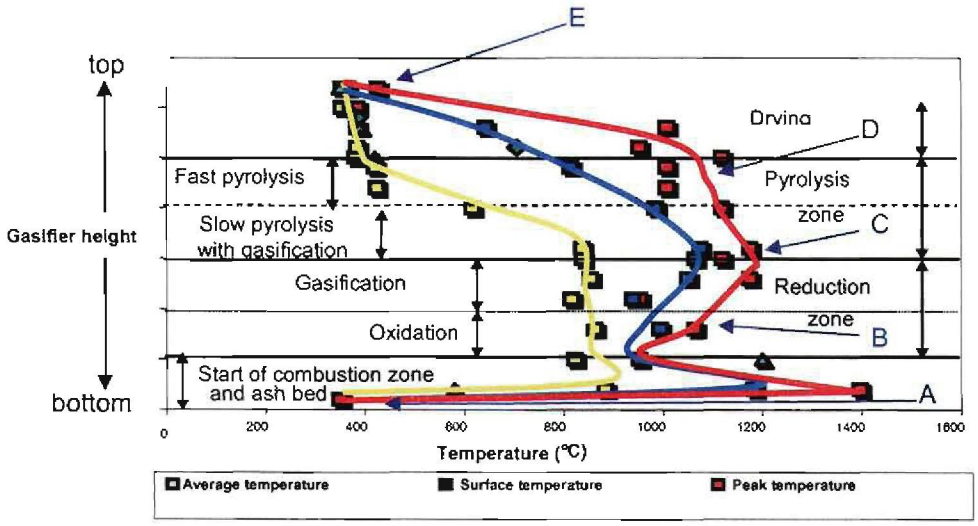

Figure 3.4: Solids temperature profiles obtained for the different samples showing the average temperature, surface temperature and peak temperatures [Bunt, 2006].

From the third sample (C) up to the last sample (A), there is a decrease in the amount of pyrrhotite and anhydrite that had formed in sample C. The decrease of pyrrhotite and anhydrite could be due to thermal decomposition of these species once they have formed. The last sample, which is the ash (A), shows the presence of only anhydrite

as a sulphur-bearing mineral in the crystalline phase. The loss of pyrrhotite from sample C can be attributed to the reaction as shown in equation 7. In the gasification zone and combustion zone, oxidising conditions prevail and pyrrhotite is transformed to metallic iron which then reacts with oxygen to form various iron oxides including hematite (Fe_2O_3) and magnetite ($FeO.Fe_2O_3$) indicated in figure 3.3.

In the work reported by Waanders and Bunt, [2006], Mössbauer spectroscopy was used to investigate the transformation of the Fe-minerals in coal during gasification. In their paper, the sample corresponding to sample E shows the presence of pyrite. As the coal is exposed to the conditions inside the gasifier, various Fe-species form from the pyrite in the feed coal. Mössbauer results indicate that samples in the pyrolysis zone contain both the pyrite and some other Fe^{2+} containing species. This is in agreement with the fact that equation 6 starts to take place in the pyrolysis zone leading to formation of pyrrhotite, which is indicated by the presence of Fe^{2+} species.

Mössbauer spectroscopy results show that in the gasification zone some of the pyrite is still observed, with Fe^{2+} and Fe^{3+} species also identified. In the combustion zone no pyrite is observed by Mössbauer spectra but only hematite and other species containing Fe^{2+} and Fe^{3+} were observed in the samples at the bottom of the gasifier, which correspond to samples A and B. XRD results indicate the presence of both hematite and magnetite in these samples, while Mössbauer spectroscopic results indicate the presence of hematite as well as other species containing Fe^{2+} and Fe^{3+}. Some of these Fe species could react with high-temperature products (metakaolinite and reactive silica) from the clay in the coal at elevated temperatures to form iron

aluminosilicate species such as hercynite ($FeAl_2O_4$), from the reaction of Fe^{2+} with alumina [Duraes et al., 2007; Paesano, 2003].

Some of the H_2S formed from the transformation of pyrite and pyrrhotite under reducing conditions (equation 6) is oxidised further down in the gasifier, where oxygen is present producing sulphur dioxide and sulphur trioxide, in the area of samples A and B. SO_2 and SO_3 can also be produced from the oxidation of pyrrhotite and organically bound sulphur species in the combustion zone of the gasifier. The produced SO_2 and SO_3 can then react with the high-temperature products of calcite, dolomite and the organically associated calcium and magnesium in the mineral matter of the coal to form $CaSO_4$ and $MgSO_4$.

The $CaSO_4$ species was identified even in the last sample (A), which is the ash. $MgSO_4$ is not detected by the XRD since it is known to be very unstable against thermal treatment [Torres et al., 1999]. This is in agreement with findings by Bryers, [1986], Ward [2004] and Raask, [1984] who reported that calcite transforms at elevated temperatures to form quicklime (CaO). This lime may react with water and sulphur oxides to form portlandite ($Ca(OH)_2$) and anhydrite ($CaSO_4$) respectively. It is this aspect of the chemistry that takes place inside the gasifier that will be crucial for sulphur capturing by SO_2 injection in a packed coal bed, exposed to different reaction conditions. The results of the findings of this aspect are discussed in the sections to follow.

3.1.2.2 Computer controlled scanning electron microscopy

From the CCSEM results given in figure 3.5, it can be deduced that the sample at the top of the gasifier (E), which is the feed coal, contained pyrite cleats (extraneous pyrite), as well as Fe, Ca and Mg associated with aluminosilicates. The extraneous pyrite particles in the feed coal sample transformed at elevated temperatures to various iron and sulphur forms. As a result, no evidence of extraneous pyrite particles in samples other than the feed sample was detected. In figure 3.5, the decrease in the amount of pyrite cleats from the first sample to the second sample from the top is accompanied by an increase in content of the mixture of pyrrhotite/Fe-S-O/Fe-Oxide, which is a high-temperature transformation product of extraneous pyrite. The extraneous pyrite could also be transformed to pyrrhotite, as suggested by equation 6. An increase in the amount of calcium, magnesium, iron aluminosilicate glass content that forms during the interaction with the included kaolinite, carbonate and pyrite is also observed within the gasifier.

It is noted from figure 3.5 that, when moving from the top to the bottom of the gasifier that the proportion of aluminosilicate glass containing Ca and Fe increases. The presence of this glass in these samples can possibly be attributed to the interaction of high-temperature transformation products of kaolinite, carbonates, and pyrite at temperatures of more than 1000 °C to form a melt. From the work by Bryers [1986], Ward [2004] and Raask [1984], it was observed that at elevated temperatures CaO interacts with more reactive aluminosilicates such as metakaolinite to form gehlenite ($Ca_2Al_2SiO_7$) and anorthite ($CaAl_2Si_2O_8$). On cooling the gasifier by using excess steam, anorthite and, to a lesser extent, mullite crystallise out from the melt

[Matjie et al., 2006]. The temperature decreases further as the ash subsides towards the rotating ash grate of the gasifier, and the residual molten materials solidify into Ca- and Fe-bearing aluminosilicate glasses.

It can also be deduced from the results in figure 3.5 that, from samples C to A, there is an increase in the concentration of iron aluminosilicate glass from the interactions of high-temperature transformation products of kaolinite and pyrite. The presence of sulphur in the ash samples could be attributed to the encapsulation of sulphur-bearing ash particles by the melt formed during coal gasification. Sulphur in the ash particles can also be derived from the remnants of pyrite and organically-associated sulphur in the unburned carbon particles, which can also be encapsulated in the melt.

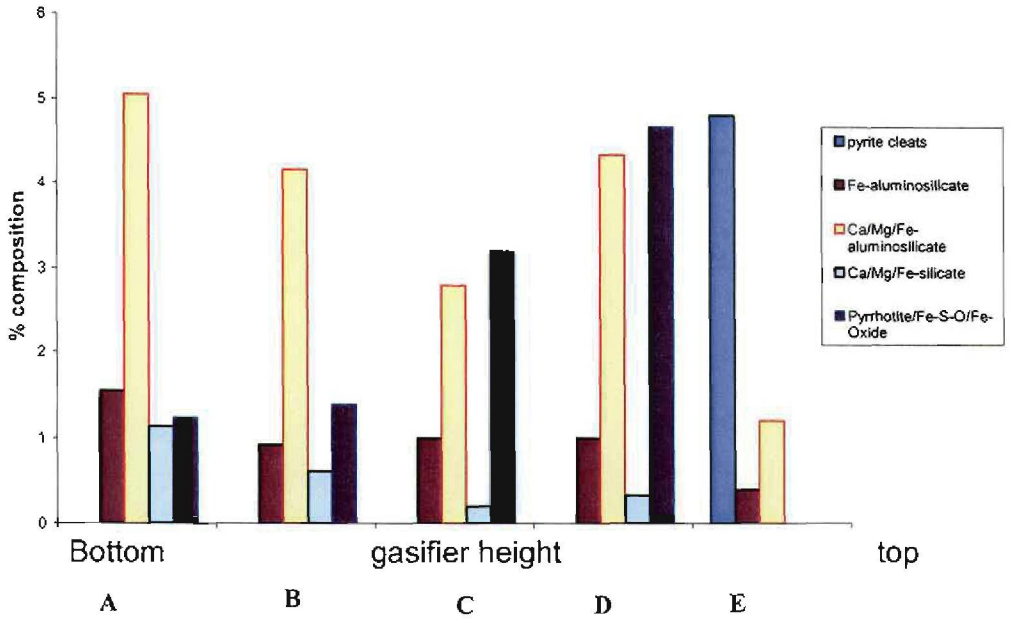

Figure 3.5: Mineral phases identification with CCSEM

CCSEM images of pyrite transformation

Selected back-scattered electron microscope images were taken during CCSEM analysis of the samples. The images discussed in this section were taken as part of the work reported by Matjie [2008], with the focus for this thesis being on the coal structure and mineral matter that impacts on sulphur behaviour. This section covers only the part of the coal structure and mineral matter related to sulphur. Table 3.4 indicates the samples with images together with the zones where they were taken from and the approximate temperatures that the sample had experienced.

Table 3.4: Samples of CCSEM images

Samples number	**Zones of the gasifier**	**Approximate temperature of sample (°C)**
E (figure 8A)	Top of gasifier	25
C (figure 8B)	Gasification	1000-1350
A (figure 8C)	Bottom of gasifier	1100-1350

From figure 3.6A (sample E) it can be deduced that the following particle types and associated minerals are present in the feed coal sample:

- Organic-rich coal particles with small concentrations of kaolinite (particle A), quartz (particle A), pyrite (particle A1) and calcite/dolomite inclusions. Fine to coarse dolomite and calcite cleats in predominantly organic-rich particles (particle A2) are common.

- Coarse to fine quartz-rich sandstone rock fragments (particles B and E). Minor kaolinite, microcline, muscovite and fine pyrite inclusions are present.
- Large (>750 μm) calcite and pyrite cleat fragments (particle D).

The CCSEM results also indicate that the included minerals which contain the fluxing elements (Ca and Mg) are also associated with the included kaolinite. The CCSEM analysis also shows that pyrite grains (white) are included in the carbon particles and some are associated with kaolinite in the coal sample.

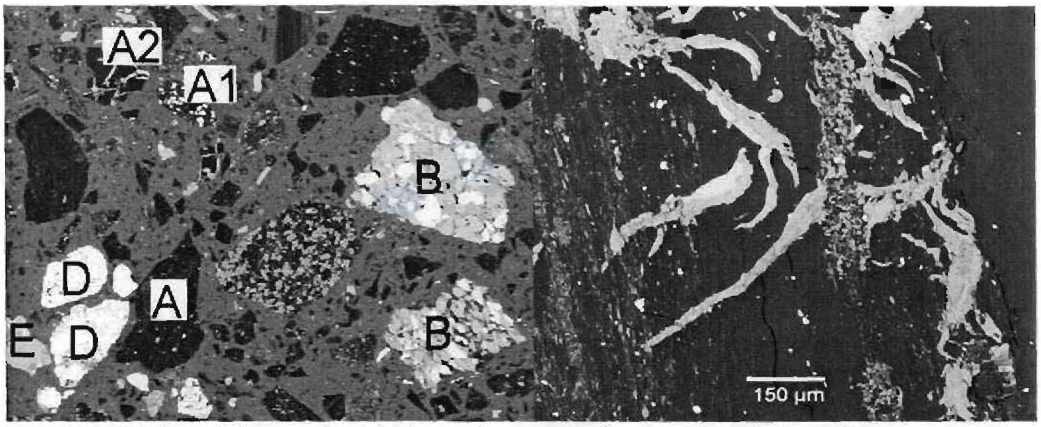

Figure 3.6A: Sample E scanning electron micrographs (back-scattered images) [Matjie 2008].

Scanning electron micrographs (back-scattered electron images) highlighting mineral attributes and deportment characteristics in gasifier feedstock. Carbon-rich particles are black, mineral matter is light grey to white and epoxy mounting resin is grey. The width of each image is approximately 3.5mm. The right BSE image of feed coal shows included kaolinite associated with dolomite/calcite, kaolinite is also associated with dolomite/calcite/pyrites (white dots). The scale bar is 150µm.

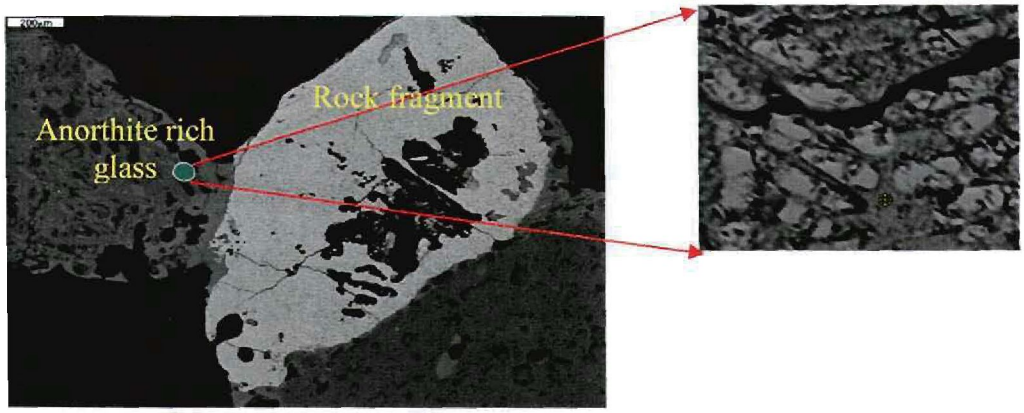

Figure 3.6B: Sample C scanning electron micrographs (back-scattered images) [Matjie, 2008].

Large extraneous "Fe-oxide/Fe-S-oxide/pyrrhotite" particle attached to rock fragment and anorthite rich glass fragment in the coarse ash: scale bar is 200µm). The scale bar of Fe-oxide/ Fe-S-oxide/pyrrhotite is 20µm.

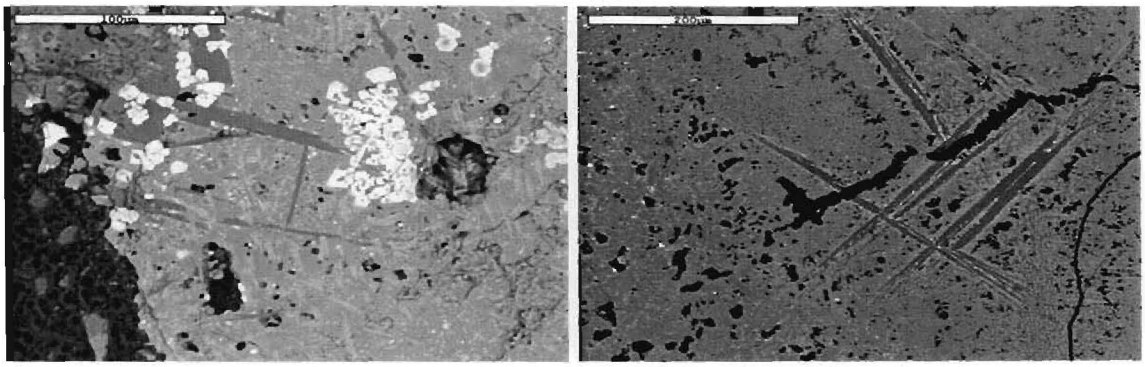

Figure 3.6C: Sample A scanning electron micrographs (back-scattered images) [Matjie 2008]. Left hand image (sample 1) consists of prominent dark anorthite laths and white hercynite in two toned glass. In the right hand image the glass is differentiated into grey and light grey phases and very small iron oxide phases (white).

Figure 3.6B represents the image obtained for sample C taken from the gasification zone. The heated rock fragment particle of sample C, shown in Figure 3.6B, comprises the Fe-oxide/Fe-S-oxide/pyrrhotite that is a high temperature transformation product of the extraneous pyrite [Matjie and van Alphen, 2008]. The spherical light grey grains in the heated rock fragment particles are pyrrhotite, the grey phase is Fe-S-oxide and the dark grey is Fe oxide. The heated rock fragment particle attached to the particle of clinker consists of anorthite crystals and glass particles [Matjie and van Alphen, 2008]. There is no evidence of reaction between the partially oxidised pyrite and dehydrated kaolinite.

The interstitial glass (sample A, Figure 3.6C) is enriched in Fe (some iron particles are derived from kaolinite/pyrite association, siderite and ankerite) and to a lesser extent Mg relative to the average field composition. This trend is expected, as Fe and Mg are not part of the anorthite structure, which is $(Ca,Na)(Si,Al)_2O_6$. On further cooling, the Fe and Mg in the interstitial glass can react with aluminosilicate or oxygen to form the following iron species: Fe-rich Mg-aluminosilicate (pyroxene or amphibole), Fe-rich hercynite ($FeAl_2O_4$) and finally wustite [Duraes et al., 2007; Paesano, 2003].

3.1.3 Summary

Sulphur-bearing minerals in the coal undergo various transformations, with some of the sulphur released with the raw gas under reducing conditions of the gasifier as H_2S and COS, and the other sulphur captured in ash glass, retained in the unburned

carbon, and released with the ash. The decomposition of pyrite to pyrrhotite and H_2S was found to be predominant in the pyrolysis zone, prior to the gasification zone.

Exposure of pyrrhotite to the conditions in the gasifier leads to further decomposition in an oxidising atmosphere in the combustion zone leading to the formation of iron oxides (magnetite and hematite), and sulphur gases such as SO_2 and SO_3.

Some of the sulphur reports to the ash as a result of remnants of pyrite and organic sulphur in unburned carbon particles of carbonaceous shales as well as by the formation of sulphur species in the glass matrix.

Some of the sulphur is also retained as sulphur oxides that react with the high-temperature transformation product (CaO) of calcite or dolomite to form anhydrite through the following reaction.

Now that the sulphur behaviour in a commercial scale fixed bed gasifier has been attained, the next sections cover the results obtained for sulphur capturing in the coal minerals such as CaO, through SO_2 injection in a packed coal bed, in a laboratory scale furnace and in a pipe reactor.

3.2 Sulphur capture in a fixed coal bed in a laboratory-scale furnace.

This section covers all results obtained from the experimental work and characterisation techniques employed for studying sulphur capturing in a fixed coal bed in a laboratory-scale furnace. The results presented and discussed in this section are the results obtained for the various parameters that were investigated, which include the effect of temperature, the monitoring of SO_2 breakthrough during the reaction, and the effect of residence time.

3.2.1 Effect of temperature

The effect of temperature on sulphur capturing in a packed coal bed in a laboratory-scale furnace was studied by following the procedure described in section 2.2.2.1. Batch samples of fresh coal were treated for 20 min at temperatures ranging from 900 to 1250 °C, in increments of 50 °C. The total sulphur content of the blank sample (sample heated without SO_2 flow) as well as the reaction sample (treated with SO_2), was determined as indicated in section 2.2.3.1. The results obtained for the reaction points are presented graphically in figure 3.7.

From the graph in figure 3.7 it can be deduced that there is an observed increase in the total sulphur content of the samples that were treated with SO_2 at the temperatures up to 1100 °C tested, compared with the samples not treated with SO_2. The blank samples show a decrease in the amount of total sulphur with increased temperature of the laboratory furnace. This can be due to the loss of sulphur with thermal treatment, as discussed in section 3.2.

The amount of total sulphur in the reaction samples tends to increase with an increase in temperature treatment from 900 °C up to 1100 °C. This increase of total sulphur with an increase in temperature treatment can be attributed to sulphur intake from the injected SO_2. This intake of sulphur could be due to the reaction of the SO_2 with the high temperature transformation products of mineral matter in the coal. For temperatures above 1100 °C, there is a decrease in the amount of total sulphur in the SO_2-treated reaction samples.

The decrease in the amount of total sulphur with higher temperature could be due to a number of factors. Firstly, decomposition of the organically bound sulphur as well as the inorganically bound species can be favored at these conditions of elevated temperatures as discussed in section 3.1 of this thesis. Secondly, the nature of the CaO formed from the calcination of limestone and dolomite could also be playing a role, since hard-burned or soft-burned lime react differently, with the hard-burned lime being less reactive than the soft-burnt variant [Gallala et al., 2008]. Formation of hard burnt lime during the limestone or dolomite calcination process will lead to formation of lime that is less reactive, and vice versa. This implies that the reaction of SO_2 with the formed CaO will be favored if a soft burnt lime is formed instead of a hard burned lime [Gallala et al., 2008].

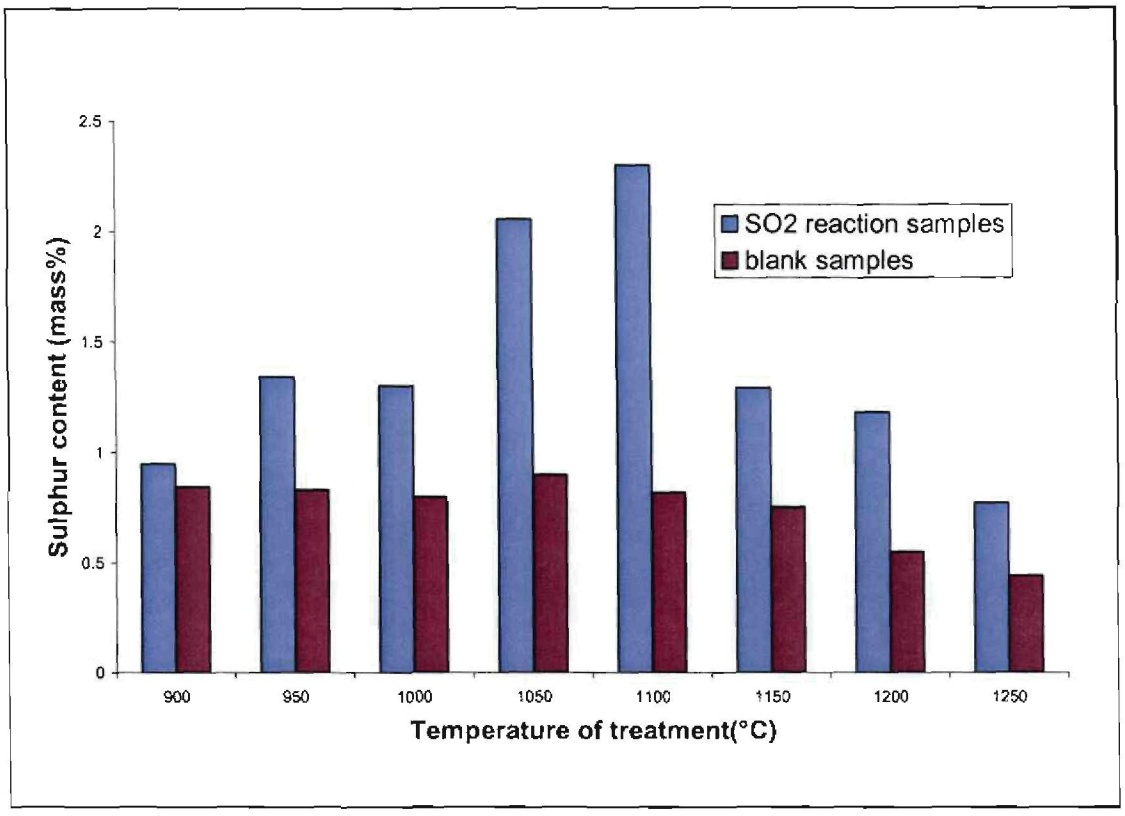

Figure 3.7: Effect of temperature on sulphur capturing.

3.2.2 Effect of residence time

The effect of residence time on sulphur capturing was investigated by conducting the reactions at 1100°C, which was found to be the optimum temperature for sulphur capturing as discussed in section 3.2.1. In this case, the reaction temperature was kept constant while varying residence time at 20 min, 40 min, 60 min, 80 min, 120 min and 240 min. The samples were analysed for both their total sulphur content and carbon content and the results are presented graphically in figure 3.8.

In figure 3.8 the time of reaction is plotted against sulphur content and carbon content. The first point indicates the blank sample, which is the sample obtained after treatment of the coal at 1100 °C for 20 min, with no SO_2 flow. From the results in figure 3.8, an increase in the amount of sulphur in the resulting ash, with an increase in time of the reaction is observed. The sulphur content in the sample treated for 80 min is 4.25%, in comparison with 0.85% in the blank sample and 80 min is the residence time resulting in the highest sulphur capturing propensity. This is indicative of the fact that from 20 min up 80 min, the reaction of sulphur capturing is favourable, and takes place without major decomposition of the formed sulphur capture products. This could also be due to the fact that beyond 80 min all of the reaction sites for SO_2 are used up, and the SO_2 does not react, but instead passes through the bed. The amount of sulphur captured thus increases up to 80 min, since within this timeframe more lime is formed from the decomposition of both the limestone and dolomite, as shown in the reactions 1 and 2 below [Hem and Debaprasad, 1986; Powell and Searcy, 2006; Wang et al., 2007].

$$CaCO_3 \rightarrow CaO + CO_2 \qquad 8$$

$$CaMg(CO_3)_2 \rightarrow CaO + MgO + 2CO_2 \qquad 9$$

On the other hand, the carbon content shown in figure 3.8 shows no major change for the first 60 min, whereafter, a decrease in the carbon content is observed. The carbon content in the sample heated for 80 min at 1100 °C (showing the highest sulphur content) was found to be 37%. The carbon content thus shows a continuous decrease with an increase in reaction time. The reaction was conducted up to 240 min (4 hours), since for a sample to pass through a combustion zone in a commercial gasifier

it will take only a couple of minutes and not more than 2 hrs. The high carbon content of the ash obtained from the reaction conditions employed is due to equipment limitations in achieving the heating efficiency necessary to drive off most of the carbon from the coal. From the results obtained it can be deduced that 80 min at 1100 °C appears to be the optimum reaction conditions for sulphur capturing in the setup used. The reaction conditions were then used for monitoring of the SO_2 breakthrough during the course of the reaction. The decrease in the sulphur content beyond 80 min reaction time corresponds with a substantial decrease in the carbon content.

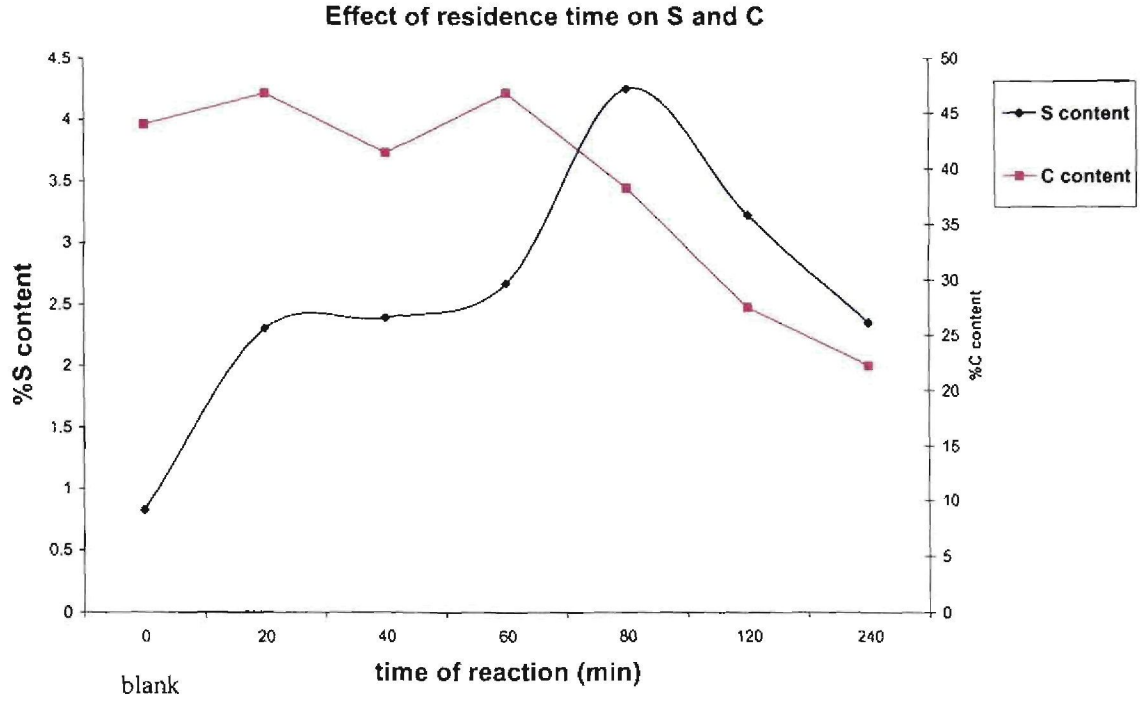

Figure 3.8: Effect of residence time at 1100 °C, on total sulphur and carbon content of the remaining coal sample.

3.2.3 Monitoring of SO_2 emission during the reaction

The off-gas from the reaction furnace was collected throughout the reaction and scrubbed in a 20 ml water solution. The water solutions were taken in 10 min intervals, with a fresh 20 ml water solution used every time. The solutions were analysed for their acid concentrations since SO_2 or SO_3 released from the reaction will react with water to form sulphuric acid (H_2SO_4) and sulphurous acid (H_2SO_3). These reactions are well known for acid rain formation from SO_2 and SO_3 emitted from coal combustion plants coming into contact with water vapour in the atmosphere to form acid rain [Hao et al., 2001; Columbia Encyclopedia, 2008]. The scrubbing solutions were subjected to pH determination using a calibrated pH meter, as well as for acid concentration determination using standard titration reactions with 0.02 M NaOH, results are shown in appendix table A.6. The results obtained are presented graphically in figure 3.9, and also given in table A.6 in the appendix.

Figure 3.9 indicates that initially, at approximately 800 °C, the SO_2 that passes through the coal bed gives rise to a scrubbing solution with low pH, of approximately 2, and acid concentration of ±0.04 M. However, as the reaction progresses and the temperature reaches 1100 °C there seems to be very little or no SO_2 that passes through the coal bed, as indicated by the pH increases to approximately 6, and the acid concentration decrease to less than 0.0001 M. This remains the case for up to approximately 80 min, which indicates that all of the SO_2 that flows through the system is consumed in the reaction. After the 80-min period lapses, the pH starts to decrease to approximately 4 and the concentration increases to ±0.00035 M. This is indicative of the fact that after the 80-min period has lapsed SO_2 breakthrough takes place. This is in agreement with the observations obtained from the results on the investigation of residence time, where 80 min was found to be an optimum period for

sulphur capturing. Once the 80 min period has lapsed, the extent of sulphur capturing was observed to be decreasing. This could be due to the exhaustion of the reactive sites, leading to the SO_2 not reacting with the sites but instead, passing through. Subsequent decomposition of the products of sulphur capturing could also lead to SO_2 emission from the reaction.

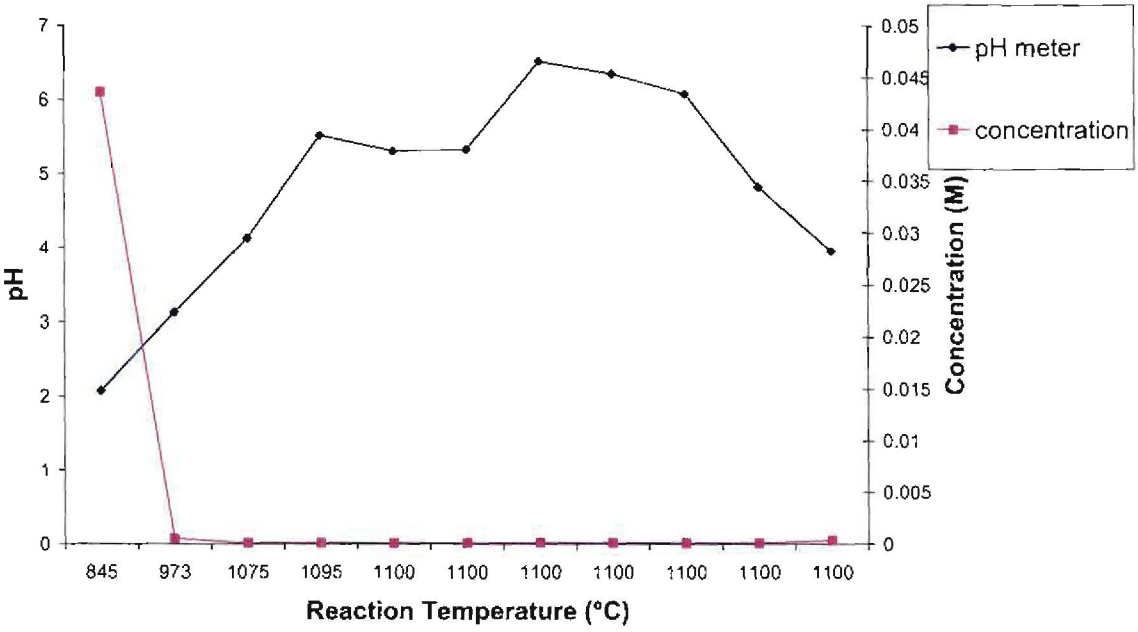

Figure 3.9: Tracking of the release of SO_2 from the reaction.

In agreement with the results shown under the impact of residence time, it can be deduced that after the 80 min time period has elapsed there seems to be an escape of SO_2. This is seen from the increase in the acidity of the scrubbing solution collected from the acidity analysis. This is in agreement with the impact of residence time results, which show that the sulphur capturing is optimum at 80 min, after which the amount of sulphur captured tends to decrease and hence the breakthrough of SO_2 after 80 min has lapsed. This indicates that there is a period during the reaction whereby no sulphur passes through the coal bed. This is evidence that there is sulphur retention, possibly through the reaction of the SO_2 injected with the coal structure.

3.2.4 Effect of thermal exposure

The determination of the amount of sulphur loss with thermal exposure was conducted by treating batch coal samples (of the sample treated with SO_2 for 80 min at 1100 °C, in air) at 1150 °C, 1200 °C, 1250 °C, 1300 °C, and 1350 °C in a tube furnace. The samples were analysed for their total sulphur content. Figure 3.10 indicates the percentage of sulphur retained at the various temperature points. The percentage sulphur retained is calculated based on the sulphur content of the sample that was used for thermal treatment.

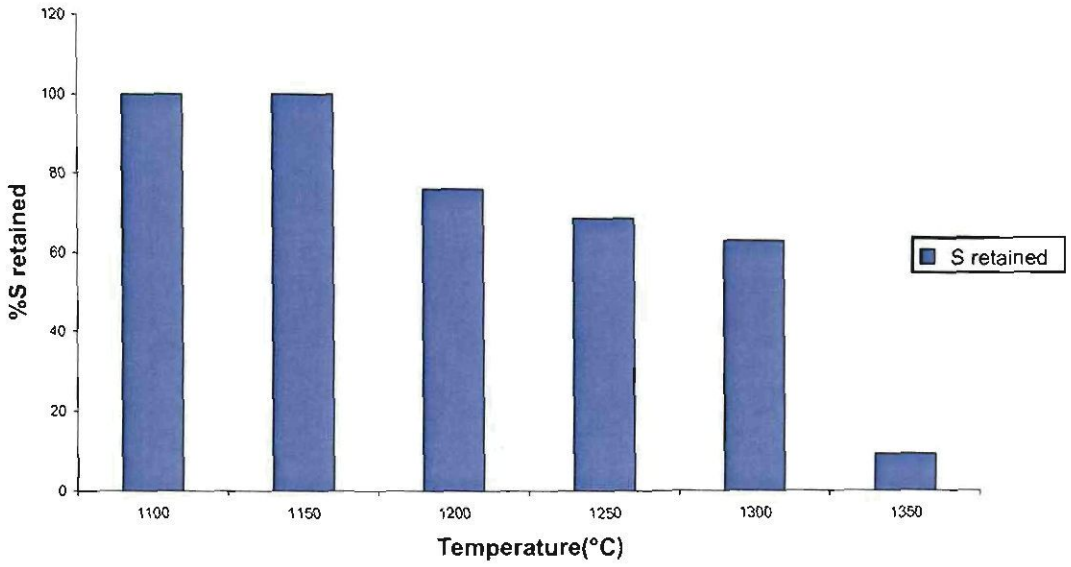

Figure 3.10: Sulphur retention with thermal exposure

Figure 3.10 indicates that there is a gradual loss of the captured sulphur with thermal exposure. At 1300 °C, only 60 % of the sulphur in the original sample is retained in the ash. A drastic decrease is observed at 1350 °C, where less than 10 % of the original sulphur content is retained. This indicates that the sulphur captured during the reaction is affected by increased temperature that leads to its decomposition and

possible loss from the structure. The loss of sulphur increases with increased temperature of exposure.

One of the possible sulphur capture products is $CaSO_4$. According to a paper by Cheng et al. [2003] $CaSO_4$ decomposes with increased temperatures of exposure under oxidising conditions starting from a temperature of 1150 °C, where a decomposition percentage of 13 %, up to a temperature of 1300 °C where a decomposition percentage of 96 % is achieved. The loss of sulphur with thermal exposure in figure 3.10 can be due to thermal decomposition of $CaSO_4$, as explained above.

3.2.5 Mineralogical analysis of selected samples before and after reactions

Mineralogical analysis was conducted (using the XRD technique) on selected samples from the reactions. The samples that were used for XRD analysis were the feed coal, the sample from the blank reaction; as well as the reaction sample at 1100 °C for 20 min; the sample from the blank reaction and reaction sample at 1100 °C for 80 min; the samples from the blank reaction and reaction sample at 1100 °C for 120 min, as well as the sample from the reaction at 1100 °C for 240 min. The XRD results on these samples are presented graphically in figure 3.11, and also in table A.7 in appendix.

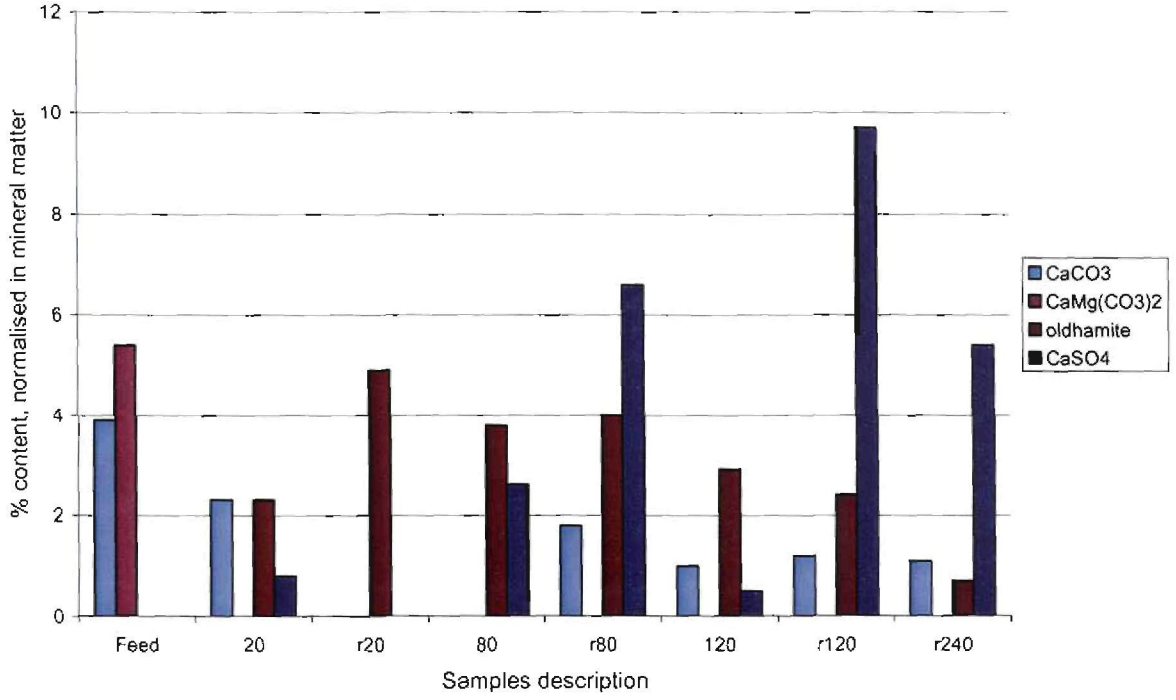

Figure 3.11: Mineral phases normalised in crystalline matter

Note: "r" indicates samples taken from SO_2 treated reactions for the given time of reaction e.g. r 20 stands for sample taken from SO_2 treated reaction conducted for 20 minutes.

The feed coal sample was found to contain all of the major low-temperature minerals such as quartz, kaolinite, muscovite, dolomite, pyrite, calcite, and alunite. The graph in figure 3.11 shows the presence of Ca-bearing minerals i.e. dolomite and calcite, for the feed coal sample. As the samples were treated at high temperatures for both the blank and reaction samples, all of the low-temperature phases have transformed and high-temperature phases are observed, such as mullite (from kaolinite transformation) anorthite (from kaolinite transformation and reaction with lime); cristoballite (from quartz and kaolinite transformation); as well as magnetite and other mineral spinnel from pyrite transformation [Bryers, 1986; Srinivasachar et al., 1990; Grim and Bradley, 1940; Benson, 1987; Ward and French, 2004].

Figure 3.11 indicates selected mineral phases identified for the selected coal ash samples from the reactions. The minerals indicated in figure 3.11 are those that take part in the sulphur capturing process that is being investigated in this study. The rest of the other mineral phases present are indicated in table A.7 in appendix. In figure 3.11, the sample description is plotted against the percentage content, normalised in crystalline phase. The first column indicates the mineralogical composition of the feed coal, followed by a column of reaction samples treated at 1100 °C for 20 min for both the blank reaction (20), and the reaction with SO_2 flow (denoted r20). The next column is for the reaction conducted for 80 min (80 and r80), 120 min (120 and r120), then reaction for 240 min, but only for the reaction with SO_2 flow (r240).

From the graph in figure 3.11, it can be deduced that dolomite and calcite are observed mainly in the feed coal, with the reduction of these phases observed in the treated samples. For all of the reaction samples, oldhamite (CaS) is formed, and is even more enhanced in the reaction samples when compared with samples obtained from the blank reactions for the 20-min sample. This suggests that there is definitely a formation of CaS during the reaction. This can be brought about by reducing conditions during the reaction due to lack of enough oxygen to get oxidising conditions. In a review by Cheng et al., the possibility of CaS transformation to $CaSO_4$, due to reducing and oxidising conditions changes was highlighted, and is indicated in figure 3.12 [Cheng et al., 2003]. In the diagram two possible routes for SO_2 reaction with CaO are depicted, depending on whether the environment is reducing or oxidising. The path for $CaSO_4$ formation takes places under oxidising conditions where CaO, SO_2 and O_2 react form $CaSO_4$. On the hand under reducing conditions CaO reacts with SO_2 in the presence of CO leading to formation of CaS.

The reaction leading to transition between CaS and $CaSO_4$ is a reversible reaction; and reductive decomposition of anhydrite can lead to the formation of CaS, as suggested by Chen and Yang [1979], who indicated that the reaction given in equation 8 can take place under reducing conditions:

$$CaSO_4 + 4H_2 \rightarrow CaS + 4H_2O \qquad 8$$

Notable amounts of anhydrite products ($CaSO_4$) are observed for samples that were exposed for longer reaction times. Gypsum is known to form through contact of the anhydrite with water leading to hydration of the anhydrite to gypsum, as shown in equation 4 [George and Stanley, 1973]. In the experimental setup and procedure followed the resulting ash samples couldn't have come into contact with water that can lead to anhydrite transformation to gypsum. It is suggested that the gypsum could be derived from bassanite ($CaSO_4.^1/_2H_2O$) that forms under reducing conditions from organically sulphur and mineral calcite [Painter et al., 1978]. The bassanite could also be derived from direct reaction of organic calcium and organic sulphur [Miller et al., 1979; Morgan et al., 1981]. From figure 3.11, it can be deduced that all of the reaction samples with SO_2 flow tended to have higher concentrations of anhydrite-based products. The presence of anhydrite indicates that there is a reaction of SO_2 with CaO in the ash, leading to the formation of anhydrite, as shown in equations 3.

The amount of CaS formed tends to decrease with an increase in the time of the reaction. The decrease in the amount of CaS is accompanied by an increase in the formation of $CaSO_4$. This is also related to the carbon content in the sample, with

samples of higher carbon contents having higher CaS and lower $CaSO_4$ contents, and vice versa. This suggests that for the samples with high carbon content, that the CaO and SO_2 reaction takes place in the presence of CO to form CaS, as shown in figure 3.12 by Cheng et al. [2003]. This observation is also supported by findings by Strydom et al., [1997]. In samples with lower carbon content, oxidising conditions prevail more and CaO reacts to a greater extent with O_2 and SO_2 to form $CaSO_4$.

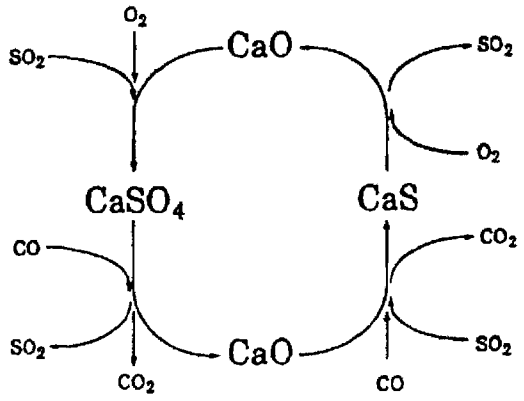

Figure 3.12: Solid phase transformation taking place when lime is exposed to alternating reducing and oxidising conditions in CFB [Cheng et al., 2003]

A correlation between carbon content and the amount of CaS in a sample was plotted and is indicated in figure 3.13. From the graph it can be deduced that a linear correlation with R^2 of 0.9258 is obtained, which indicates a linear relationship between carbon content and the amount of CaS in the samples. From the graph it is illustrated that for samples treated with SO_2, the amount of calcium sulphide decreases as the carbon content decreases. This is accompanied by an increase in the formation of anhydrite and gypsum, as indicated in figure 3.11.

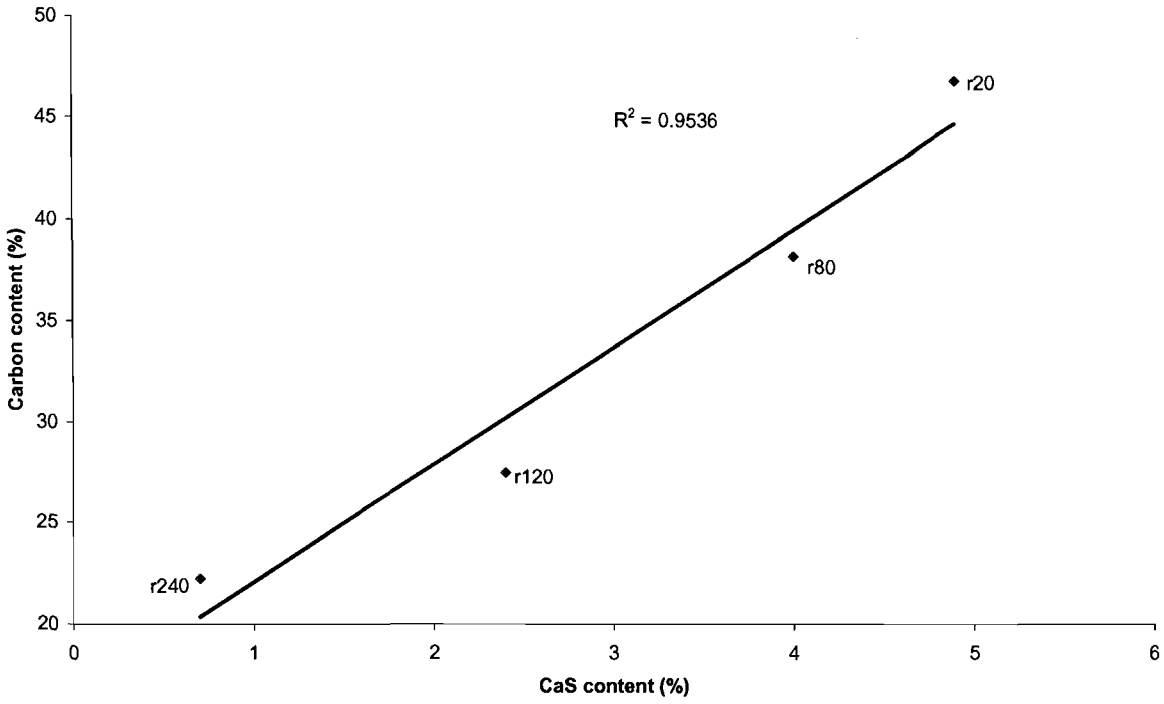

Figure 3.13: Correlation between carbon content and amount of CaS in SO_2 treated samples

From these observations it can thus be concluded that SO_2 injection in a packed coal bed leads to sulphur capturing by CaO derived from calcite and dolomite in the coal mineral matter. The reaction of CaO with SO_2 leads to the formation of oldhamite, anhydrite and gypsum. The sulphur-capturing products formed depend on the severity of the conditions, whether oxidising or reducing and the composition of these are related to the carbon content in the sample.

3.2.6 Summary

The results obtained from the investigation of sulphur capturing in a fixed coal bed in a laboratory-scale furnace were presented in this section. It was observed that SO_2 injection in a packed coal bed at elevated temperatures and various reaction times

leads to sulphur capturing by the Ca-bearing coal minerals. The extent of sulphur capturing was found to be related to the temperature of the reaction as well as the residence time for the reaction.

The optimum conditions for sulphur capturing were found to be the temperature of 1100 °C for a period of 80 min under specific experimental conditions. Monitoring of SO_2 breakthrough from the reaction confirmed that there is a time during the reaction when no SO_2 is emitted from the reactor bed, which suggests that the SO_2 reacts with the reactive species in the coal structure. The sulphur, once captured, can undergo decomposition or loss due to exposure at high temperatures, with about 70 % of the sulphur retained at 1250 °C, and approximately 60 % retained at 1300 °C.

Mineralogical analysis of the ash samples obtained from the experiments, using XRD, indicates that the sulphur-capture products that are formed include CaS and $CaSO_4$. The existence of these compounds is dependent on the extent of oxidising or reducing conditions during the reaction, with CaS favoured in reducing conditions and $CaSO_4$ favoured under oxidising conditions. A linear correlation between the carbon content and the amount of CaS in the samples was obtained.

Nonetheless, given the equipment limitations discussed, valuable insight into the sulphur capturing propensity within a fixed bed environment has been successfully obtained.

3.3 Sulphur capture in a fixed coal bed in a pipe reactor

This section covers all results obtained for the investigation of sulphur capturing through SO_2 injection in a packed coal bed in a pipe reactor. Results discussed in this section include results on sulphur elemental analysis, sulphur forms analysis and mineralogical analysis using XRD. The residual solid samples collected after each of the reactions were divided into 7 equal portions from the top to the bottom of the pipe reactor. The fractions were labelled samples 1 to 7 with sample 1 being the sample on top, and sample 2 the following all the way with sample 7, being the last sample at the bottom of the reactor, constituting the ash bed sample.

The pipe reactor employed for this study was shown to be simulating the conditions in a commercial fixed-bed gasification process by Bunt and Waanders [2009]. In the work reported, the pipe reactor samples were compared to the gasifier samples from a gasifier turnout, and the trends were found to be in agreement with those observed for a Sasol-Lurgi Fixed Bed Dry Bottom (SLFBDB) MKIV gasifier [Bunt and Waanders, 2009]. Profiles of the volatile matter, fixed carbon and ash for the pipe reactor and the SLFBDB MKIV gasifier indicated similarities in the trends obtained for the two systems. From the findings it was concluded that the pipe reactor can be used to simulate the Sasol-Lurgi gasifier with the reaction zone clearly identified [Bunt and Waanders, 2009]. The zones of the gasifier, namely drying zone, pyrolysis zone, gasification zone and combustion zone, were identified and are indicated in all of the graphical representation of the results. Results for both the base-case reaction, i.e. the reaction without SO_2 flow, as well as the reaction with SO_2 flow, are discussed for comparison.

3.3.1 Elemental analysis

The samples were analysed for their total sulphur content, and the results are presented graphically in figure 3.14. The graph in figure 3.14 indicates results for both the base-case and the reaction samples.

From figure 3.14 it can be deduced that the total sulphur content for the base-case samples show a decrease from the top sample to the bottom of the pipe reactor. This decrease in total sulphur content of the base-case samples can be ascribed to loss of sulphur due to thermal treatment of the samples. As indicated in section 3.1, sulphur-bearing pyrite undergoes decomposition to form pyrrhotite and H_2S. The pyrrhotite further decomposes to form iron oxides and sulphur gases such as SO_2, SO_3 and H_2S, depending on the atmosphere whether reducing or oxidising.

The total sulphur content profile for the SO_2 treated reaction samples (indicated as reaction in the graph) is also shown in figure 3.14. It can be seen that the total sulphur content shows a decrease in the first three samples, which are in the top of the pipe reactor, from a total sulphur content of 1.2 % for sample 1 to 1 % for sample 2 and then to about 0.8 % for sample 3. This indicates that there was no impact of the injected SO_2 at this level of the reactor height. However, from sample 4 down to sample 6 there is a notable increase in the total sulphur content, with the content up to more than 1.8 % for sample 6. This increase in the total sulphur content in this region of the pipe reactor suggests that there is sulphur capturing of the SO_2 by the coal mineral structure. Sample 7 shows lower sulphur content than samples 4, 5 and 6.

This is expected since sample 7 was allowed to reach 1250 °C before the flow of SO_2 was injected, as discussed in detail in chapter 2.

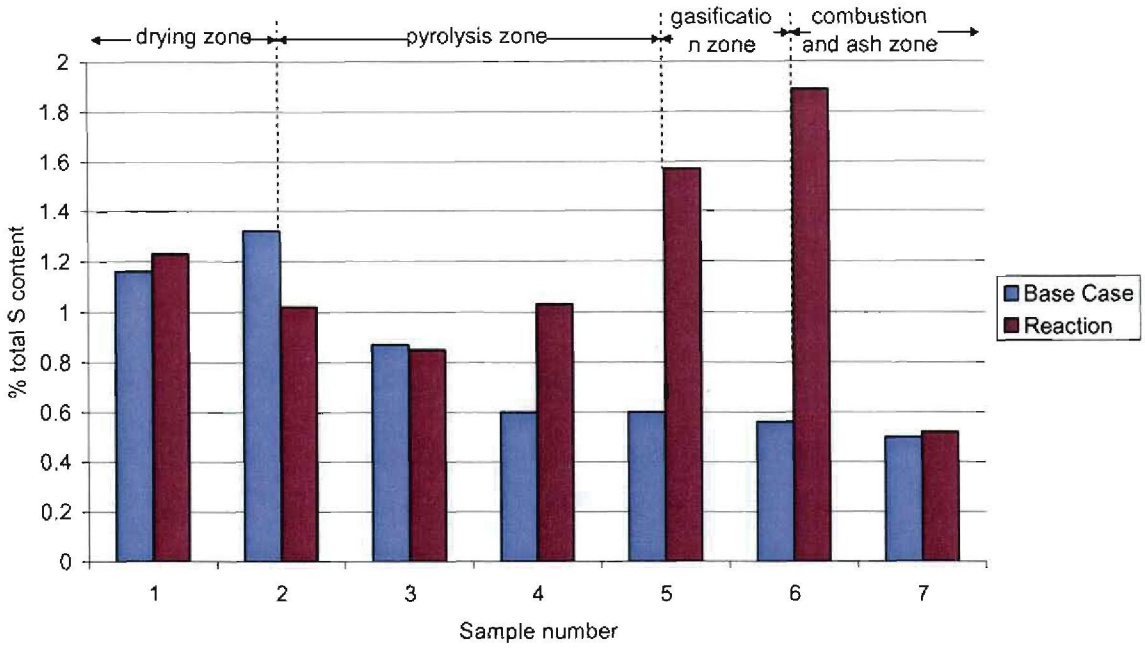

Figure 3.14: Total sulphur on the pipe reactor fractions for blank and SO_2 treated samples

The total sulphur content as well as the mass of the individual samples was used to calculate the amount of sulphur captured in relation to the sulphur introduced to the system. Table 3.5 indicates the sulphur content as well as the mass of sulphur for both the reaction samples as well as the samples from the base-case reactions. These are calculated from the mass of each fraction, and this is indicated in appendix table A.8. From table 3.5 it can observed that the mass of sulphur decreases from the top to the bottom of the reactor for the base-case samples. The mass of sulphur for the reaction samples shows a decrease initially for the first 3 samples, and this is followed by an increase from samples 4 to 6. The information in table 3.5 was used to calculate the

amount of sulphur captured in the coal structure from the amount injected. The details of the calculation are presented in appendix table A.8.

Table 3.5: Percentages and total sulphur amounts in total ash in the indicated samples for the reference and SO_2 treated experiments.

	Reference samples		**SO_2 treated reaction samples**	
Sample	**% S**	**Mass S(kg) in coal/mass ash**	**% S**	**Mass S(kg) in coal/mass ash**
1	1.16	0.34	1.23	0.36
2	1.32	0.48	1.02	0.35
3	0.87	0.30	0.8	0.29
4	0.60	0.20	1.03	0.34
5	0.6	0.16	1.57	0.56
6	0.59	0.15	1.89	0.65
7	0.55	0.13	0.52	0.18
Total		1.76		2.73

From table 3.5 the following can be calculated:

- Total mass of sulphur in the base case samples: 1.76 kg
- Total mass of sulphur in the reaction samples: 2.73 kg
- Mass of S captured (retained) into the coal mineral structure:

  Total sulphur in reaction samples - Total sulphur in base case samples

  = 2.73 – 1.76 kg

  = 0.97 kg
- Mass of S added (from cylinder): 40 ml/min for 2hrs = 2.38 kg

- % S captured:

  = Sulphur added (and retained) to coal structure/ sulphur added from cylinder × 100

  = 0.97 kg/2.38 kg X 100

  = 41 %

From the calculations it can be seen that 41% of sulphur added to the pipe reactor was captured in the coal ash. This implies that the other 59 % of the sulphur added was released and was never captured in the coal matrix. This amount of sulphur that was not captured could have been released without reacting with the coal ash, or it could have been released after reacting with the coal structure through decomposition of the formed sulphur species. Based on the reaction procedure and results obtained so far, it can be deduced that the sulphur emitted from the SO_2 added is likely to be due to decomposition of the formed sulphur species brought about by long reaction times necessary for cooling down the reactor.

The samples were also subjected to ash elemental analysis, and the results are indicated in table A.9 in the appendix. The results of the SO_3 content, determined from XRF, are plotted and presented graphically in figure 3.15. From the results in the graph it can be observed that the amount of SO_3 in the samples shows a decrease from sample 1 to sample 3, followed by an increase from sample 3 to sample 5, and then a decrease from sample 5 to sample 7. This is in agreement with the observation of the total sulphur behaviour on the blank samples. Samples 1 and 2 of SO_2 treated samples show higher SO_3 content than for sample 3, after which there is a decrease to 2 % in sample 3. From sample 3 there is an increase in the SO_3 content with an increase in

pipe reactor bed depth, from about 2 % for sample 3, to 3 % and 4.5 % for samples 4 and 5 respectively. Sample 5 shows an SO_3 content of 4.5 % which is still much higher than the corresponding sample of the base-case reaction. The observation here is in line with the observation for the total sulphur content results which indicated that sulphur capturing seems to be prevalent in samples 4, 5 and 6.

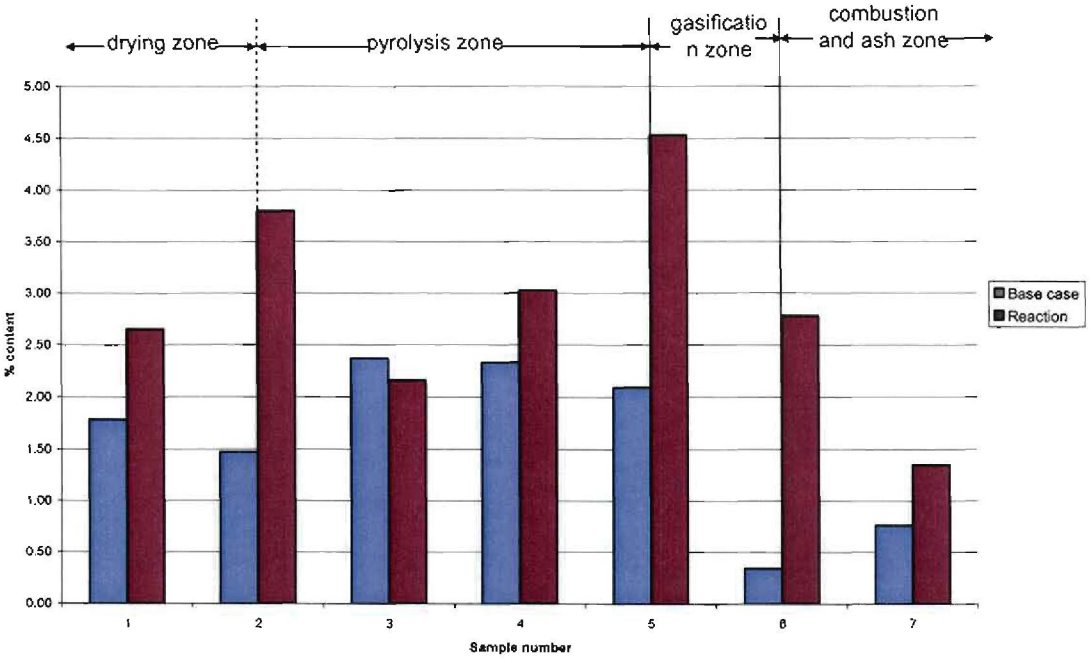

Figure 3.15: SO_3 content from ash analysis of the fractions

3.3.2 Sulphur forms analysis

Sulphur forms analysis was conducted on all the samples from both the base-case reaction and the reaction with SO_2 flow. The graph in figure 3.16 shows the sulphur forms composition for the base-case samples. From the graph it can be deduced that the amount of total sulphur shows a decrease throughout the pipe reactor from the top to the bottom. The amount of mineral sulphur follows the profile of total sulphur and shows a decrease from the top to the bottom of the pipe reactor. Organic sulphur

doesn't show much change throughout the pipe reactor with only a marginal decrease observed for sample 2 to sample 3, and from sample 4 to sample 5. Sulphate sulphur is very low in all the samples and does not show any notable changes in the axial direction within the pipe reactor, with only a marginal decrease observed throughout the reactor.

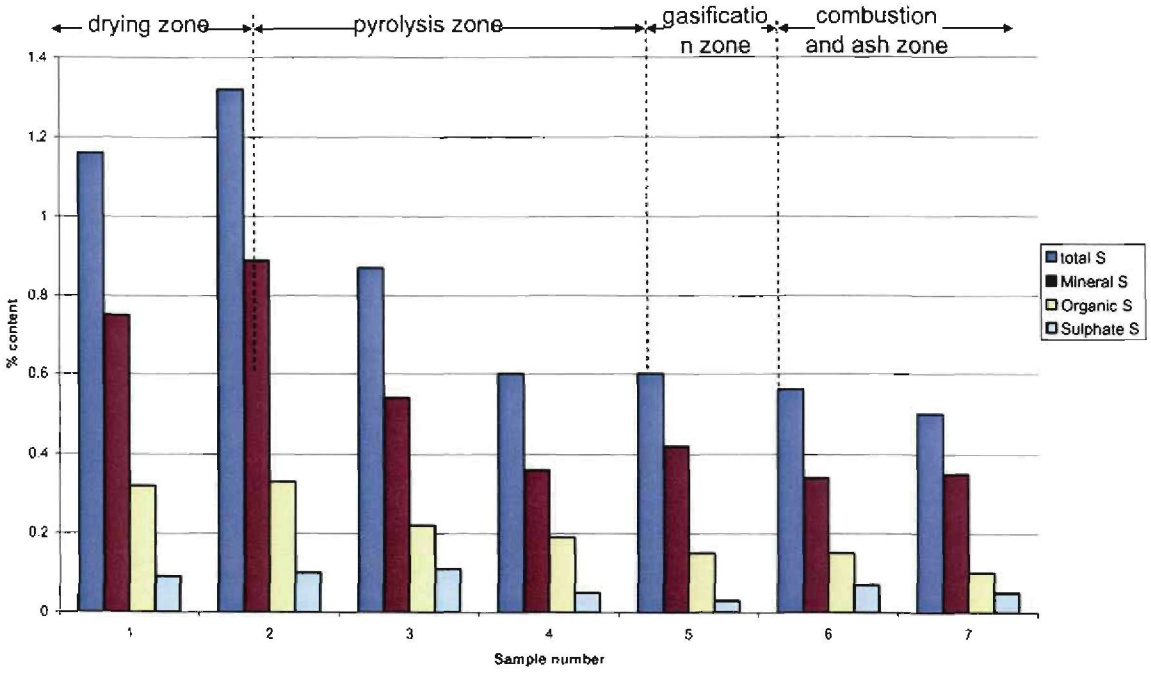

Figure 3.16: Sulphur forms for fraction of base-case reaction samples

The results obtained from the sulphur forms analysis of the samples obtained from reaction with SO_2 flow are presented graphically in figure 3.17. From the graph it can be seen that from sample 4 down to sample 6, that there is an increase in the amount of both total sulphur and mineral sulphur. This is indicative of the fact that there is sulphur capturing occurring in this region of the pipe reactor. The capturing here leads to the formation of mineral sulphur which is probably a sulphide form. Organic sulphur does not show much axial change within the reactor, as was the case with the

base-case reaction. A marginal increase is observed from sample 4 to sample 5, which suggests possible reaction of the introduced SO_2 with the organic structure of the coal.

No major changes are observed with the sulphate sulphur. Sample 7 shows low proportions of total sulphur, mineral sulphur and sulphate sulphur. This is due to the fact that this sample was exposed to 1250 °C before the SO_2 flow was allowed, as described in chapter 2.

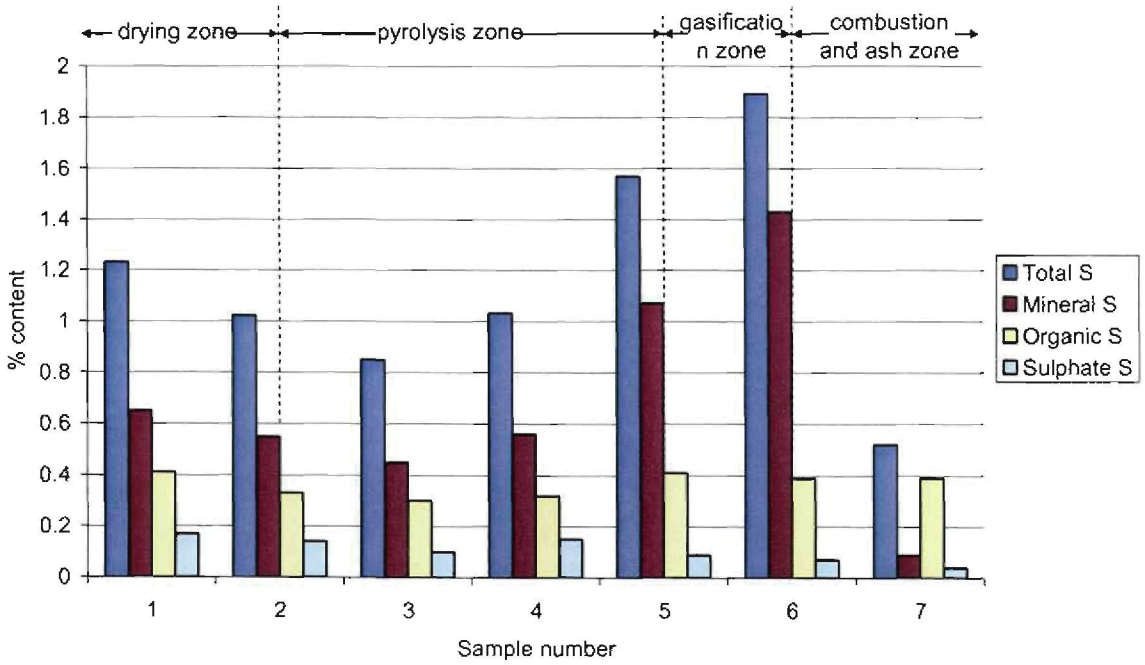

Figure 3.17: Sulphur forms for fraction of SO_2 treated reaction samples.

Sulphur forms analysis for both the base-case samples as well as reaction samples indicated that SO_2 injection into a packed coal bed in a pipe reactor at controlled conditions leads to sulphur capturing in the coal ash. The capturing was found to be taking place in the region of samples 4, 5 and 6. The increase in total sulphur content in these regions is accompanied by an increase in the amount of mineral sulphur. This

indicates that the form in which the sulphur binds to the coal ash is in the mineral sulphur form.

3.3.3 Mineralogical analysis using XRD analysis

Mineralogical analysis was conducted using XRD analysis of the samples taken from the pipe reactor. Table A.11, in the appendix, shows the detailed XRD data for the samples taken. The data are represented as percentage content in crystalline matter. From these results, mineral phase transformation due to thermal treatment is observed. Transformation of kaolinite, calcite and dolomite in the samples in the upper regions of the pipe reactor (samples 1 to 4) led to the formation of high-temperature phases anorthite and mullite which are observed in the samples below (samples 5 to 7) that have been exposed to temperatures in excess of 1000 °C.

Pyrite is also observed to be present in samples 1 to 4, and beyond this no pyrite is observed. This is due to the fact that samples 5 to 7 are exposed to higher temperatures (more than 700 °C), which give rise to pyrite transformation as discussed in section 3.1 of this thesis. Calcite and dolomite are also observed in the top samples (samples 1 to 4), and for samples in the lower half of the pipe reactor no calcite and dolomite is observed. This indicates that these species undergo transformation as they are exposed to high temperatures. Cristoballite, which is a high temperature transformation product of kaolinite and quartz, was observed in samples 6 and 7.

Figure 3.18 indicates graphically the composition of the mineral phases that are associated with sulphur behaviour in the pipe reactor's reaction samples. The graph is a plot of sample number against the percentage content of the various mineral phases. On the secondary Y-axis is the carbon content in the samples as determined from the ultimate analysis. From the graph it can be observed that dolomite and calcite are present in sample 1 to sample 4. It is also noted that no major changes are observed for the carbon content for these samples as well as for sample 5. This indicates that the samples 1 to 4 have not been exposed to a high enough temperature that can effect calcite and dolomite transformation (>850 °C).

Carbon content is not expected to decrease yet, since these samples are still in the devolatilasation zone and have not been exposed to the gasification zone conditions as indicated in the diagram. Sample 5 also indicates no major change in carbon content compared to the preceding samples. This indicates that the sample is at the beginning of the gasification zone as indicated in the diagram. Sample 5 also has a small amount of calcite still present with no dolomite detected, but MgO, which is a transformation product of dolomite, is observed. No CaO is detected in sample 5, which suggests that all of the CaO formed from calcite and dolomite decomposition reacts with SO_2 to form CaS, observed to be more than 6 % in sample 5.

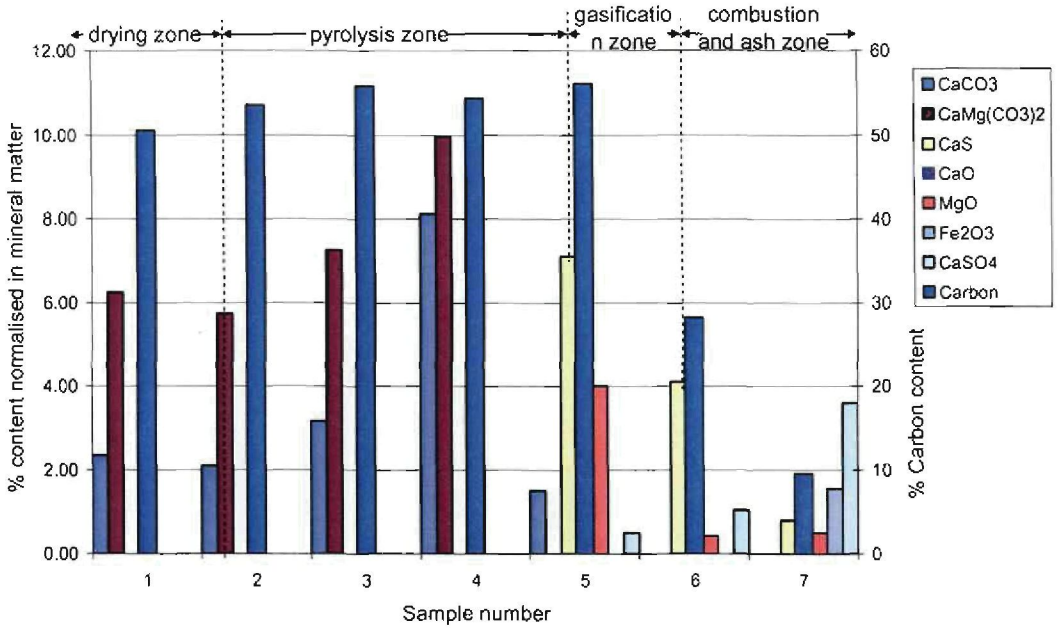

Figure 3.18: Mineral composition for the fractions of the pipe reactor experiments

A decrease in carbon content is observed in samples 6 and 7 and samples 5, 6 and 7 show the presence of CaS. However the content of CaS shows a decrease from sample 5 to 7, which is also the trend for the carbon content. The content of $CaSO_4$ shows an increase from sample 5 to 7, which is the direct inverse of what is observed for CaS and carbon content. This is in agreement with the observation discussed in section 3.2, where CaS and $CaSO_4$ formation was shown to be alternating depending on whether the atmosphere is reducing or oxidising, as reported by Cheng et al. [2003] and indicated in figure 3.12 in section 3.2. Sample 5, which still has a high carbon content (more than 50 %), favours the formation of CaS instead of $CaSO_4$; on the other hand, sample 7, with a low carbon content of 10 %, shows the formation of $CaSO_4$.

Comparison of the mineral phase content for the base-case samples as well as samples generated by the reaction with SO_2 was carried out using XRD analysis of samples 5, 6 and 7. The results obtained are presented graphically in figures 3.19 a, b, c and d, as

well as in table A.12 in the appendix. All the results are presented as percentage content in crystalline matter.

Figure 3.19a indicates the percentage content of CaS in samples 5, 6 and 7 for both base-case and SO_2 treated reaction samples. From the graph it can be deduced that reaction samples contain notable amounts of CaS relative to the base-case samples. Reaction sample 5 was found to contain more than 7 % of CaS, while the corresponding base-case sample was found to contain 2 % of CaS in the crystalline matter. This suggests that the CaS in the reaction samples must have formed during the reaction by the reaction of CaO and SO_2 in the presence of CO, since the carbon content in this sample is more than 50 % (refer to figure 3.18). The reaction path followed is as follows, as suggested by Cheng et al., [2003].

$$CaO + SO_2 + CO \rightarrow CaS + CO_2 \qquad 9$$

However the amount of CaS in the reaction samples was found to decrease as the samples in the reactor are exposed to higher temperature, as seen for sample 6 with (CaS 4 %) and sample 7 (CaS of less than 1 %). The decrease in the amount of CaS with an increase in bed depth is accompanied by an increase in the amount of $CaSO_4$, as observed in figure 3.19b. This phenomenon is in agreement with the observation for the results obtained using a laboratory-scale furnace reported in section 3.2, where carbon content was also found to have an impact on this phenomenon.

Referring to figure 3.19b, it can be seen that the base-case samples also contained small amount of $CaSO_4$ in samples 5, 6 and 7. Sample 5 has approximately 5 % of

$CaSO_4$, and samples 6 and 7 have 3.2 % and 2.7 % respectively. This suggests that even in the samples without SO_2 flow that there is a possibility of in-situ reaction of inherent CaO and SO_2 released from the coal structure, leading to the formation of anhydrite and oldhamite. The amount of $CaSO_4$ in both the base-case run and the reaction run is too low to make a credible conclusion regarding whether it is actually forming from the SO_2 injected into the reactor.

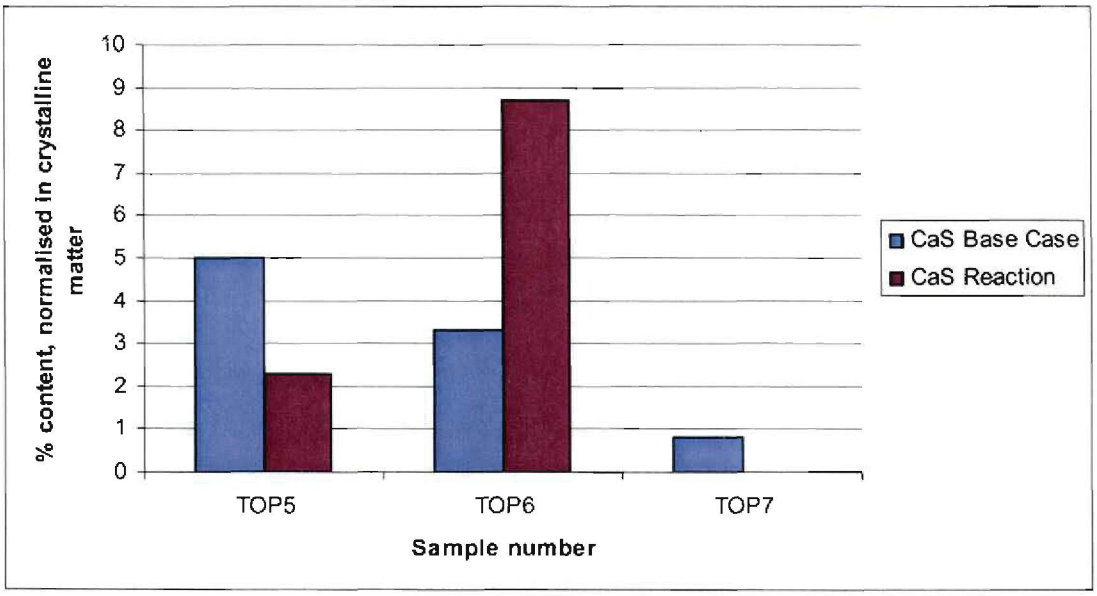

Figure 3.19a: CaS content in the samples from blank reaction and SO_2 treated reaction samples

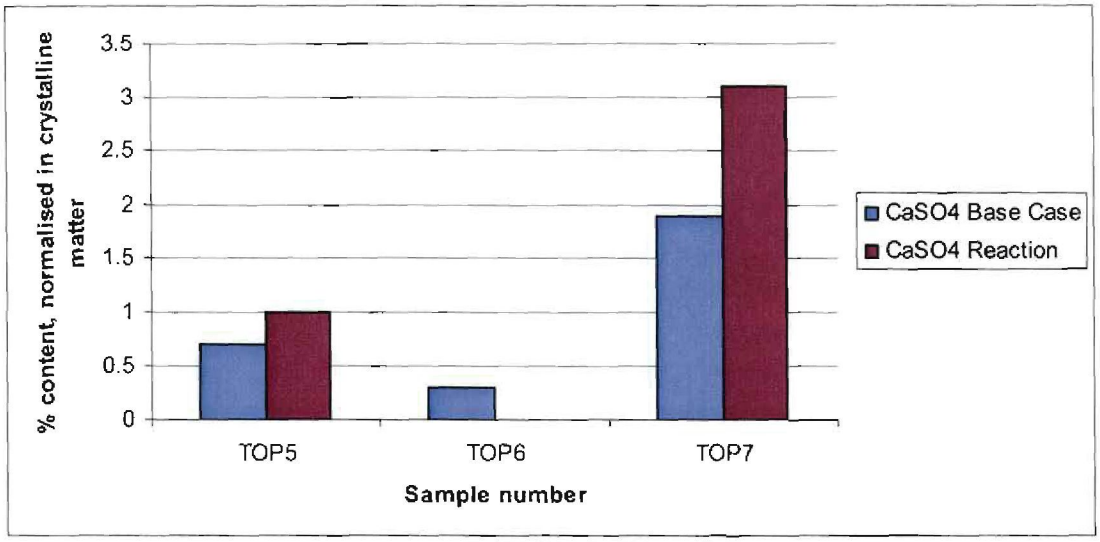

Figure 3.19b: $CaSO_4$ content in the samples from blank reaction and SO_2 treated reaction samples

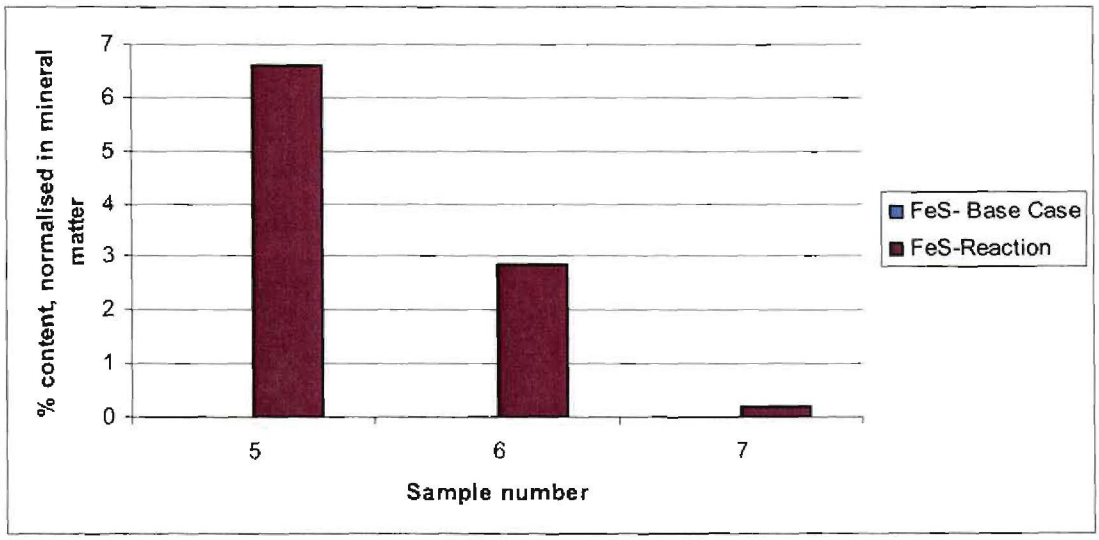

Figure 3.19c: FeS content in the samples from blank reaction and SO_2 treated reaction samples

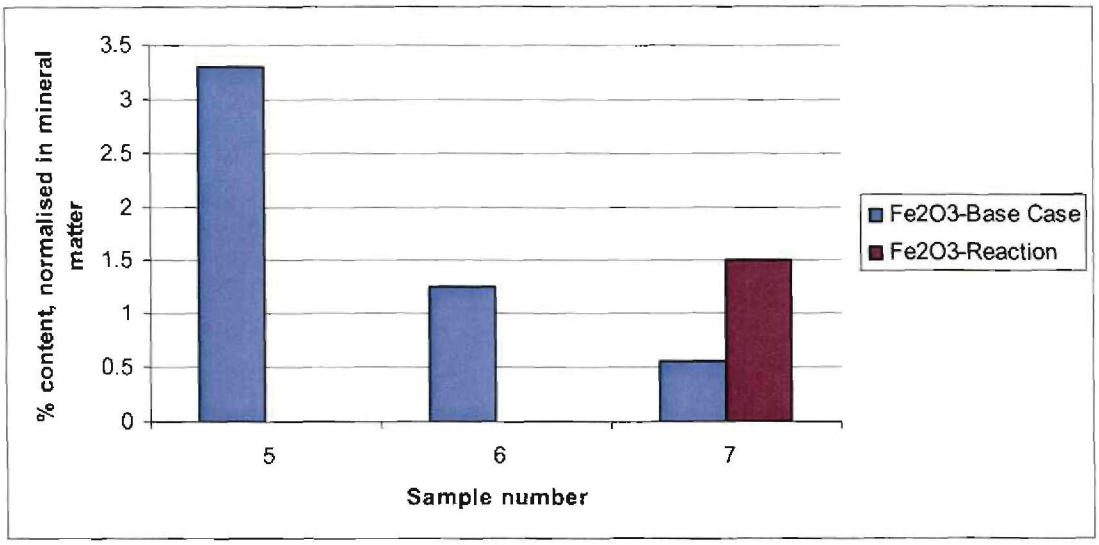

Figure 3.19d: Fe_2O_3 content in the samples from blank reaction and SO_2 treated reaction samples

Troilite, a species similar to pyrrhotite, was observed to form in the reaction samples (samples 5, 6 and 7), and no troilite was observed in the blank samples. Figure 3.19c shows the amount of troilite in the base-case sample as well as in the reaction sample. Sample 5 of the reaction run contains more than 6 % of troilite in crystalline matter. Whereas, sample 6 contains about 3 %, and sample 7 contains about 0.2 %. The troilite formation is seen to reach a maximum in sample 5, and shows a decrease as the samples are exposed to higher temperature towards the base of the reactor. The troilite has formed from the reaction of Fe, from pyrite decomposition, with any H_2S present to form FeS. The troilite could also be derived from the decomposition of pyrite in the feed coal.

Various authors have reported the possibility of troilite formation from the reaction of hydrogen sulphide with metallic iron [Murowchick and Barnes, 1986; Imae and Kitamura, 1993; Lauretta et al., 1996; Jiang et al., 1998;]. In a paper by Li and Hung [2003], hydrogenation of sulphur dioxide to hydrogen sulphide over Fe catalysts was

reported. This hydrogenation of the SO_2 introduced into the pipe reactor, and subsequent formation of H_2S, and reaction of the H_2S with Fe to form troilite might have been the case during the reaction run.

The decrease in the amount of troilite towards the base of the reactor can be due to decomposition through oxidation, of the formed troilite towards the formation of metallic Fe that reacts with oxygen to form iron oxide. Figure 3.19d indicates the formation of hematite in sample 7 only, which suggests that the decomposition of troilite does lead to the formation of hematite, as observed by Lee and Montana [1984]. This is in agreement with the observations from the investigation of sulphur behaviour in a commercial-scale fixed bed gasifier (section 3.1).

3.3.4 Summary

Results obtained from an investigation of sulphur capturing via SO_2 injection in a packed coal bed in a pipe reactor were presented in this section. From the results of the total sulphur analysis and ash analysis, it was observed that there is indeed sulphur capturing in the reaction samples, mainly in the region of samples 4, 5, and 6 of the pipe reactor. From the total sulphur results it can be concluded that up to 41% of the sulphur injected in the form of SO_2 from the cylinder was captured and retained in the coal ash.

Results from the sulphur forms analysis also indicated capturing of sulphur in the reaction samples for samples in the region of samples 4, 5 and 6. The increase in total sulphur content in this region was accompanied by the formation of mineral sulphur,

which suggests that the sulphur is captured mainly in mineral sulphur form, i.e. in a sulphide form.

Results from XRD analysis of the samples indicated the formation of notable amounts of CaS in the region of sample 5 in the pipe reactor. The amount of CaS was also found to decrease with an increase in bed depth in the pipe reactor up to sample 6 and 7. This was found to be accompanied by a decrease in carbon content and a marginal increase in $CaSO_4$ content for the reaction samples. The presence of anhydrite in the base-case samples (5, 6 and 7) suggests that there is a possibility of in-situ reaction of the inherent Ca and S during the processing of the coal in the pipe reactor. The amount of $CaSO_4$ in both the base-case and reaction samples is however too low to make a conclusion regarding its formation. Results from the XRD analysis also suggest the formation of troilite (a form of pyrrhotite) from the reaction of Fe and sulphur species generated during the reaction. The troilite could also be derived from pyrite decomposition.

Chapter 4

Conclusions and recommendations from the study

Understanding of sulphur behaviour during the fixed bed gasification process is an important step towards devising means for the reduction of sulphur emissions from the gasification processes. In the study presented in this thesis, sulphur behaviour in a commercial fixed bed gasifier and the possibility of sulphur capturing via injection of SO_2 in a packed coal bed was investigated. The hypothesis of the study carried out was that injection of SO_2 in a packed coal bed, under controlled conditions such as in the fixed bed gasification process, can lead to sulphur capturing by high temperature transformation products of coal mineral matrix through a series of reactions involving Ca-bearing minerals such as limestone and dolomite.

The main objective of the study was to investigate the possibility and extent of sulphur capturing via SO_2 injection in a packed coal bed using an experimental setup capable of simulating specific reaction zones of a fixed bed gasifier. This was investigated using a laboratory-scale furnace (simulating the combustion zone) as well as in a pilot-scale pipe reactor unit simulating the entire fixed bed gasifier. A further objective of the study was to understand the behaviour of sulphur in the coal as the coal is exposed to various conditions in a commercial-scale fixed bed gasifier. Conclusions and recommendations from the findings of the study conducted are discussed in this section.

4.1 Conclusions

From the investigation of sulphur behaviour in a commercial fixed bed gasifier, the following conclusions can be made.

It is concluded that when the coal is subjected to coal processing at elevated temperatures, sulphur is liberated from the coal structure and coal minerals. This is brought about by amongst other factors, the transformation of sulphur-bearing coal minerals such as pyrite. During the fixed bed gasification process, pyrite undergoes various transformation steps including; transformation of pyrite to pyrrhotite, which takes place predominantly in the reduction zone of the fixed bed gasifier, leading to the liberation of sulphur as H_2S and COS. This is followed by subsequent transformation of pyrrhotite to metallic Fe which reacts with O_2 in the oxidation zone of the fixed bed gasification process, to form various oxides of Fe.

During fixed bed gasification, small proportions of sulphur report to the ash in three possible forms namely:

- as part of remnants of pyrite and pyrrhotite as well as sulphur species trapped in the glass matrix
- as organic sulphur in unburned carbon particles of carbonaceous shale, as well as;
- sulphur retained as SO_2 or SO_3 that reacts with the high-temperature transformation product (CaO) of limestone and dolomite to form anhydrite.

The understanding of the manner in which the sulphur is bound to the coal mineral structure, and also the manner in which the sulphur is released under various conditions can be of importance in establishing various processes that can be used to reduce the H_2S emissions from the gasification plant, especially those processes involving manipulation of the coal structure for in-situ sulphur capturing. The presence of anhydrite in the ash indicates the possibility of sulphur capturing through in-situ reactions of Ca and sulphur in the coal structure. The investigation of sulphur capturing in a packed coal bed via injection of SO_2 into a packed coal bed under controlled conditions, investigated as part of this thesis, was motivated by the findings on sulphur behaviour in a commercial fixed bed gasifier.

Sulphur injection into a packed coal bed under controlled conditions leads to sulphur capturing within the high temperature transformation products of coal minerals observed by an increase in total sulphur content of the resulting ash.

Laboratory-scale results obtained in this investigation indicated that sulphur capturing at elevated temperatures indeed occurs, and that the extent of sulphur capturing was found to be dependent on the temperature as well as the time of the reaction. The optimal temperature and time of reaction for the reactions in a laboratory-scale furnace was found to be 1100 °C and 80 min respectively. The sulphur captured was found to be further influenced by elevated temperatures (i.e. 1350 °C) leading to the loss of sulphur due to thermal decomposition. SO_2 breakthrough monitoring confirmed that there was a period during the reaction where no SO_2 or SO_3 breaks through from the reaction.

XRD results of the investigation of sulphur capturing in a laboratory-scale furnace suggests that sulphur capturing takes place through the reaction of the injected sulphur from the added SO_2, with the Ca in the coal minerals such as dolomite and calcite. However, decomposition of calcite and dolomite towards the formation of lime (CaO) is necessary for the SO_2 to react with lime. As per the hypothesis of the study, the envisaged reaction for sulphur capturing is as shown below.

$$CaO + SO_2 + {}^1/_2O_2 \rightarrow CaSO_4$$

XRD results indicated that there was formation of CaS and $CaSO_4$ in notable amounts in the ash samples obtained from SO_2 reaction with the coal. In samples with high carbon content (>30 %), CaS was formed instead of $CaSO_4$, with the latter forming as the carbon content decreased. This suggests that CaO reacts with the added SO_2 leading to the formation of CaS instead of $CaSO_4$, in the presence of a high carbon content, thus in a reducing atmosphere. This was also related to a carbon content of about 30 % in the ash fraction obtained from the reaction. The 30 % carbon content in ash was found to be the lowest carbon content that was obtained due to limitations of the experimental equipment employed. The findings were in agreement with earlier findings in the literature where it was proven that in the presence of carbon products i.e. CO and CO_2, that the reaction of CaO with SO_2 will take place, but will only lead to the formation of CaS instead of $CaSO_4$. A linear correlation between the carbon content in ash with the amount of CaS was obtained, which suggested that the higher the carbon content in the ash after SO_2 treatment, the higher the CaS content versus that of $CaSO_4$.

Results obtained from the investigation of sulphur capturing in a packed bed in a pipe reactor indicates that there is indeed sulphur capturing occurring with SO_2 injection in a packed coal bed at elevated temperatures. From the total sulphur results the sulphur capturing extent was found to be 41 %. This suggests that 41 % of the sulphur injected was found to be captured permanently by high temperature transformation products of the coal mineral structure. Most of the sulphur capturing was found to be taking place in the region corresponding to the gasification zone of the fixed bed gasifier.

XRD results indicated notable amounts of CaS in the region where most of the capturing takes place. This was also related to the carbon content of the same samples which was found to be about 30 %, which suggests that the carbon content had an impact on the sulphur-capture products formed. This is in agreement with the observation from the results obtained for the laboratory-scale furnace results where the presence of carbon was found to lead to the formation of CaS instead of $CaSO_4$. Evidence of in-situ sulphur capturing was also obtained for the base-case reaction samples, where it was found that anhydrite formation seemed to be taking place without any addition of SO_2. However, the amount of $CaSO_4$ in both the base-case and reaction samples is considered to be too low to make a conclusion regarding its formation.

The observed sulphur capturing around the combustion zone of the pipe reactor is in agreement with the observations obtained from the laboratory-scale furnace. The furnace was operated such that it simulates the conditions in the combustion zone. Whereas, with the pipe reactor the maximum sulphur capturing was observed to be

taking place around the combustion zone of the reactor. This illustrates that the region where the reaction of CaO with SO_2 is taking place, is around the combustion zone. This observation is agreement with literature findings where the reaction of CaO and SO_2 was reported to be taking place from 900 °C to higher temperatures. The formation of both CaS and CaSO4, as well as the impact of the extent of the formation of each due to reducing or oxidisind conditions influences discussed in this thesis, was found to be a similar for both scale of reactors used.

4.2 Recommendations

From the investigation of sulphur capturing in a packed coal bed in a laboratory-scale furnace and in a pipe reactor, it was evident that sulphur capturing does take place through the reaction of the injected sulphur with the Ca-bearing high temperature transformation coal mineral matrix. Despite, some obvious limitations in the equipment used for the experimental work in simulating a commercial fixed bed gasifier, valuable insight into the sulphur capturing propensity within a fixed bed environment has been successfully obtained. It is recommended that the concept be tested in a commercial scale gasifier, where real gasification conditions are introduced.

Troilite a form of pyrrhotite was observed to be forming in some of the reaction samples in the pipe reactor. Investigation into the possibility of sulphur capturing through troilite formation is an area that needs to be further investigated for future studies on sulphur capturing. This will have an impact on the propensity of sulphur

capturing as it means more sulphur will be captured in other forms other than in Ca-bearing minerals.

Addition of sorbent such as limestone and dolomite can be investigated for their impact of sulphur capturing in a setup simulating fixed bed gasification using lump size coal. This can give an indication of the impact of the addition of these sorbents on the propensity of sulphur capturing under conditions similar to those of a fixed bed gasification process.

REFERENCES

Abbasian J., Rehmat A., Leppin D. and Banerjee D.D.; Desulphurization of fuels with calcium-based sorbents; Fuel Processing Technology; 25(1); 1990; 1-15.

ASTM standard D4239-08; 2002; Standard Test Methods for Sulphur in the Analysis Sample of Coal and Coke Using High-Temperature Tube Furnace Combustion Methods.

ASTM standard D5373- 08; 2002; Standard Test Methods for Instrumental Determination of Carbon, Hydrogen, and Nitrogen in Laboratory Samples of Coal.

Benson S.A.; Laboratory Studies of Ash Deposit Formation During the Combustion of Western U.S. Coals; Doctor of Philosophy Thesis; The Pennsylvania State University; University Park, PA; May 1987.

Bethell F.V., Gill D.W. and Morgan B.B.; Mathematical modelling of the limestone-sulphur dioxide reaction in a fluidized-bed combustor; Fuel; 52(2); 1973; 121-127.

Botha P.H; An Investigation of the flotation of three South African coals; Journal of the South African Institute of Mining and Metallurgy; 1980; 395-400.

Bryers R.W.; Influence of segregated mineral matter in coal, In Mineral matter and ash in coal, Symposium of American Chemical Society, Vorres K (Ed.); Elsevier; 1986; 351-374.

Bunt J.R.; A New Dissection Methodology and Investigation into Coal Property transformational behaviour impacting on a commercial-scale Sasol-Lurgi MKIV fixed-bed gasifier; PhD Thesis; North-West University; Potchefstroom, South Africa; 2006.

Casagrande D. J. , Idowu G., Friedman A., Rickert P., Siefert K. and Schlenz D.; H_2S incorporation in coal precursors: origins of organic sulphur in coal; Nature; 282; 1979; 599 – 600.

Chen T. and Saxena S.C.; Mathematical modelling of coal combustion in fluidized beds with sulphur emission control by limestone or dolomite; Fuel; 56(4); 1977; 401-413.

Chen J.M. and Yang R.T.; Fluidized bed combustion of coal with lime additives. Kinetics and mechanism of regeneration of lime sorbent; Indian Engineering Fundamentals; 18; 1979; 134-138.

Cheng J., Zhou J., Liu J., Zhou Z., Huang Z., Cao X., Zhao X. and Cen K.; Sulphur removal at high temperature during coal combustion in furnaces: a review; Progress in Energy and Combustion Science; 29; 2003; 381-405.

Coetzee C.B.; "Delfstowwe van die Republiek van Suid-Afrika".Dept. of Mining. Geological survey. Fifth Edition. Handbook no. 7; Edited by Coetzee C.B.; 1976; 363-404.

Coburn T.T'; Forster K.G.; Gregg H.R. and Lindsay J.A.; Tests of a mechanism for H_2S release during coal pyrolysis; Proceedings for the 1991 International Conference on Coal Science, Newcastle, UK; 16-20 September 1991.

Crnkovic P.M., Milioli F.E. and Pagliuso J.D.; Kinetics study of the SO_2 sorption by Brazilian dolomite using thermogravimetry; Thermochimica Acta; 447(2); 2006; 161-166.

Dahlin R.S. and Landhman E.C.; Factors affecting Dustcake Drag in a Hot-gas Filter system Collecting coal gasification ash, 6th international Symposium on Gas Cleaning at High temperatures; Osaka; Japan; October 20-22, 2005.

Dalai A.K. and Tollefson E.L., Kinetics and Reaction Mechanism of Catalytic Oxidation of Low Concentrations of Hydrogen Sulfide in Natural Gas over Activated Carbon; Canadian Journal of Chemical Engineering; 76; 1986, p. 902.

Davidson M.D., Galloway E.N., Guan X., Hendrix H.L., Scarborough P.T., Dahlin R.S., Landhman E.C., and Spain J.D.; Power Systems Development Facility: High temperature, high pressure filter system operations in a combustion gas, proceeds of the 15th International Conference on Fluidized-bed combustion; American Chemical Engineers; New York; 1999.

Day N.; Batch basket filtration centrifuges for FGD pay their way; Filtration & Separation; 41(6); 2004; 28-30.

Deberry D.W.; Process for removal of H_2S from gas streams; US Patent 5733516; 1998.

Durães L., Costa B.F.O., Santos R., Correia A., Campos J., and Portugal A.; Fe_2O_3/aluminum thermite reaction intermediate and final products characterization; Materials Science and Engineering: A; 465(1-2); 2007; 199-210.

England T, Hand P.E, Michael D.C, Falcon L.M. and Yell A.D.; Coal Preparation in South Africa; compiled by the South African Coal Processing Society; 2002.

Falcon R.M.S.; Coal in South Africa – Part I: "The quality of South African coal in relation to its uses and world energy resources"; Minerals Science and Engineering; 9(4); 1977; 198- 217.

Fischlowitz-Roberts B.; Earth policy institute; 2002; http://www.eart-policy.org/updates/update17.htm

Fuerstenau M.C.; Flotation; The American Institute of Mining, Metallurgical and Petroleum Engineers, Inc.; New York; A.M. Gaudin Memorial Volume 2; 1976;1235-1259

Gallala W., Gaied M. E., Tlili A., Montacer M.; Factors Influencing the reactivity of quicklimes; Proceedings, Construction Materials; 61(1), 2008; 25 – 30, Publisher: Thomas Telford - ICE Virtual Library.

Galuskina I.; Inorganic matter in coal: Yakov E. Yudovich and Marina P. Ketris, Russian Academy of Science, Ural Division, Ekaterinburg, 2002, 422 pp. (in Russian); International Journal of Coal Geology; 58(4); 2004; 269-270.

Gangwal S. K., Gupta R. and McMichael W.J.; Hot-gas cleanup—sulphur recovery technical, environmental, and economic issues; Heat Recovery Systems & CHP; 15 (2); 1995, 205-214.

García-Labiano F., Hampartsoumian E. and Williams A.; Determination of sulphur release and its kinetics in rapid pyrolysis of coal; Fuel; 74(7); 1995; 1072-1079.

Gardner T.H., Berry D.A., Lyons K. D., Beer S.K., Monahan M.J. and Freed A.D., 2001; Fuel processor integrated H_2S catalytic partial oxidation technology for sulphur removal in fuel cell power plants; Fuel; 81(17); 2002; 2157-2166.

George; James Stanley; Process for the conversion of anhydrite into gypsum; US Patent 3906083; 1973.

Glover G.; An experimental study of the physical and chemical processes occurring with a Lurgi Mark IV coal gasifier with a view to determine an optimization path. Part 2: The Sasol One gasifiers, Sasol Technology R&D unpublished internal report, 1988.

Glover G., An experimental study of the physical and chemical processes occurring with a Lurgi Mark IV coal gasifier with a view to determine an optimization path. Part 1: Rational and Preliminary observations, Sasol Technology R&D unpublished internal report, 1988.

Grim R.E., Bradley W.F.; Investigation of the effect of heat on the clay minerals illite and montmorillonite; Journal of American Ceramic Society; 1940; 242-248

Gryglewicz G., Sulphur transformations during pyrolysis of a high sulphur Polish coking coal; Fuel; 74(3); 1995; 356-361.

Gryglewicz G. and Jasieńko S.; The behaviour of sulphur forms during pyrolysis of low-rank coal; Fuel; 71(11); 1992; 1225-1229.

Guan X., Gardner B., Martin R.A.; Demonstration of hot gas filtration in advanced coal gasification systems; Paper presented at the 24th Annual International Pittsburgh Coal Conference, Johannesburg; South Africa; 2007.

Guilin H.; Dam-Johansen K.; Wedels S. and Hansen J.P.; Decomposition and oxidation of pyrite; Progress in energy and combustion science; 32(3); 2006; 295-314.

Haji-Sulaiman M.Z., Scaroni A.W. and Yavuzkurt S.; Optimum sulfation temperature for sorbents used in fluidized bed coal combustion; Fuel Processing Technology; 25(3); 1990; 227-240.

Hao J.; Wang S.; Liu B. and He K.; Plotting of acid rain and sulfur dioxide pollution control zones and integrated control planning in China; Water, Air, and Soil Pollution; 130(1-4); 2001; 259-264.

Hawke M.I., Martini I.P. and Stasinki L.D.; A comparison of temperate and boreal peats from Ontario, Canada: possible modern analogues for Permian coals; International Journal of Coal Geology; 41(3); 1999; 213-238.

Hem S. R. and Debaprasad D. C.; The moving boat technique and practical studies on the decomposition of carbonates. Part 1. Comparative assessment of the decomposition rates of limestone and dolomite samples; Thermochimica Acta; 101(1); 1986; 119-130.

Hepol J.; Sulphur transformations in catalytic hot-gas cleaning of gasification gas; VTT Technical Research Center of Finland; 2000; http//www.vtt.fi/inf/pdf/publications/2004/p425_pdf.

Horsfall D.W.; Coal Preparation and usage: Coal Processing for Management; 3; Coal Publications (Pty) Ltd.; 1993.

Hu Y., Watanabe M., Aida C. and Horio M.; Capture of H_2S by limestone under calcination conditions in a high-pressure fluidized-bed reactor; Chemical Engineering Sciences; 61(6); 2006; 1854-1863.

Ibarra J., Munoz E. and Moliner R.; FTIR study of the evolution of coal structure during the coalification process; Organic Geochemistry; 24(6-7); 1996; 725-735.

Imae N. and Kitamura M.; FeS formation reaction between metallic iron and H_2S gas in primordial solar nebula; Antarctic Meteorites XVIII. Papers presented to the 18th

Symposium on Antarctic Meteorites; NIPR; Tokyo; May 31 - June 2; 1993; p. 129-131.

ISO 157: Coal - Determination of forms of sulphur, 1996.

Jiang J. Z., Larsen R. K. , Lin R. , Mørup S. , Chorkendorff I. , Nielsen K., Hansen K. and West K.; Mechanochemical synthesis of Fe–S materials; Journal of Solid State Chemistry; 138(1); 1998; 114-125.

Kay D.A.R., and Wilson W.G.; Methods of desulphurisation of iron and steel and gases such as stack gases and the like; US Patent 4; 084,525, 1978.

Keyser M.J., van Dyk J.C., Coertzer R.L.C. and Wagner N.J., Full Scale Sasol-Lurgi Fixed Bed Test Gasifier Project: Impact of Particle Size Distribution, Destoning and Gasifier Operating Conditions on Sulfur Production ; Paper present at the 18th International Pittsburgh Coal Conference: Newcastle: New South Wales; Australia; 3-7 December; 2001.

Koss U. and Schlichting H.; Lurgi's MPG gasification plus Rectisol gas purification-Advanced process combination for reliable syngas production, Gasification Technologies Conference; San Francisco; October 9-12, 2005.

Korens N., Simbeck D.R., Wilhelm D.J.; Process screening analysis of alternative gas treating and sulphur removal; SFA Pacific Inc. for US Department of Energy, Mountain View, CA, December 2002.

Krishnudu T., Madhusudhan B., Narayan R.S., Seshagiri R.K. and Vaidyeswaran R.; Moving bed pressure gasification of some Indian coals; Fuel Processing Technology; 23; 1989 (a); 233-256.

Krishnudu T., Madhusudhan B., Reddy S.N., Sastry V.S.R., Seshagiri R. K. and Vaidyeswaran R.; Studies in a moving-bed pressure gasifier: Prediction of reaction zones and temperature profile; Indian Engineering and Chemistry Research; 28;1989 (b); 438-444.

Lambert J. M.; Simkovich G. and Walker P.L.; The Kinetics and Mechanism of the Pyrite-to-Pyrrhotite Transformation; Metallurgical and Materials Transactions. B, Process Metallurgy and Materials Processing Science; 29(2); 1998; 385-396.

Lauretta D. S., Kremser D. T. and Fegley Jr. B.; The rate of iron sulfide formation in the solar nebula; Icarus; 122(2); 1996; 288-315.

Lee Y. C. and Montano P. A.; An Auger and EELS study of iron sulfide (FeS_2, F_7S_8 and FeS) surfaces; Surface Science; 143(2-3); 1984; 442-468.

Li K. and Hung Y; Hydrogenation of sulphur dioxide to hydrogen sulphide over Fe/Al_2O_3; Applied Catalysis B: Environmental; 40; 2003; 13–20.

Macias-Perez M.C., Bruno-Lopez A., Lillo-roderas M.A., Salinas-Martinez de Lecea C. and Linares-Solano A.; SO_2 retention on CaO/activated carbon sorbents. Part I: Importance of calcium loading and dispersion; Fuel; 86; 2007; 677-683.

Maes I.I., Gryglewicz G., Yperman J., Franco D.V., Mullens J. and Van Poucke L.C.; Effect of calcium and calcium minerals in coal on its thermal analysis; Fuel; 76(2); 1997; 143-147.

Mastral A.M., Callén M.S., Murillo R. and Garcia T.; Organic emissions from Coal AFBC; Proceedings of the 15th International Conference on Fluidized Bed Combustion, Savannah, Georgia; May 16 - 19, 1999.

Matjie R.H.; Sintering and slagging of mineral matter in South African coals during the coal gasification process; PhD thesis; University of Pretoria; Pretoria, South Africa; 2008.

Matjie R.H. and van Alphen C.; Mineralogical features of size and density fractions in Sasol coal gasification ash, South Africa and potential by-products; Fuel; 87; 2008; 1439-1445.

Matjie R.H., van Alphen C. and Pistorius P.C.; Mineralogical characterisation of Secunda gasifier feedstock and coarse ash; Minerals Engineering; 19(3); 2006; 256-261.

Merkel T.C., Turk B., Gupta R., Cicero D.C. and Jain S.C., A hybrid gas cleaning process for production of ultra-clean syngas; Paper presented at the 24th Annual International Pittsburgh Coal Conference, Johannesburg, South Africa, 2007

Meyers R.A.; Coal structure. Academic Press. New York; 1982

Miller R.N., Yarzab R. F. and Given P.H.; Determination of the mineral-matter contents of coals by low-temperature ashing; Fuel; 58 (1); 1979; 4-10.

Morgan M.E., Jenkins R.G., and Walker P.L. Jr.; Inorganic constituents in American lignites; Fuel; 60 (3); 1981; 189-193.

Murowchick J.B. and Barnes H.L.; Formation of cubic FeS; American Mineralogist; 71, 1986; 1243-1246.

Ocampo A., Arenas E., Chejne F., Espinel J., Londoño C., A., Aguirre J. and Perez J. D.; An experimental study on gasification of Colombian coal in fluidised bed; Fuel; 82(2); 2003; 161-164.

Osborne D.G.; Coal preparation technology – Volume one; Graham & Trotman; London; 1988; 172-174.

Özum B., Kovacik G., Chambers A.; Coal gasification gas cleanup; International journal of hydrogen energy; 18(10); 1993; 847-851.

Paesano, Jr A., Matsuda C. K., da Cunha J. B. M., Vasconcellos M. A. Z., Hallouche B. and Silva S. L.; Synthesis and characterization of Fe-Al_2O_3 composites; Journal of Magnetism and Magnetic Materials; 264 (2-3); 2003; 264-274.

Painter P. C., Coleman M.M., Jenkins R.G., Whang P.W. and Walker P.L. Jr.; Fourier Transform Infrared study of mineral matter in coal. A novel method for quantitative mineralogical analysis; Fuel; 57(6); 1978; 337-344.

Pearce B. C., Hill J. W. F. and Kerry I.; Use of X-ray fluorescence spectrometry for the direct multi-element analysis of coal powders; Analyst; 115; 1990; 1397 – 1403.

Pearson D.E. and Kwong J.; Mineral matter as a measure of oxidation of caking coal; Fuel; 58; 1979; 66-68.

Popiel E.S.; Kromranse J.L. and Stancky K.; Chemical transformations of iron compounds during the process of hard coal pyrolysis; Hyperfine Interactions; 58 (1-4); 1990; 2613-2616.

Powell E. K. and Searcy A.W.; Kinetics and thermodynamics of decomposition of dolomite to a metastable solid product; Journal of the American Ceramic Society; 61(5-6); 2006; 216 – 221.

Raask E.; Creation, capture and coalescence of mineral species in coal frame. Journal of the Institute of Energy; 57; 1984; 231-239.

Reyers F., Perez-Alcazar G.A., Barraza J.M., Bohorques A., Tabarez J.A. and Speciali N.L.; Mössbauer and XRD characterization of then mineral matter of coal from the Guachinte mine in Colombia; Hyperfine Interactions, 148-149, 2004, 39-46.

Ripley E. M. and Snyder K.; Experimental sulphur isotope studies of the pyrite to pyrrhotite conversion in a hydrogen atmosphere; Economic Geology; 95(7); 2000; 1551-1554.

Ryan, B.D. and Ledda, A. (1997): A Review of Sulphur in Coal: With Specific Reference to the Telkwa Deposit, North-Western British Columbia; in Geological Fieldwork 1997, *B.C. Ministry of Employment and Investment*, Paper 1998-1, pages 29-1 to 29-21.

Saxena S. C. and Gabor J. D.; Mechanisms of heat transfer between a surface and a gas-fluidized bed for combustor application; Progress in Energy and Combustion Science; 7(2); 1981; 73-102.

Schlather J. and Turk B., Comparison of a new warm-gas desulphurisation process versus traditional scrubbers for a commercial IGCC Power plant, Paper at the 24th

Annual International Pittsburgh Coal Conference, Johannesburg, South Africa, 2007.

Shao L., Zhang P., Ren D., and Lei J.; Late Permian coal-bearing carbonate successions in southern China: coal accumulation on carbonate platforms; International Journal of Coal Geology; 37(3-4); 1998; 235-256.

Siriwardane R.V., Cicero D.C., Jain S., Gupta R.P. and Turk B.S.; Durable zinc oxide-based regenerable sorbents for desulphurisation of syngas in a fixed bed reactor; Paper at the 24th Annual International Pittsburgh Coal Conference; Johannesburg; South Africa; 2007.

Slaghuis J.H.; Coal gasification: A study guide for the national diploma in Fuel technology; Coal Processing III; Part A. Sasol Technology R&D; Sasolburg; 1993.

Slimane R.B., Lau F.S., Abbasian J. and Ho K.H.; New ZnO-based regenerable sulfur sorbents for fluid-bed/transport reactor applications; Paper at the 24th Annual International Pittsburgh Coal Conference; Johannesburg; South Africa; 2007.

Smith W.H.; "The constitution of coal"; Lecture prepared for the South African Processing School.; 1984.

Sotichos S.V.; Removal of H_2S and SO_2 by $CaCO_3$-based sorbents at high pressure; Semi Annual Report to the US DOE, GRANT **NO.:** DE-FG22-95PC95217; 1998.

Spears D.A., Rippon J.H. and Cavender P.F.; Geological controls on the sulphur distribution in British Carboniferous coals: a review and reappraisal; International Journal of Coal Geology; 40(1); 1999; 59-81.

Speight J.G.; The Chemistry and Technology of Coal, 2nd edition, Marcel Dekker, New York; 1994; 41-79.

Srinivasachar S., Helble J. J. and Boni A. A.; Mineral behaviour during coal combustion 1. Pyrite transformations; Progress in Energy and Combustion Science; 16(4); 1990; 281-292.

Strydom C. A.; Groenewald E. M.; Potgieter J. H. ; Thermogravimetric studies of the synthesis of CaS from gypsum, $CaSO_4.2H_2O$ and phosphogypsum; Journal of Thermal Analysis; 49(3); 1997; 1501-1507.

Teichmuller M. and Teichmuller R.; Chapter 8; Diagenesis of Coal (Coalification); Developments in Sedimentology; 8; Chilingar G.V., Bisseli H.J., and Fairbridge R.W., (editors); AGID Canada Catalogue 2001/1; 1967; 391-415.

Torres J., Mendez J. and Sukiennik M.; Transformation enthalpy of the alkali-earths sulfates ($SrSO_4$, $CaSO_4$, $MgSO_4$, $BaSO_4$); Thermochimica Acta; 334 (1-2); 1999; 57-66.

Tsai S.C.; Fundamentals of coal beneficiation. Amsterdam: Elsevier, 1982, 372.

Ulerich N. H., Newby R. A. and Keairns D. L.; A thermogravimetric study of the sulfation of limestone and dolomite — prediction of pressurized and atmospheric fluidized-bed desulfurization; Thermochimica Acta; 36(1); 1980; 1-16.

Undengaard N.R. and Berzins V.; Catalytic Conversion of COS for Gas Clean-up; Energy Progress; 1984; 115-117.

van Alphen C.; Automated mineralogical analysis of coal and ash products – Challenges and requirements; Minerals Engineering; 20; 2007; 496–505.

van Alphen, C., Falcon, L., 2000. Application of CCSEM to coal processing. Coal – the future. In: Proceedings of the 12th International Conference on Coal Research, SAIMM; Johannesburg; 12 -15 September 2000.

Vermaire S. and de Haan R.; Influence of sodium carbonate/vanadium concentration ratios on vanadate (V) equilibria and on the reoxidation of V(1V) in a hydrogen sulfide removal process; Indian Engineering and Chemistry Research; 27; 1988; 1242-1245.

Vidaurri J., Larsen R., Martin J., Looker M., Gebhard S., and Srinivas G.; Multicontaminant warm gas cleanup; Paper at the 24th Annual International Pittsburgh Coal Conference; Johannesburg; South Africa; 2007.

Vlakovic V.; Trace Elements in Coal; 1; CRC Press; New York; 1983.

Waanders F. and Bunt J.; Transformation of the Fe-mineral associations in coal during gasification; Hyperfine Interactions; 171(1-3); 2006; 287-292.

Wang Y., Lin S., and Suzuki Y.; Study of limestone calcination with CO_2 capture: Decomposition behaviour in a CO_2 atmosphere; Energy Fuels; 21 (6); 2007; 3317–3321.

Ward C.R. and French D.; Analysis and significance of mineral matter in coal. The Society for organic petrology; Short course notes, The University of New South Wales; Sydney; NSW; Australia; 2004; 7-68.

Watt, J.D.; The physical and chemical behaviour of the mineral matter in coal under conditions met in combustion plants, ECURA Industrial Laboratories, Leatherhead, Surrey, Part II, 1969.

Wiedemann H. -G. and Boller A.; Thermogravimetric studies of the reactions between dolomite and sulphur dioxide; Solid State Ionics; 43; 1990; 53-60.

Xie W., Chang C., Song H., Liu X., Xie K., Wall T. and Yu J.; Two-step hot-gas desulphurisation process integrated with direct production of elemental sulphur using iron-based sorbents: A preliminary study; Paper at the 24th Annual International Pittsburgh Coal Conference; Johannesburg; South Africa; 2007.

Zevenhoven R. and Kilpinen P.; Control of pollution in flue gases and fuel gases, for the Helsinki University of technology course EWE-47.;153; 2005; 3.1-3.24.

Zhang L., Sato A. and Ninomiya Y.; CCSEM analysis of ash from combustion of coal added with limestone; Fuel; 81; 2002; 1499-1508.

Appendices

Table A.1 Sulphur forms analysis report

Date : 2007/04/23

CMT No			135102	135106	135107	135103	135108
Sample			S0 01	S0 08	S0 16	S0 24	S0 32
Description			A	B	C	D	E
Tot.Sulp.	%	ASTM D4239	0.39	0.45	0.85	1.11	2.12
Min.Sulp	%	ISO 157	0.21	0.22	0.35	0.67	1.67
Sul.Sulp	%	ISO 157	0.04	0.08	0.03	0.03	0.15
Org.Sulp	%	ISO 157	0.18	0.23	0.50	0.44	0.46

Table A.2 XRF analysis results

Element/ % composition	Fe2O3	MnO	Cr2O3	V2O5	TiO2	CaO	K2O	P2O5	SiO2	AL2O3	MgO	Na2O	SO3
Sample													
A	4.56	0.05	0.05	0.02	1.5	8.63	0.92	0.80	54.73	26.42	1.56	0.50	0.25
B	4.48	0.08	0.06	0.04	1.44	8.14	1.02	0.74	54.29	26.68	1.81	0.50	0.73
C	4.02	0.11	0.1	0.05	1.42	7.31	0.95	0.76	54.26	26.10	1.93	0.59	2.39
D	3.51	0.16	0.1	0.09	1.37	9.07	0.94	0.83	52.07	26.34	0.56	0.65	4.29
E	3.94	0.20	0.1	0.12	1.27	10.1	0.84	0.91	49.17	26.13	0.77	0.81	5.61

Table A.3 CCSEM analysis results

	Mass % phase proportion, normalised in ash				
Sample	pyrite cleats	Kaolinite(pyrite)	Kaolinite(carbonate,pyrite)	Quartz(carbonate,pyrite)	Extraneous Pyrrhotite/Fe-S-O/Fe-oxide
A	0	1.55	5.05	1.13	1.24
B	0	0.92	4.15	0.62	1.38
C	0	1.00	2.80	0.20	3.20
D	0	1.00	4.33	0.33	4.67
E	4.8	0.40	1.20	0.00	0.00

Table A.4 Effect of temperature on sulphur content

Coal A used							
SO_2 flow rate 40cc/min, air @ 5l/min							
Reaction time: Ramping to 450 at 50°C/min keep at 450°C for 1 hr ramp to desired temp and keep there for 20 min							
			based on ultimate analysis				
			not treated	SO_2 treated			
		Temp	S in ash (mass %)	S in ash (mass %)			
		900	0.605	0.95			
		950	0.42	1.34			
		1000	0.6	1.3			
		1050	0.9	2.055			
		1100	0.82	2.3			
		1150	0.753	1.29			
		1200	0.55	1.18			
		1250	0.44	0.7734			

Table A.5 Effect of residence time on sulphur and carbon content.

Time of reaction at desired temperature(min)	Sample temperature and period	S	C	CaS content based on XRD
0	1100	0.82	44	0
20	1100 20min	2.3	46.8	4.9
40	1100 40min	2.39	41.39	5
60	1100 60min	2.67	46.82	4.8
80	1100 80min	4.25	38.22	4
120	11002hr	3.22	27.49	2.4
240	11004hr	2.35	22.21	0.7

Table A.6 pH and acidity concentrations determination

Vinitial	20
Cfinal	0.02

sample	time taken	temp	corresponding temperature	pH (paper)	pH(meter)	Vfinal	Cinitial
1	14:35	815	845	1	2.07	43.59	0.04359
2	14:45	943	973	4	3.13	0.53	0.00053
3	14:55	1045	1075	4	4.13	0.1	0.0001
4	15:05	1065	1095	5	5.52	0.1	0.0001
5	15:15	1070	1100	6	5.31	0.1	0.0001
6	15:25	1070	1100	6	5.33	0.1	0.0001
7	15:35	1070	1100	6	6.52	0.1	0.0001
8	15:45	1070	1100	6	6.35	0.1	0.0001
9	15:55	1070	1100	6	6.08	0.1	0.0001
10	16:05	1070	1100	5	4.82	0.101	0.000101
11	16:15	1070	1100	5	3.95	0.35	0.00035

Table A.7 : XRD analysis on selected sulphur capture reaction samples of the laboratory-scale furnace, normalised to crystalline matter.

Mineral phase	Chemical Formula	Feed	20	r20	80	r80	120	r120	r240
Quartz	SiO_2	20.8	47.7	21.6	22.6	18.5	18.9	27.8	27.7
Kaolinite	$Al_2(Si_2O_5)(OH)_4$	58.4	0	0	0	0	0	0	0
Muscovite	$KAl_2Si_3O_{10}(OH)_2$	5.7	2.3	0	0	0	0	0	0
Pyrite	FeS_2	1.4	0	0	0	0	0	0	0
Calcite	$CaCO_3$	3.9	2.3	0	0	1.8	1	1.2	1.1
Dolomite	$CaMg(CO_3)_2$	5.4	0	0	0	0	0	0	0
Alunite	$KAl_3(SO_4)_3(OH)_6$	4.3	0	0	0	0	0	0	0
Brushite	$Ca(HPO_4)(H_2O)_2$	0	0	0	0	0	0	0	0
Rutile	TiO_2	0	0.8	0.7	0.5	1.1	0	0.7	0.2
Anatase	TiO_2	0	0	0	0	0	0	0	0.2
Mullite	$Al_6Si_2O_{13}$	0	3.8	50.2	47.1	36.4	36.7	30.5	53.3
Anorthite	$CaAl_2Si_2O_8$	0	0.8	18.9	14.4	4.7	9.5	4.1	6.8
Cristobalite	SiO_2	0	0	4.1	3.6	1.3	1.7	2.7	3.2
Oldhamite	CaS	0	2.3	4.9	3.8	4	2.9	2.4	0.7
Anhydrite compounds	$CaSO_4$	0	0.8	0	2.6	6.6	0.5	9.7	5.4
Magnetite (or other	Fe_3O_4	0	0.8	0	1	17.9	11.9	12.6	0.2
Hematite	Fe_2O_3	0	6.2	0	0.5	5.8	0.2	5.8	0
Periclase	MgO	0	6.2	0	1.2	1.6	17	1.7	0.9
Lime	CaO	0	0	0	0	0	0	0	0
Diopside	$CaMgSi_2O_2$	0	0	0	2.6	0	0	0	0
Crystalline matter		100	100	100	100	100	100	100	100

Table A.8: Calculation of the sulphur capturing efficiency in a pipe reactor.

	Reference samples		**SO_2 treated reaction samples**	
Sample	**% S**	**Mass S(kg) in coal/mass ash**	**% S**	**Mass S(kg) in coal/mass ash**
1	1.16	0.34	1.23	0.36
2	1.32	0.48	1.02	0.35
3	0.87	0.30	0.8	0.29
4	0.60	0.20	1.03	0.34
5	0.6	0.16	1.57	0.56
6	0.59	0.15	1.89	0.65
7	0.55	0.13	0.52	0.18
Total		1.76		2.73

s added by reaction/kg	**0.97**
Sulphur added from SO2	
SO_2 added/ml/min	40
over 2hours/ml	4800
amount/l	4.8
SO_2 density/kg/l	0.99
mass SO_2 used/kg	4.752
mass SO_2 used/g	4752
%sulphur captured	40.76

Mr SO_2/g/mol	64
Mr O_2/g/mol	16
Mr S/g/mol	32
n SO_2/mol	74.25
n S/mol	74.25
mS/g	2376
mS/kg	**2.376**

Table A.9: Ash analysis of the sample from both the base case and the SO_2 reaction sample

	Coal A - Reaction samples									
	oxides analysis (%)									
	SiO_2	Al_2O_3	Fe_2O_3	P2O5	TiO_2	CaO	MgO	K_2O	Na_2O	SO_3
1	55.90	28.70	3.79	0.08	1.72	2.94	2.69	0.95	0.40	2.65
2	58.10	25.80	4.16	0.08	1.36	2.81	3.06	0.95	0.40	3.80
3	54.30	29.90	2.72	0.11	1.36	4.01	3.88	1.02	0.51	2.16
4	56.50	28.00	3.01	0.07	1.41	3.38	3.37	1.25	0.48	3.03
5	57.80	25.40	3.87	0.11	0.98	3.19	2.96	0.99	0.44	4.53
6	59.30	25.40	4.22	0.09	1.11	2.86	2.61	1.12	0.54	2.78
7	57.00	28.50	3.89	0.08	1.35	3.97	2.89	1.01	0.43	1.35
	Coal A - Base Case									
1	64.40	21.00	3.80	0.63	1.31	2.56	2.13	1.66	0.30	1.78
2	60.70	26.30	2.88	1.08	1.08	2.94	1.19	1.80	0.49	1.47
3	57.60	27.30	3.21	0.47	1.10	3.61	2.35	1.26	0.45	2.37
4	56.70	30.00	3.45	0.17	1.18	2.73	1.71	1.27	0.37	2.33
5	60.90	26.00	3.73	0.14	1.08	2.63	1.59	1.35	0.45	2.09
6	60.00	27.00	5.19	0.13	1.36	3.00	1.67	0.80	0.35	0.34
7	59.50	25.30	5.02	0.11	1.52	3.96	1.88	1.16	0.41	0.76

Table A.10: Sulphur forms analysis for base case reaction and SO_2 treated reaction samples for pipe reactor reactions

	Base Case Samples (%)				
Sample	**Tot. S**	**min. S**	**organic S**	**sulp. S**	**Carbon**
1	1.16	0.75	0.32	0.09	47.44
2	1.32	0.89	0.33	0.1	48.32
3	0.87	0.54	0.22	0.11	50.03
4	0.60	0.36	0.19	0.05	49.63
5	0.6	0.42	0.15	0.03	51.9
6	0.56	0.34	0.15	0.07	50.4
7	0.5	0.35	0.1	0.05	14.51

Sample	Reaction samples (%)				
Sample	**Tot. S**	**min. S**	**organic S**	**sulph. S**	**Carbon**
1	1.23	0.65	0.41	0.17	50.6
2	1.02	0.55	0.33	0.14	53.5
3	0.85	0.45	0.3	0.1	55.77
4	1.03	0.56	0.32	0.15	54.32
5	1.57	1.07	0.41	0.09	56.05
6	1.89	1.43	0.39	0.07	28.2
7	0.520	0.090	0.390	0.040	9.52

Table A.11: Mineral phases identification and quantification in reaction samples for the pipe reactor in percentage.

mineral phase	1	2	3	4	5	6	7
Quartz	28.39	24.54	22.40	32.47	61.00	23.25	19.4
kaolinite	51.82	55.87	59.94	43.54	7.00	0.00	0.00
muscovite	1.04	2.35	2.84	2.95	0.00	0.00	0.00
pyrite	4.95	3.66	0.95	0.37	0.00	0.00	0.00
marcasite	0.00	1.04	0.00	0.00	0.00	0.00	0.00
calcite	2.34	2.09	3.15	8.12	1.50	0.00	0.00
dolomite	6.25	5.74	7.26	9.96	0.00	0.00	0.00
alunite	3.91	3.92	2.52	1.11	0.00	0.00	0.00
anatase	1.04	0.78	0.95	1.48	0.00	0.00	0.00
mullite	0.00	0.00	0.00	0.00	18.50	46.25	42.80
anorthite	0.00	0.00	0.00	0.00	1.5	20.95	22.00
cristoballite	0.00	0.00	0.00	0.00	0.4	13.60	11.00
oldamite	0.00	0.00	0.00	0.00	7.1	4.1	0.8
anhydrite	0.00	0.00	0.00	0.00	0.50	1.05	3.6
Troilite	0.00	0.00	0.00	0.00	6.6	2.85	0.2
hematite	0.00	0.00	0.00	0.00	0.00	0.00	1.5
periclase	0.00	0.00	0.00	0.00	4.00	0.42	0.5
lime	0.00	0.00	0.00	0.00	0.00	0.00	1.5

Table A.12: Comparison of the base-case and reaction samples by XRD.

	Reaction samples			Base Case samples		
Mineral (%)	**5**	**6**	**7**	**5**	**6**	**7**
CaS	**7.1**	**4.1**	**0.8**	**2**	**1.65**	**0.95**
$CaSO_4$	**0.7**	**1.05**	**3.6**	**4.85**	**3.25**	**2.6**
$CaSO_4.2H_20$	**0**	**0**	**0**	**0**	**1.1**	**0**
FeS	**6.6**	**2.85**	**0.2**	**0**	**0**	**0**
Fe_2O_3	**0**	**0**	**1.5**	**3.3**	**1.25**	**0.55**